

Nonlinear phenomena on metric and discrete necklace graphs

Von der Fakultät für Mathematik und Physik der Universität Stuttgart
zur Erlangung der Würde eines
Doktors der Naturwissenschaften (Dr. rer. nat.)
genehmigte Abhandlung

Vorgelegt von
Daniela Maier
aus Schwäbisch Gmünd

Hauptberichter:	Prof. Dr. Guido Schneider
Mitberichter:	Prof. Dr. Wolfgang Reichel Prof. J. Douglas Wright, PhD

Tag der mündlichen Prüfung: 19. Juli 2019

Institut für Analysis, Dynamik und Modellierung
der Universität Stuttgart

2019

Für Markus

Abstract

Nonlinear phenomena on periodic necklace graphs constitute the central theme of this thesis. Applications of periodic graphs arise in many fields of science, for instance as models for complex physical structures such as photonic crystals, nano-tubes or graphene.

In the first part we provide a rigorous proof for the existence of breather solutions for nonlinear Klein-Gordon equations on periodic metric necklace graphs with Kirchhoff boundary conditions. In particular, we construct long-wave breathers that are symmetric with respect to the semi-circles of the necklace graph. The proof relies on a spatial dynamics approach. Thus, the existence question is approached by considering an infinite-dimensional system of ordinary differential equations on subintervals of the real line that are coupled by suitable boundary conditions. A careful analysis of the Floquet-Bloch spectrum of the associated linear operator and an appropriate fixation of the temporal period of the breather allow us the application of a center manifold reduction. The persistence of the approximately constructed pulse solutions on the center manifold under higher order perturbations is obtained by symmetry and reversibility arguments.

Furthermore, we consider a nonlinear diffusion equation on a metric necklace graph. We prove that terms which are irrelevant with respect to linear diffusion on the real line are irrelevant on the graph, too. The proof is based on L^1 - L^∞ -estimates combined with Bloch wave analysis.

In the second part of this thesis we deal with a discrete version of the necklace graph. We prove dispersive estimates for Klein-Gordon systems with small symmetric initial conditions. In particular, we use explicit integral representations of the semi-group and van der Corput's lemma to obtain a temporal decay rate of $(1+t)^{-\frac{1}{3}}$. Note that anti-symmetric initial conditions correspond to eigenvalues and will not lead to any temporal decay. Moreover, asymptotic stability of the vacuum state for nonlinear Klein-Gordon systems with power nonlinearity is shown.

Finally, we prove the existence of strongly localized breather solutions, which are not symmetric with respect to the periodic branching of the discrete graph. The main ingredient of the proof is the Theorem of Crandall and Rabinowitz (bifurcation from a simple eigenvalue). For this purpose we request a non-resonance condition.

Zusammenfassung

Nichtlineare Phänomene auf periodischen Perlenschnur-Graphen bilden das zentrale Thema dieser Arbeit. Periodische Graphen finden Anwendung in vielen naturwissenschaftlichen Disziplinen, beispielsweise als Modelle für komplexe physikalische Strukturen wie photonische Kristalle, Nanoröhren oder Graphen.

Im ersten Teil der Arbeit beweisen wir die Existenz so genannter Breather Lösungen von nichtlinearen Klein-Gordon Gleichungen auf periodischen, metrischen Perlenschnur-Graphen mit Kirchhoff Randbedingungen. Insbesondere konstruieren wir langwellige Breather Lösungen, die symmetrisch bezüglich der Halbkreise des Graphen sind. Der Beweis beruht auf einem Fourierreihenansatz, der auf ein System mit räumlicher Dynamik führt. Die Existenzfrage wird somit auf ein unendlich dimensionales System von gewöhnlichen Differentialgleichungen auf Teilintervallen der reellen Achse zurück geführt, die über geeignete Randbedingungen gekoppelt sind. Eine sorgfältige Analyse des Floquet-Bloch Spektrums des zugehörigen linearen Operators und eine geeignete Wahl der zeitlichen Periode der Breather Lösungen erlaubt uns die Durchführung einer Zentrumsmannigfaltigkeitenreduktion. Dabei erhalten wir die Persistenz der näherungsweise konstruierten Pulslösungen auf der Zentrumsmannigfaltigkeit unter Störungen höherer Ordnung mithilfe von Symmetrie- und Reversibilitätsargumenten.

Zudem betrachten wir eine nichtlineare Diffusionsgleichung auf einem metrischen Perlenschnur-Graphen. Wir zeigen, dass vernachlässigbare Terme hinsichtlich Diffusion auf der reellen Achse auch vernachlässigbar auf dem Graphen sind. Der Beweis basiert auf L^1 - L^∞ -Abschätzungen kombiniert mit einer Blochwellenbetrachtung.

Im zweiten Teil dieser Arbeit beschäftigen wir uns mit einer diskreten Version des Perlenschnur-Graphen. Wir beweisen dispersive Abschätzungen für Klein-Gordon Systeme mit kleinen, symmetrischen Anfangsbedingungen. Hierzu benutzen wir eine explizite Integraldarstellung der Halbgruppe und das Lemma von van der Corput um zeitliche Abfallraten der Form $(1 + t)^{-\frac{1}{3}}$ zu

erreichen. Antisymmetrische Anfangsbedingungen gehören zu Eigenwerten und werden zu keinem zeitlichen Abfall führen. Des Weiteren wird die asymptotische Stabilität des Vakuumzustandes einer nichtlinearen Klein-Gordon Gleichung mit polynomieller Nichtlinearität gezeigt.

Letzlich beweisen wir die Existenz von stark lokalisierten Breather Lösungen, die nicht symmetrisch bezüglich der periodischen Zweige des diskreten Graphen sind. Der Hauptbestandteil des Beweises ist das Theorem von Crandall und Rabinowitz (Bifurkation von einem einfachen Eigenwert), wofür wir eine Nichtresonanz-Bedingung fordern.

Acknowledgements and declaration

First and foremost I would like to thank my advisor Guido Schneider for his extensive advice, support and encouragement over the past three years. I am very grateful for many fruitful mathematical discussions and thank him very much for introducing me to exciting areas of research.

I would also like to thank Wolfgang Reichel and Douglas Wright for their readiness to act as referees for this thesis. I thank Wolf-Patrick Düll for agreeing to be a member of my audit committee and providing helpful comments and suggestions on my work. Moreover, I would like to express my gratitude to Martina Chirilus-Bruckner and Douglas Wright for stimulating discussions during my research stays in Leiden and Philadelphia.

And not least, I gratefully acknowledge the financial support by the German Research Foundation through GRK 1838: Spectral theory and dynamics of quantum systems.

My colleagues and friends at the mathematics department in Stuttgart deserve my special thanks for creating an enjoyable and inspiring atmosphere.

It was a great pleasure.

I hereby certify that this thesis has been composed by myself and describes my own work unless otherwise acknowledged in the text. All references and verbatim extracts have been quoted and all sources of information have been specifically acknowledged.

Stuttgart, April 2019

Daniela Maier

Contents

1	Introduction	1
1.1	Motivation and state of the art	1
1.1.1	Breather solutions	2
1.1.2	Diffusive and dispersive phenomena	3
1.2	Brief summary of results	4
1.2.1	Metric necklace graph	4
1.2.2	Discrete necklace graph	6
I	Nonlinear phenomena on a metric necklace graph	9
2	Construction of breather solutions on a metric necklace graph	11
2.1	Introduction	11
2.1.1	Statement of the problem	13
2.1.2	Statement of the main theorem	14
2.1.3	Outline of the proof	15
2.2	Spatial dynamics formulation	17
2.3	Time- P -maps	19
2.4	Spectral situation and center manifold reduction	20
2.4.1	Trace of monodromy matrix and choice of breather frequency	21
2.4.2	Discrete center manifold reduction	23
2.5	Analysis of the reduced system	25
2.5.1	Relating the reduced discrete systems to an ordinary differential equation	25

2.5.2	Existence of homoclinic orbits to zero of the lowest order approximation on the center manifold	27
2.5.3	Persistence of the homoclinic orbits under higher order perturbations	28
2.6	Discussion	30
2.7	Appendices	31
2.7.1	Floquet-Bloch theory	31
2.7.2	The discrete center manifold theorem	33
3	Diffusive stability on metric necklace graphs	37
3.1	Introduction	37
3.2	The PDE on the metric graph	40
3.3	Spectral analysis	42
3.4	The functional analytic set-up	45
3.4.1	The system in Bloch space	45
3.4.2	The function spaces	46
3.5	Diffusive and exponentially damped modes	48
3.6	The nonlinear decay estimates	50
3.6.1	Preliminaries	50
3.6.2	Irrelevance of the nonlinear terms	53
3.7	Appendix	58
3.7.1	Local existence and uniqueness	58
II	Nonlinear phenomena on a discrete necklace graph	61
4	Dispersive estimates and asymptotic stability on a discrete necklace graph	63
4.1	Introduction	63
4.2	Spectral situation and Bloch transform	65
4.3	Explicit integral representation of the solution	67
4.4	Dispersive decay and energy estimates	70
4.4.1	Dispersive estimates	71
4.4.2	Energy estimate	75

4.5	Global existence for the nonlinear problem with sufficiently large power nonlinearity	76
5	Construction of breather solutions on discrete necklace graphs	79
5.1	Introduction	79
5.2	Spectral situation	82
5.3	Existence of breather solutions for non-vanishing local forces . .	85
6	Outlook	91
	Bibliography	94

Chapter 1

Introduction

1.1 Motivation and state of the art

Differential operators on metric graphs with appropriate vertex conditions recently attracted a lot of interest, cf. [KP07, Noj14, EK15, AST16]. These so called quantum graphs first appeared in the 1930s as models of free electrons in organic molecules [Pau36]. In modern physics they arise as models for nanostructures and microwave cavities, for instance, if one considers wave propagation through a quasi-one-dimensional system with geometric structure. Prominent examples are graphene and graphene sheets with a cylindrical structure (nanotubes). Quantum graphs form a rapidly growing branch of mathematical physics lying on the border between differential operators, spectral theory and operator theory. We recommend the textbook [BK13] and the survey [Kuc02] for further motivations.

Korotyaev and Lobanov [KL07] found a unitarily equivalence between the periodic Schrödinger operator on a class of zigzag nanotubes and the direct sum of its corresponding Hamiltonians on a one-dimensional periodic metric graph consisting of rings and lines. Thus, they reduced the spectral problem on zigzag nanotubes to the spectral problem of periodic Schrödinger operators on one-dimensional graphs with necklace structure. In contrast to operators on the real line, spectral properties of operators on necklace graphs are explicitly computable. Their periodicity leads to a band gap structure with spectral gaps.

Nonlinear Schrödinger equations posed on specific periodic necklace graphs, cf. Figure 1.2.1, were studied by recent works [GPS16, PS17, Pan18]. In particular, the existence of small localized standing waves for frequencies lying below the linear spectrum of the associated stationary Schrödinger equation have been established in the work of Pelinovsky and Schneider [PS17]. Pankov [Pan18] proved the existence of a non-small finite energy ground state solution by a variational approach.

The theory of quantum graphs is a relatively young branch of mathematics with many open problems and a broad perspective. Studies of properties of solutions on quantum graphs are very important for applications in physics and natural sciences.

1.1.1 Breather solutions

We are interested in the existence of localized structures on periodic necklace graphs. A main part of this work is the analysis of the existence of real-valued, time-periodic and spatially localized solutions for nonlinear wave equations. From a mathematical point of view there is a phenomenological interest, because the existence of these so called breather solutions for such systems is very rare. There is a competition between linear decay and the focusing effect of the nonlinearity, which allows for the existence of localized solutions. Hence, breathers are an inherently nonlinear phenomenon. In the spatially homogeneous situation, a nonlinear wave equation known to admit small-amplitude breather solutions of pulse form is the Sine-Gordon equation. However, these solutions do not persist under analytic perturbations. In particular, up to rescaling, the Sine-Gordon equation is the only one of the form

$$\partial_t^2 u - \partial_x^2 u + u + g(u) = 0$$

with $g(u) = \mathcal{O}(u^3)$ for $u \rightarrow 0$ possessing breather solutions, cf. [Den93]. In general, only the existence of generalized pulse solutions with small non-vanishing tails can be shown, cf. [GS01, GS05, GS08]. The rareness of breathers in PDEs makes it hard to believe that these non-generic, structurally unstable objects describe phenomena in nature.

However, the situation on spatial domains with periodic structures is different and breather solutions are back. Our approach is motivated by the existence result of small-amplitude breathers of Blank, Chirilus-Bruckner, Lescarret, and Schneider [BCBLS11]. They considered a nonlinear Klein-Gordon equation

$$s(x)\partial_t^2 u - \partial_x^2 u + q(x)u - u^3 = 0$$

on the real line with specifically chosen, spatially periodic step functions s and q . More recently, Hirsch and Reichel [HR17] showed the existence of breather solutions of a semi-linear wave equation with a periodically extended delta potential. Their variational approach leads to large amplitude solutions.

MacKay and Aubry [MA94] constructed breathers in Hamiltonian lattices with anharmonic on-site potentials and weak coupling. In their proof breathers are obtained by continuation from the uncoupled case in which trivial breathers exist. This means that only one oscillator is excited and the others are at rest. With the same technique the existence of breathers was proved for diatomic Fermi-Pasta-Ulam (FPU) chains, cf. [LSM97]. Aubry et al. [AK01] have proved the existence of breathers in FPU lattices with frequencies above the phonon spectrum if the potential V is a strictly convex polynomial of degree 4. These results are obtained via a variational method. In the class of infinitely extended periodic lattice differential equations, discrete necklace graphs are related to poly-atomic FPU models and are discretized versions of nonlinear partial differential equations on metric necklace graphs. While discrete graphs reflect the topology of the system, metric graphs take into account distances between the nodes and the way different bonds are connected to each other. Understanding the relation between discrete and continuous graphs is a challenging area, which has not been studied systematically so far.

1.1.2 Diffusive and dispersive phenomena

We are interested in diffusive and dispersive phenomena on necklace graphs. The knowledge of stability properties of spatially localized structures is fundamental for many fields in nature. A basic concept in stability theory is the control of nonlinear terms by the linearized problem if energy is dissipated fast enough.

Typically, the L^∞ norm decays with an algebraic rate of type $(1+t)^{-\beta}$ for some constant $\beta > 0$. In the dispersive case, this is because initially localized solutions are dispersed by different group velocities associated with different wave numbers.

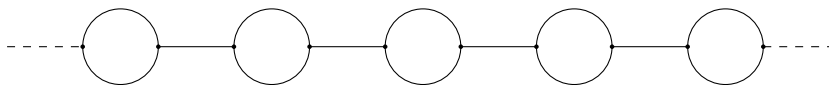
The first stability result for a diffusive equation on the real line goes back to [Wei81]. This result has been transferred to more complicated problems such as the stability of spatially periodic equilibria in the Ginzburg-Landau equation [CEE92, BK92] and in pattern forming systems [Sch96, Sch98]. There are various approaches to establish such stability results, namely the discrete and continuous renormalization approach, the use of Lyapunov functions and L^1 - L^∞ -estimates, see [SU17, Chapter 14] for more details.

In general, dispersive properties are well-studied for partial differential equations on the real line. These effects are also expected in discrete systems. Mielke and Patz [MP10] derived dispersive stability results for oscillator chains such as the FPU or discrete Klein-Gordon chain.

1.2 Brief summary of results

1.2.1 Metric necklace graph

A metric graph is a network of edges connected by vertices, i.e., it consists of edges considered as intervals on the real axis that are joined together at the vertices. The graph is equipped with a differential operator that acts on functions defined on the edges (Hamiltonian) together with appropriate boundary conditions that guarantee the self-adjointness of the operator. The geometry of the metric graph, which we will consider subsequently, is displayed in Fig. 1.2.1. We impose Kirchhoff boundary conditions at the vertex points, which consist of continuity and conservation of the flows.

Figure 1.2.1: Geometry of the metric necklace graph Γ **Result 1: Construction of breather solutions on the necklace graph**

For an odd integer k and sufficiently small $\varepsilon > 0$ the nonlinear, cubic Klein-Gordon equation

$$\partial_t^2 u(t, x) = \partial_x^2 u(t, x) - (k^2/4 + \varepsilon^2)u(t, x) + u(t, x)^3, \quad t \in \mathbb{R}, x \in \text{int } \Gamma,$$

with Kirchhoff boundary conditions at the vertices, possesses breather solutions of amplitude $\mathcal{O}(\varepsilon)$ and frequency $\omega = k/2$. In particular, these solutions are symmetric with respect to the upper and lower semicircles.

Our method of proof relies on a spatial dynamics ansatz combined with center manifold reduction. It requires a careful control of the Floquet Bloch spectrum of the underlying linearized differential operators. We show the existence of small amplitude solutions bifurcating from the trivial solution. The major challenge arises from the irregularity of the solutions due to Kirchhoff boundary conditions. As a consequence, the flow on the center manifold is no longer continuous at the vertex points. The resulting non-autonomous system makes it necessary to modify the persistence proof of the approximately constructed pulses under higher order perturbations. *The construction is shown in Chapter 2, see also [Mai18].*

Result 2: Diffusive stability on the necklace graph

We consider the nonlinear diffusion equation

$$\partial_t u(t, x) = \partial_x^2 u(t, x) + u^p(t, x), \quad t \in \mathbb{R}, x \in \text{int } \Gamma,$$

for $p > 3$ posed on the metric necklace graph Γ from Figure 1.2.1. We prove that terms which are irrelevant with respect to linear diffusion on the real line are also irrelevant on the periodic metric graph.

Diffusive equations posed on necklace graphs come with new challenges since the underlying function spaces contain very irregular functions. The major difficulty is to bring together well-known diffusive estimates, cf. [MSU01], and local existence and uniqueness theory, which is based on the domain of the Laplacian \mathcal{H}^2 . We think that the presented approach for handling this problem is conceptually more transparent than the general approach in [SU17, Chapter 14] and easier to apply to other situations. Moreover, our result is a first step in answering similar problems for dispersive equations, cf. [Str89], such as Klein-Gordon or nonlinear Schrödinger equations. *This result is explained in Chapter 3, which coincides with [CMS18].*

1.2.2 Discrete necklace graph

We consider the discrete Klein-Gordon system

$$\begin{aligned} \partial_t^2 u_j &= f(v_j^+ - u_j) + f(v_j^- - u_j) - h(u_j - w_{j-1}) - r_u(u_j), \\ \partial_t^2 v_j^+ &= g(w_j - v_j^+) - f(v_j^+ - u_j) - r_v(v_j^+), \\ \partial_t^2 v_j^- &= g(w_j - v_j^-) - f(v_j^- - u_j) - r_v(v_j^-), \\ \partial_t^2 w_j &= h(u_{j+1} - w_j) - g(w_j - v_j^+) - g(w_j - v_j^-) - r_w(w_j), \end{aligned} \tag{1.1}$$

with interaction potentials f, g, h , local potentials r_u, r_v, r_w and coordinates u_j, v_j^\pm, w_j , for all $j \in \mathbb{Z}$, on the subsequent discrete graph with periodic branching, cf. Figure 1.2.2. We assume that all forces vanish at the origin and consider expansions $f(x) = f_1 x + f_2 x^2 + \dots$ of the forces. The coordinates $(u_j, v_j^+, v_j^-, w_j)^T = X_j \in \mathbb{R}^4$ correspond to the horizontal displacement of the mass particles from its equilibrium positions.

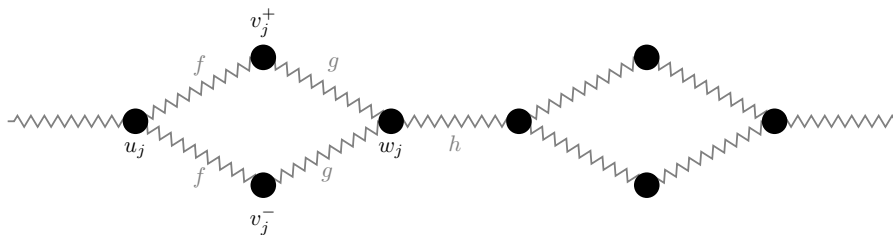


Figure 1.2.2: Topology of the discrete necklace graph

Result 3: Dispersive estimates and asymptotic stability of the vacuum state for nonlinear problems

We show that solutions with localized initial data that are symmetric w.r.t. the semi-circles decay with a rate of $(1+t)^{-1/3}$ in the L^∞ norm.

Furthermore, we prove asymptotic stability of the vacuum state for these kind of initial data. In particular, we show that solutions with small localized initial data decay exactly as in the linear case if the power nonlinearity is of degree higher than five. *These results can be found in Chapter 4.*

To our knowledge, global existence results based on dispersive estimates do not exist for equations posed on non-trivial infinite periodic metric graphs yet. However, Kaminaga and Mine [KM16] showed dispersive estimates for finitely many spectral bands for a periodic δ -potential on the real line, but not for the complete semigroup.

Result 4: Existence of breather solutions on the discrete necklace graph

Under a number of non-resonance conditions there exists a one-parameter family of breather solutions mainly supported in one periodicity cell of the discrete graph.

The idea of proof, namely the application of the Theorem of Crandall-Rabinowitz within an invariant subspace of solutions, is a first step towards

constructing breathers on the metric necklace graph, which are not symmetric w.r.t. the semi-circles and therefore exploit the branching of the graph structure. *This result is explained in Chapter 5.*

For the reader's convenience we keep the chapters self-contained and introduce the setting at the beginning of each chapter.

Part I

Nonlinear phenomena on a metric necklace graph

Chapter 2

Construction of breather solutions on a metric necklace graph

The purpose of this chapter is to construct small-amplitude breather solutions for a nonlinear Klein-Gordon equation posed on a periodic metric graph via spatial dynamics and center manifold reduction. The major difficulty occurs from the irregularity of the solutions. The persistence of the approximately constructed pulse solutions under higher order perturbations is obtained by symmetry and reversibility arguments.

2.1 Introduction

Korotyaev and Lobanov [KL07] found a unitary equivalence between the periodic Schrödinger operator on a class of zigzag nanotubes and the direct sum of its corresponding Hamiltonians on a one-dimensional periodic metric graph consisting of rings and lines. Thus, they reduced the spectral problem on zigzag nanotubes to the spectral problem of periodic Schrödinger operators on one-dimensional graphs with necklace structure. Recent works [GPS16, PS17, Pan18] studied nonlinear Schrödinger equations posed on this necklace graph. Particularly, the existence of small localized standing waves for frequencies ly-

ing below the linear spectrum of the associated stationary Schrödinger equation has been established in the work of Pelinovsky and Schneider [PS17]. The purpose of this article is to construct time-periodic, spatially localized solutions in nonlinear cubic Klein-Gordon equations. From a mathematical point of view, the existence of these so called breather solutions is very rare. Breathers are an inherently nonlinear phenomenon. In the spatially homogeneous situation, a wave equation known to admit small-amplitude breather solutions of pulse form is the Sine-Gordon equation. However, these solutions do not persist under analytic perturbations. In particular, up to rescaling, the Sine-Gordon equation is the only one of the form

$$\partial_t^2 u = \partial_x^2 u - u - g(u)$$

with $g(u) = \mathcal{O}(u^3)$ for $u \rightarrow 0$ possessing breather solutions, [Den93]. In general, only the existence of generalized pulse solutions with small non-vanishing tails can be shown, cf. [GS01, GS05, GS08]. Our approach is motivated by the existence result of Blank, Chirilus-Bruckner, Lescarret, and Schneider [BCBLS11]. They considered a nonlinear Klein-Gordon equation

$$s(x)\partial_t^2 u - \partial_x^2 u + q(x)u = u^3$$

on the real line with specifically chosen, spatially periodic step functions s and q . More recently, Hirsch and Reichel [HR17] showed the existence of breather solutions of a semilinear wave equation with a periodically extended delta potential.

The spectral picture necessary for the construction of breather solutions appears on the necklace graph in a natural way. For a detailed spectral analysis for general necklace graphs we refer to [MV05, KL07]. The major difficulty will occur from the irregularity of the solutions caused by the imposed Kirchhoff boundary conditions, which lead to jumps of the first derivatives. As a consequence, the flow on the center manifold for the spatial dynamics formulation is no longer continuous as in [BCBLS11] with respect to the spatial evolution variable x .

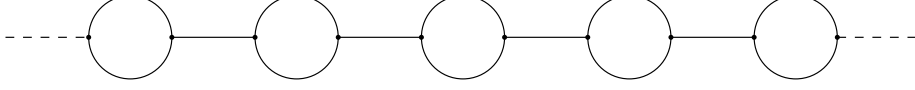


Figure 2.1.1: The necklace graph is of the form $\Gamma = \bigoplus_{n \in \mathbb{Z}} \Gamma_n$ with $\Gamma_n = \Gamma_n^0 \oplus \Gamma_n^+ \oplus \Gamma_n^-$, where the Γ_n^0 are the horizontal links between the circles and the Γ_n^\pm the upper and lower semicircles. The part Γ_n^0 is isometrically identified with the interval $I_n^0 = [nP, nP + L]$ and the Γ_n^\pm with the intervals $I_n^\pm = [nP + L, (n + 1)P]$. The horizontal links are of lengths $L > 0$, whereas the semicircles have length π . Hence, the periodicity of the graph is $P = L + \pi$. For a function $u : \Gamma \rightarrow \mathbb{C}$, we denote the part on the interval I_n^0 with u_n^0 and the parts on the intervals I_n^\pm with u_n^\pm .

2.1.1 Statement of the problem

We consider a cubic, nonlinear Klein-Gordon equation

$$\partial_t^2 u(t, x) = \partial_x^2 u(t, x) - (\alpha + \varepsilon^2)u(t, x) + u(t, x)^3, \quad t \in \mathbb{R}, x \in \text{int } \Gamma, \quad (2.1)$$

with a real-valued constant α and sufficiently small $\varepsilon > 0$ on the periodic necklace graph Γ from Figure 2.1.1. Note that this equation does not possess breather solutions if posed on the real line. Throughout this section we impose Kirchhoff boundary conditions at the vertex points $\{nP\}_{n \in \mathbb{Z}}$ and $\{nP + L\}_{n \in \mathbb{Z}}$, which consist of the continuity condition at the vertex points

$$\begin{aligned} u_n^0(nP + L) &= u_n^\pm(nP + L), \quad n \in \mathbb{Z}, \\ u_{n+1}^0((n + 1)P) &= u_n^\pm((n + 1)P), \quad n \in \mathbb{Z}, \end{aligned}$$

and the conservation of the fluxes

$$\begin{aligned} \partial_x u_n^0(nP + L) &= \partial_x u_n^+(nP + L) + \partial_x u_n^-(nP + L), \quad n \in \mathbb{Z}, \\ \partial_x u_{n+1}^0((n + 1)P) &= \partial_x u_n^+((n + 1)P) + \partial_x u_n^-((n + 1)P), \quad n \in \mathbb{Z}, \end{aligned}$$

cf. Figure 2.1.1.

Remark 2.1.1. *It turns out that time-periodic, spatially localized solutions can be constructed within the invariant subspace of functions that are symmetric with respect to the semicircles. In this subspace, the necklace graph Γ can be identified with the real line equipped with jump conditions of the first derivatives.*

2.1.2 Statement of the main theorem

Theorem 2.1.2. *Let $L \in \{l\pi, l \in \mathbb{N}_{\text{odd}}\}$ be the length of the horizontal links. For an odd integer k and a sufficiently small $\varepsilon > 0$ the nonlinear, cubic Klein-Gordon equation*

$$\partial_t^2 u(t, x) = \partial_x^2 u(t, x) - \left(\frac{k^2}{4} + \varepsilon^2 \right) u(t, x) + u(t, x)^3, \quad t \in \mathbb{R}, x \in \text{int}\Gamma, \quad (2.2)$$

with Kirchhoff boundary conditions at the vertices possesses breather solutions of amplitude $\mathcal{O}(\varepsilon)$ and frequency $\omega = k/2$. These solutions are symmetric in the upper and lower semicircles. Precisely, there exist functions $u : \mathbb{R} \times \mathbb{R} \rightarrow \mathbb{R}$ satisfying

- $u(t, x) = u(t + \frac{2\pi}{\omega}, x)$ for all $t, x \in \mathbb{R}$,
- $\lim_{|x| \rightarrow \infty} u(t, x)e^{\beta|x|} = 0$ for all $t \in \mathbb{R}$ and a constant $\beta > 0$.

Remark 2.1.3. *The major challenge is the irregularity of the solutions due to Kirchhoff boundary conditions $(u^0)'(v) = 2(u^+)'(v)$ at the vertex points v , which leads to a non-autonomous system and makes it necessary to modify the persistence proof of the approximately constructed pulse under higher order perturbations. In contrast to the previous work [BCBLS11], the first derivative has jumps. As a consequence the flow on the center manifold is no longer continuous at the vertex points. Therefore, we use a discrete center manifold reduction of the time- P -mappings.*

Remark 2.1.4. *In particular, we construct four breathers up to discrete translational invariance. They arise from homoclinics on the center manifold that are purely positive, respectively purely negative and obey symmetries about the midpoint of horizontal link, respectively the midpoint of the semicircle, cf. Figure 2.1.2.*

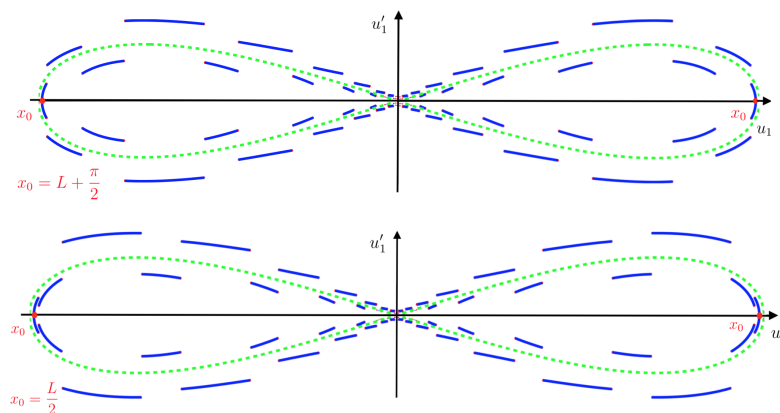


Figure 2.1.2: Phase portraits of the four homoclinic orbits of the reduced system on the center manifold with symmetry about the midpoint $x_0 = L + \frac{\pi}{2}$ in the upper panel and with symmetry about the midpoint $x_0 = \frac{L}{2}$ in the lower panel.

Remark 2.1.5. *In principle, our method of proof allows to treat any odd nonlinearities, i.e.*

$$N(u) = u^p, \quad p \in \mathbb{N}_{\text{odd}}.$$

2.1.3 Outline of the proof

Using a Fourier series expansion with respect to time

$$u(t, x) = \sum_m u_m(x) e^{im\omega t},$$

the evolutionary problem (2.1) transforms into countably many coupled second order ordinary differential equations for the Fourier coefficients

$$-m^2\omega^2 u_m(x) = \partial_x^2 u_m(x) - (\alpha + \varepsilon^2)u_m(x) + (u * u * u)_m(x), \quad x \in \mathbb{R}, \quad (2.3)$$

where $m \in \mathbb{N}_{\text{odd}}$ and new dynamic variable x , the so called spatial dynamics formulation. The cubic nonlinearity transforms into a discrete convolution. Since

we are interested in spatially localized solutions, i.e.

$$\lim_{|x| \rightarrow \infty} u(t, x) = 0, \quad t \in \mathbb{R},$$

we construct a homoclinic orbit to zero in the phase space of this infinite dimensional system (2.3). The key idea is to perform a center manifold reduction in order to reduce (2.3) to a finite dimensional system. However, because of the Kirchhoff boundary conditions, the system is non-autonomous and the first derivatives of the solutions have jumps and the flow on the center manifold is no longer continuous. Therefore, we apply a discrete version of the center manifold theorem to the family of time- P -maps.

We explain the core of our argument, which makes use of Floquet-Bloch theory. Linearizing (2.3) at the origin leads to the (decoupled) spectral problems

$$-\partial_x^2 u_m(x) = (m^2 \omega^2 - \alpha) u_m(x) = \lambda_m u_m(x), \quad x \in \text{int } \Gamma, \quad m \in \mathbb{N}_{\text{odd}}, \quad (2.4)$$

with Kirchhoff boundary conditions at the vertex points. Let $M(\lambda_m)$ denote the monodromy matrix of (2.4), which is the canonical fundamental matrix evaluated after one period of the system and conjugated to the linearization of the time- P -maps at the origin. A complex number λ_m lies in the spectrum of the negative Laplacian on the necklace graph if and only if the eigenvalues of $M(\lambda_m)$ (Floquet multipliers) lie on the complex unit circle. Further, the number of Floquet multipliers on the complex unit circle determines the dimension of the center manifold. Thus, we shall choose the constants ω and α such that λ_1 corresponds to the spectrum of the negative Laplacian, whereas the positive numbers λ_m for $3 \leq m \in \mathbb{N}_{\text{odd}}$ fall into spectral gaps of the negative Laplacian. This is possible, since the spectral gaps open linearly. Hence, the infinite dimensional spatial dynamics system (2.3) can then be reduced to a two-dimensional real system on the center manifold. To summarize, our method of construction heavily relies on the spectral properties of the linear system, which allows us to choose a frequency in the spectrum, whose harmonics fall into spectral gaps.

In fact, the lowest order approximation of the dynamics on the discrete center

manifold can be described via a single ordinary differential equation

$$\partial_x^2 u_c(x) = \varepsilon^2 u_c(x) - u_c^3(x), \quad x \in \text{int } \Gamma, \quad (2.5)$$

with imposed Kirchhoff boundary conditions on the graph. The existence of pulse solutions for (2.5) has been established in [PS17] via a detailed analysis of the stable and unstable manifold of the time- P -mapping. In order to show persistence of these homoclinic orbits under higher order perturbations, we use reversibility and symmetry arguments.

The chapter is organized as follows. In Section 2.2 we introduce the spatial dynamics formulation and its symmetries. The family of time- P -mappings is investigated in Section 2.3. Section 2.4 is dedicated to the linear spectral analysis on the periodic metric graph Γ . Moreover, we explain how to choose an appropriate breather frequency and apply a discrete version of the center manifold theorem to the family of time- P -mappings. In Section 2.5 we relate these abstract center manifold constructions to a nonlinear cubic ordinary differential equation and show that the homoclinic orbits persist under higher order perturbations. Section 2.6 contains a short discussion about the situation when arbitrary horizontal lengths of the necklace graph are allowed. Finally, we have an appendix in Section 2.7, which contains short summaries of Floquet-Bloch theory and discrete center manifold reductions.

2.2 Spatial dynamics formulation

The central purpose of this chapter is to find time-periodic, spatially localized solutions of the nonlinear Klein-Gordon equation

$$\partial_t^2 u(t, x) = \partial_x^2 u(t, x) - (\alpha + \varepsilon^2)u(t, x) + u(t, x)^3, \quad t \in \mathbb{R}, x \in \text{int } \Gamma, \quad (2.6)$$

with a real-valued constant α and

$$u(t) \in D(\partial_x^2|_\Gamma) = \{C^0(\Gamma) \cap H^2(\text{int } \Gamma) : \text{satisfying Kirchhoff b.c. at } \partial\Gamma\}.$$

The Laplacian with domain $D(\partial_x^2|_\Gamma)$ is self-adjoint, cf. [BK13]. Breather solutions can be constructed within the invariant subspace of symmetric functions with respect to the semi-circles. In this case, equation (2.6) can be considered as a Klein-Gordon equation on the real line equipped with a very singular periodic potential. The proof is based on spatial dynamics w.r.t. the spatial variable x . Searching for $\frac{2\pi}{\omega}$ -periodic solutions

$$u(t, x) = u\left(t + \frac{2\pi}{\omega}, x\right), \quad t, x \in \mathbb{R},$$

Fourier series expansion leads to

$$u(t, x) = \sum_{m \in \mathbb{Z}} u_m(x) e^{im\omega t}. \quad (2.7)$$

The real-valued constant ω has to be chosen suitably later on, such that the linearization possesses two Floquet exponents on the complex unit circle, whereas the others are bounded away from the unit circle. As a consequence, there will be a two-dimensional center manifold. The evolutionary problem (2.6) transforms into countably many coupled second order ordinary differential equations

$$-m^2\omega^2 u_m(x) = \partial_x^2 u_m(x) - (\alpha + \varepsilon^2)u_m(x) + (u * u * u)_m(x), \quad m \in \mathbb{Z}, \quad (2.8)$$

where the cubic nonlinearity is given by the discrete convolution

$$((u * u * u)_m)_{m \in \mathbb{Z}} = \left(\sum_{n_1, n_2 \in \mathbb{Z}} u_{m-n_1} u_{n_1-n_2} u_{n_2} \right)_{m \in \mathbb{Z}}.$$

The dimension of the problem can be reduced by considering symmetries of the problem. Real-valued solutions satisfy $u_m = \overline{u_{-m}}$, $m \in \mathbb{Z}$. Moreover, the system is invariant under the transform $(t, u, u') \mapsto (-t, -u, -u')$, which leads to the condition $u_m = -u_{-m}$, $m \in \mathbb{Z}$. As an immediate consequence of the cubic nonlinearity, the space of solutions with $u_{2m} = 0$, $m \in \mathbb{Z}$, is an invariant subspace. These conditions particularly lead to $\text{Re}(u_m) = 0$, $m \in \mathbb{Z}$. We prefer to replace u_m by iu_m , where iu_m satisfies the same equation with an opposite sign in front of the nonlinearity. To conclude, we consider solutions in the

invariant subspace

$$\hat{X} = \{(u_m)_{m \in \mathbb{Z}} \mid u_m \in \mathbb{R}, u_{2m} = 0, u_m = u_{-m}, m \in \mathbb{Z}\} \quad (2.9)$$

of the system

$$-m^2 \omega^2 u_m(x) = \partial_x^2 u_m(x) - (\alpha + \varepsilon^2) u_m(x) - (u * u * u)_m(x), \quad (2.10)$$

for $m \in \mathbb{Z}_{\text{odd}}$ with Kirchhoff boundary conditions at the vertex points.

2.3 Time- P -maps

A canonical first order reduction of system (2.10) leads to

$$\partial_x \begin{pmatrix} u_m \\ u'_m \end{pmatrix} = \begin{pmatrix} 0 & 1 \\ -m^2 \omega^2 + \alpha & 0 \end{pmatrix} \begin{pmatrix} u_m \\ u'_m \end{pmatrix} + \begin{pmatrix} 0 \\ \varepsilon^2 u_m + (u * u * u)_m \end{pmatrix}, \quad (2.11)$$

with $m \in \mathbb{Z}_{\text{odd}}$ and Kirchhoff boundary conditions at the vertex points. Interpreting the bifurcation parameter ε as an independent variable, we treat the terms $\varepsilon^2 u_m$ in (2.11) as nonlinear and use the notation

$$\partial_x v_m = \Lambda_m v_m + N_m(\varepsilon, v), \quad m \in \mathbb{Z}_{\text{odd}}. \quad (2.12)$$

Denote by

$$v_{n,m}(\check{x}) = \begin{pmatrix} u_m(\check{x} + nP; \check{x}, \check{v}) \\ u'_m{}^+(\check{x} + nP; \check{x}, \check{v}) \end{pmatrix}, \quad \check{x} \in [0, P), \quad n \in \mathbb{Z}, \quad (2.13)$$

a solution v_m with initial conditions $v(\check{x}) = \check{v}$ given at \check{x} . With a little abuse of notation, we use the index m to label the system of ODEs and the index n for the spatial discretization. We use right-hand sided derivatives at $\check{x} \in \{0, L\}$, since the Kirchhoff boundary conditions lead to jumps of the first derivative at the vertex points. Now, the action of the time- P -mappings associated to (2.12)

can be written as

$$T^P v_{n,m}(\check{x}) := v_{n+1,m}(\check{x}), \quad n \in \mathbb{Z}, m \in \mathbb{Z}_{\text{odd}}. \quad (2.14)$$

(The notation time- P -mapping is chosen, since the spatial variable \check{x} is the new dynamic variable.) The standard uniqueness theorem for second order ordinary differential equations with non-vanishing coefficient at the second derivative claims that if a solution and its derivative vanish at a point, it is identically zero. Therefore, the vector $v_{n,m}$ is well-defined on the invariant subspace of symmetric functions. The linearizations at the origin of the associated discrete dynamical systems (2.12) are decoupled and the time- P -map of the linearization is given by monodromy matrices $M_{\check{x}}(m^2\omega^2 - \alpha)$. These matrices coincide with the canonical fundamental matrix of the linearization of (2.12) evaluated after one period of the problem and are conjugated to each other for any $\check{x} \in [0, P)$, cf. 2.7.1. For example, we explicitly compute for $\check{x} = 0$ that

$$M_0(m^2\omega^2 - \alpha) = \begin{pmatrix} 1 & 0 \\ 0 & 2 \end{pmatrix} e^{\Lambda_m \pi} \begin{pmatrix} 1 & 0 \\ 0 & \frac{1}{2} \end{pmatrix} e^{\Lambda_m L}. \quad (2.15)$$

In particular, we get

$$v_{n+1} = \Lambda_{\check{x}} v_n + \check{N}(\check{x}, \varepsilon, v_n), \quad n \in \mathbb{Z}, \quad (2.16)$$

with a linear operator $\Lambda_{\check{x}} = \text{diag}(M_{\check{x}}(m^2\omega^2 - \alpha))_{m \in \mathbb{Z}_{\text{odd}}}$ and a nonlinear map $\check{N}(\check{x}, \varepsilon, v)$. Since the matrices $M_{\check{x}}(m^2\omega^2 - \alpha)$ are conjugated to each other, the eigenvalues of $\Lambda_{\check{x}}$ do not depend on \check{x} . Our objective is to apply a discrete center manifold reduction to system (2.16), cf. 2.7.2.

2.4 Spectral situation and center manifold reduction

The discrete center manifold Theorem 2.7.5 states that the dimension of the center manifold is equal to the dimension of the spectral subspace corresponding to all eigenvalues lying in the unit circle. The essential hypothesis 2.7.4 is the

spectral separation of Λ , which requires a spectral gap around the unit circle. Motivated by the important relation for the monodromy matrices, cf. 2.7.1,

$$\boxed{|\operatorname{tr}(M(\lambda))| \leq 2 \quad \Leftrightarrow \quad \begin{array}{l} \text{two eigenvalues (Floquet multipliers) on} \\ \text{the complex unit circle,} \end{array}}$$

we adjust the parameters ω and α in (2.10), such that $|\operatorname{tr}(M(\omega^2 - \alpha))| \leq 2$ and $|\operatorname{tr}(M(m^2\omega^2 - \alpha))| > 2$ for any odd number $m \geq 3$. Since the Fourier coefficients u_1 and u_{-1} are related via $u_{-1} = \overline{u_1}$ in the invariant subspace \hat{X} defined in (2.9), two Floquet multipliers will appear on the unit circle. This leads to a two-dimensional center manifold, cf. our considerations in Subsections 2.4.1 and 2.4.2.

Remark 2.4.1. *A detailed analysis of the spectrum of the Laplacian on the necklace graph is given in [MV05]. In contrast to periodic self-adjoint elliptic second order differential operator on the real line, we have a non-empty point spectrum on necklace graphs. The eigenfunctions on the necklace graph are given by simple loop states, which are anti-symmetric with respect to the semicircles and vanish at the horizontal links, cf. [BK13, GPS16]. Since we search for breathers within the invariant subspace of symmetric functions with respect to the semicircles, this remark just provides additional information.*

2.4.1 Trace of monodromy matrix and choice of breather frequency

The monodromy matrices with varying evaluation points $\tilde{x} \in [0, P)$ are conjugated to each other. Thus, their eigenvalues are independent of the evaluation points and so is $\operatorname{tr}(M_{\tilde{x}}) = \operatorname{tr}(M)$ and $\det(M_{\tilde{x}}) = \det(M)$. Therefore, we omit the index \tilde{x} . An explicit evaluation of the exponential function in (2.15) leads to the formula

$$\operatorname{tr}M(\lambda_m) = \frac{1}{4} \left(9 \cos((L + \pi)\sqrt{\lambda_m}) - \cos((L - \pi)\sqrt{\lambda_m}) \right), \quad (2.17)$$

with $\lambda_m = m^2\omega^2 - \alpha$, cf. Figure 2.4.1. The mapping $\sqrt{\lambda} \mapsto \operatorname{tr}M(\lambda)$ is 1-periodic for $L \in \{l\pi, l \in \mathbb{N}_{\text{odd}}\}$. One of the major tasks is to find an appropriate frequency ω_0 and a constant α , such that the operator $\Lambda = \operatorname{diag}(M(m^2\omega_0^2 -$

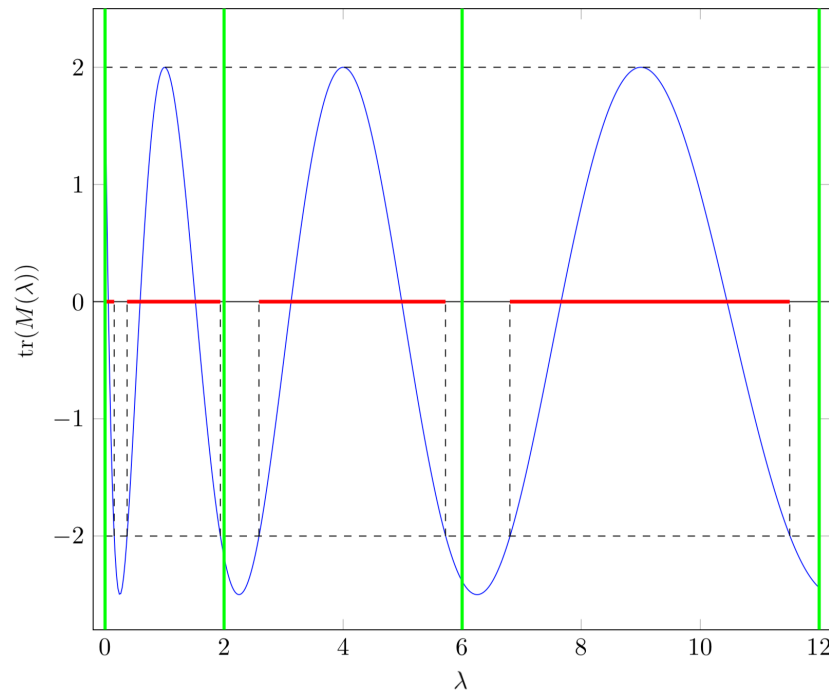


Figure 2.4.1: Trace of the monodromy matrix for $L = \pi$. The red lines show the spectrum of the Laplacian. The areas satisfying $|\text{tr}M(\lambda)| > 2$ lead to spectral gaps of the Laplacian on the graph. The points $\{(m^2 - 1)\lambda : 3 \leq m \in \mathbb{N}_{\text{odd}}\}$ (green lines) fall into spectral gaps.

$\alpha))_{m \in \mathbb{Z}_{\text{odd}}}$ has the property of spectral separation with precisely two Floquet multipliers, which coincide, lying on the unit circle, cf. Figure 2.4.2.

Choice of ω . Choosing $\omega_0^2 = k/2$, $k \in \mathbb{N}_{\text{odd}}$ equal to an odd multiple of one half period, we compute

$$\text{tr}M(m^2\omega_0^2) = \begin{cases} -5/2, & \text{for } |m| \in \mathbb{N}_{\text{odd}}, \\ 2, & \text{for } |m| \in \mathbb{N}_{\text{even}}. \end{cases} \quad (2.18)$$

The fact that there are infinitely many Floquet multipliers on the unit circle prevents at a first view the application of the discrete center manifold theorem. However, we only need to look for integers $m \in \mathbb{Z}_{\text{odd}}$, because we consider solutions within the invariant subspace \hat{X} defined in (2.9). (Essential for the symmetries of \hat{X} was the odd power of the nonlinearity.)

Choice of α . Varying the parameter α , we can achieve that $|\text{tr}M(\omega_0^2 - \alpha)| = 2$, whereas $|\text{tr}M(m^2\omega_0^2 - \alpha)| > 2$ for all $|m| \geq 3$. In particular, we choose $\alpha = \omega_0^2$, which implies $|\text{tr}M(\omega_0^2 - \alpha)| = |\text{tr}M(0)| = 2$. Since the impact of α becomes smaller with increasing m , we find $\text{tr}M(m^2\omega_0^2 - \alpha) \rightarrow -5/2$ as $\mathbb{N}_{\text{odd}} \ni |m| \rightarrow \infty$. As a consequence, we have two Floquet multipliers on the unit circle, which collide at -1 , cf. Figure 2.4.2. Small perturbations of $\omega_0 = k/2$ where $k \in \mathbb{N}_{\text{odd}}$, will destroy these properties.

2.4.2 Discrete center manifold reduction

The purpose of this subsection is to apply the discrete center manifold Theorem 2.7.5 to the family of time- P -mappings introduced in Subsection 2.3. We chose ω_0 and α in Subsection 2.4.1 such that linear operator $\Lambda = (M(m^2\omega_0^2 - \alpha))_{m \in \mathbb{Z}_{\text{odd}}}$ has the property of spectral separation. In what follows, we use weighted sequence spaces defined by their norms

$$\|u\|_{l_s^2}^2 := \sum_{m \in \mathbb{Z}} (1 + m^2)^s |u_m|^2.$$

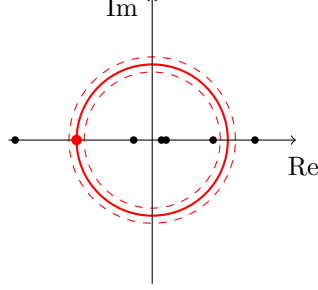


Figure 2.4.2: We adjust the breather frequency such that there are two Floquet multipliers on the unit circle, which collide at -1 , and the others are bounded uniformly away.

The linear operator Λ maps $\ell_2^2(\mathbb{Z}, \mathbb{R}^2)$ into $\ell^2(\mathbb{Z}, \mathbb{R}^2)$ and Young's inequality implies

$$\|u * u * u\|_{\ell_2^2} \leq C \|u\|_{\ell_2^2}^3.$$

The nonlinearity satisfies $\check{N}(\check{x}, \cdot, \cdot) \in C^\infty(U \times V, \ell_2^2(\mathbb{Z}, \mathbb{R}^2))$ for a neighborhood $U \times V$ of 0 in $\mathbb{R} \times \ell_2^2(\mathbb{Z}, \mathbb{R}^2)$ and

$$\check{N}(\check{x}, 0, 0) = 0, \quad \partial_3 \check{N}(\check{x}, 0, 0) = 0.$$

Therefore, the requirements of Theorem 2.7.5 are satisfied. Hence, the discrete center manifold Theorem 2.7.5 shows the existence of an invariant center manifold M_ε . Let Π_c , respectively Π_h , denote the projections on the center and the hyperbolic subspace of the time- P -mapping T^P . We obtain

$$\Pi_c v_n = (v_{n,1}, v_{n,-1}), \quad \Pi_h v_n = (v_{n,3}, v_{n,-3}, v_{n,5}, v_{n,-5}, \dots). \quad (2.19)$$

Moreover, there exists a reduction function $\Phi_{\check{x}, \varepsilon}$ for $\varepsilon \in (-\varepsilon_0, \varepsilon_0)$ and $\varepsilon_0 > 0$ sufficiently small, with the following property

$$\Pi_h v_n = \Phi_{\check{x}, \varepsilon}(\Pi_c v_n). \quad (2.20)$$

Since the nonlinearity does not possess quadratic terms, we deduce $\Pi_h v_n = \mathcal{O}((\Pi_c v_n)^3)$. Thus, we can reduce the local study of (2.16) to the dynamics of $\Pi_c v_n$ on the center manifold. Further, we remind of the symmetry restrictions in Subsection 2.2,

$$v_{n,-m} = v_{n,m}. \quad (2.21)$$

This leads to the family of two-dimensional reduced discrete systems

$$v_{n+1,1} = M_{\check{x}}(0)v_{n,1} + (\check{N}_1)_{\check{x}}(v_{n,1}, \Phi_{\check{x},\varepsilon}(v_{n,1})), \quad (2.22)$$

with $\check{x} \in [0, P)$.

2.5 Analysis of the reduced system

2.5.1 Relating the reduced discrete systems to an ordinary differential equation

In order to analyze the reduced system (2.22) on the center manifold we relate the abstract center manifold construction to an ordinary differential equation. Let

$$v_{c,n} = \Pi_c v_n.$$

From the P -periodicity of the system we deduce

$$v(\check{x} + (n+1)P; \check{x}, \check{v}) = v(\check{x} + P; \check{x}, v(\check{x} + nP; \check{x}, \check{v})). \quad (2.23)$$

This leads to

$$v_{c,n+1} = v_c(\check{x} + (n+1)P; \check{x}, \check{v}) = v_c(\check{x} + P; \check{x}, v(\check{x} + nP; \check{x}, \check{v})). \quad (2.24)$$

The projections Π_c and Π_h provide a decomposition of the Hilbert space $H = \ell^2$ into two invariant subspaces H_c and H_h and Theorem 2.7.5 guarantees the existence of a reduction function $\Phi_{\check{x},\varepsilon}$. Since the nonlinearity does not possess

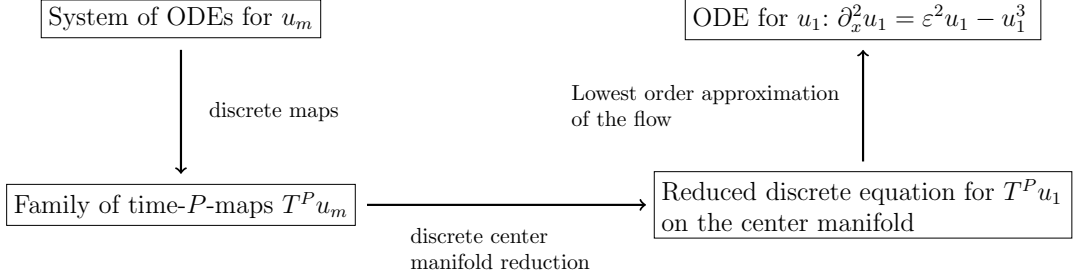


Figure 2.5.1: Schematic representation

quadratic terms, we deduce $v_h = \Phi_{\check{x}, \varepsilon}(v_c) = \mathcal{O}(v_c^3)$. Thus, we derive

$$v = (\Pi_c v) \oplus (\Pi_h v) = v_c \oplus \Phi_{\check{x}, \varepsilon}(v_c) = v_c \oplus \mathcal{O}(v_c^3). \quad (2.25)$$

Inserting this relation leads to

$$\begin{aligned} v_{c, n+1} &= v_c(\check{x} + P; \check{x}, v(\check{x} + nP; \check{x}, \check{v})) \\ &= v_c(\check{x} + P; \check{x}, v_c(\check{x} + nP; \check{x}, \check{v}) \oplus \Phi_{\check{x}, \varepsilon}(v_c(\check{x} + nP; \check{x}, \check{v}))) \\ &= v_c(\check{x} + P; \check{x}, v_c(\check{x} + nP; \check{x}, \check{v}) \oplus 0) + \mathcal{O}(v_c^5) \\ &= v_c(\check{x} + P; \check{x}, v_{c, n} \oplus 0) + \mathcal{O}(v_c^5). \end{aligned} \quad (2.26)$$

Hence, in order to compute the flow on the center manifold up to $\mathcal{O}(v_c^3)$, it is sufficient to consider the discrete flow for v_c on the center manifold with $v_h = 0$. However, this discrete flow for any \check{x} can be obtained by solving the ordinary differential equation for u_1 with $u_m = 0$ for all $|m| \geq 3$ and neglecting all terms of order $\mathcal{O}(u_1^4)$ and higher. Hence, the cubic equation

$$\partial_x^2 u_1(x) = \varepsilon^2 u_1(x) - u_1^3(x), \quad (2.27)$$

for $\varepsilon \in (0, \varepsilon_0)$ will appear as the lowest order approximation of the dynamics on the center manifold.

2.5.2 Existence of homoclinic orbits to zero of the lowest order approximation on the center manifold

The differential equation which arises as lowest order approximation of the dynamics on the center manifold had been studied in [PS17]. The existence of homoclinics to the origin is proved via a detailed analysis of the stable and unstable manifold of the time- P mapping in [PS17] Theorem 1.1, which we revise below.

Theorem 2.5.1. *There are positive constants ε_0 and C_0 , such that for every $\varepsilon \in (0, \varepsilon_0)$, the equation*

$$\partial_x^2 u = \varepsilon^2 u - u^3$$

admits four non-trivial bound states $u_{hom} \in D(\partial_x^2|_\Gamma)$ (up to discrete translational invariance) such that

$$\|u_{hom}\|_{H^2(\Gamma)} \leq C_0 \varepsilon, \tag{2.28}$$

where $H^2(\Gamma)$ denotes the Sobolev space on the graph Γ . Two bound states satisfy

$$u_{hom,1}\left(x - \frac{L}{2}\right) = u_{hom,1}\left(\frac{L}{2} - x\right) \text{ for all } x \in \Gamma, \tag{2.29}$$

and the other satisfy

$$u_{hom,2}\left(x - \left(L + \frac{\pi}{2}\right)\right) = u_{hom,2}\left(L + \frac{\pi}{2} - x\right) \text{ for all } x \in \Gamma, \tag{2.30}$$

where L is the length of the horizontal link and π the length of the upper and lower semicircle. In each case, there exist strictly positive and strictly negative solutions, i.e. $u_{hom,i}^+(x) > 0$ and $u_{hom,i}^-(x) < 0$ for $i = 1, 2$ and every $x \in \Gamma$. Moreover, the bound states obey the properties

- i) u_{hom} is symmetric in the upper and lower semicircles,*
- ii) $u_{hom}(x) \rightarrow 0$ as $|x| \rightarrow \infty$ exponentially fast.*

It remains to prove persistence of these homoclinic solutions under higher order perturbations, what we will show in Subsection 2.5.3.

2.5.3 Persistence of the homoclinic orbits under higher order perturbations

The homoclinic orbit lies in the intersection of the stable and the unstable manifold. In general this intersection will break up, if higher order terms are added. However, the situation is different in reversible systems. By proving a transversal intersection of the stable manifold with the fixed space of reversibility in x_0 , we can construct the homoclinic solutions by reflecting the semi-orbit for $x \in (-\infty, x_0]$ at the u_1 -axis.

We rescale the ODE on the center manifold (2.27) and obtain

$$\partial_X^2 v_1 - v_1 + v_1^3 + \mathcal{O}(\varepsilon^2 v_1^5) = 0. \quad (2.31)$$

As a consequence of these rescaling the new jump points are εnP and $\varepsilon(nP + L)$, where $n \in \mathbb{Z}$.

Reversibility: The spatial dynamics system (2.10) is reversible with respect to the symmetries

$$R : (X_{i,\varepsilon} + X, v) \mapsto (X_{i,\varepsilon} - X, v), \quad \text{for } i = 1, 2, \quad (2.32)$$

where $X_{1,\varepsilon} = \frac{\varepsilon L}{2}$ and $X_{2,\varepsilon} = \varepsilon(L + \frac{\pi}{2})$, i.e., if $v(X)$ is a solution, then $Rv(-X)$ is also a solution. This is due the periodic structure of the graph and standard ordinary differential equation theory. The corresponding time- P -maps admit a cut-off preserving reversibility, because they are derived from an even order explicit recurrence relation. According to Theorem 2.7.6 cited from [Jam03], the reduced system on the center manifold is also invariant under the mapping (2.32).

Transversal intersection: The homoclinic orbits are symmetric about the points $X_{i,\varepsilon}$, $i = 1, 2$, i.e.,

$$v_{hom,i}(X - X_{i,\varepsilon}) = v_{hom,i}(X_{i,\varepsilon} - X) \text{ for } i = 1, 2 \text{ and all } X \in \mathbb{R}, \quad (2.33)$$

cf. Theorem 2.5.1. Note that the points $X_{i,\varepsilon}$ are no jump points. Since the reduced equation on the center manifold (2.27) involves only second-order derivatives, existence and uniqueness theory for differential equations implies that the symmetries (2.33) are satisfied if and only if

$$\partial_X v_{hom,i}(X_{i,\varepsilon}) = 0.$$

As a consequence, the homoclinic orbits intersect the v -axis transversally in the (v, v') -plane in the sense of smooth manifolds. It remains to show that these transversal intersections remain for $X_{i,\varepsilon}$, if perturbations of order ε^2 coming from the $\mathcal{O}(v_1^5)$ -terms are added.

The constructed manifolds in Section 2.4.2 are piecewise smooth w.r.t. \check{X} with jumps at the vertex points. Thus, we have two periodically arranged smooth families of manifolds in the extended phase space $(\check{X}, v, v') \in \mathbb{R} \times \mathbb{R}^2$. Since the points $X_{i,\varepsilon}$ are far away from the vertex points, the discrete time- P -mappings will not jump from one family of manifolds to the other. The smooth parts of length $\varepsilon\pi$, respectively εL , are of order ε in the (v, v') -plane in the unperturbed system, cf. the asymptotic expansions in [PS17]. Adding the perturbation, their lengths are stretched or compressed by a factor of order ε^2 . Since the (unperturbed) homoclinics are reversible, these modifications are symmetric w.r.t. the v_1 -axis, cf. Figure 2.5.2. Therefore, the perturbation of order $\mathcal{O}(\varepsilon^2)$ will only lead to an $\mathcal{O}(\varepsilon^2)$ change of the homoclinic solutions.

Hence, the reduced system is invariant under $(X, v_1, v'_1) \mapsto (-X, v_1, -v'_1)$, i.e., the phase portrait is reflection symmetric at the v_1 -axis. In presence of the higher order perturbations, the homoclinic solutions can be constructed by reflecting the semi-orbits for $X \in (-\infty, X_{i,\varepsilon}]$ at the v_1 -axis.

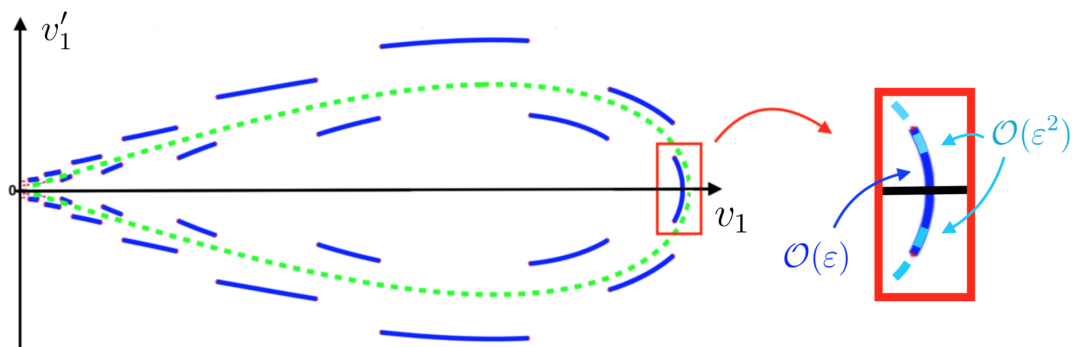


Figure 2.5.2: Left side: The blue sections correspond to the homoclinic on the graph with symmetry (2.30). The green dashed line shows the solitary wave solution on the real line. Right side: The perturbation of order ε^2 will not destroy the transversal intersection of the v_1 -axis.

Corollary 2.5.2. *There exist four homoclinic orbits to the origin in the phase space on the center manifold, cf. Figure fourhomo.*

These homoclinic solutions of the spatial dynamics formulation (2.8) in the phase space correspond to breather solutions in the original system (2.6).

2.6 Discussion

Our previous arguments heavily rely on the fact that the trace of the monodromy matrix is periodic. For general lengths $L \neq \pi$ this trace can be written as sum of cosine-terms, one of period $2\pi/(L + \pi)$ and the other one of period $2\pi/(L - \pi)$, cf. equation (2.17). The sum of two periodic functions is periodic if and only if the ratio of the two periodicity constants is a rational number. Therefore, the trace is periodic if and only if

$$\frac{2\pi}{L + \pi} / \frac{2\pi}{L - \pi} = \frac{L - \pi}{L + \pi} \in \mathbb{Q},$$

which is the case for $L = l\pi$, $l \in \mathbb{Q}$. This means that the spectral picture necessary for our construction will not appear for horizontal links of length $L = l\pi$, $l \notin \mathbb{Q}$. Additionally, in [FW98], they give reasons, why breathers will disappear if the harmonics of the breather frequency are not located in spectral

gaps. To summarize this discussion, our method of construction of breather solutions will definitely not work for horizontal links of length $L = l\pi$, $l \notin \mathbb{Q}$.

Remark 2.6.1. *Since we do not expect breather solutions if the ratio of the lengths is irrational, we predict that breather solutions will not persist under perturbations of the lengths.*

2.7 Appendices

2.7.1 Floquet-Bloch theory

To investigate the spectral problem

$$-\partial_x^2 u = \lambda u, \quad x \in \text{int } \Gamma, \quad (2.34)$$

with constants $\lambda \in \mathbb{R}$ and Kirchhoff boundary conditions at the vertex points, we use tools from Floquet-Bloch theory, cf. [RS79, Eas75, BK13]. Let u_1 be the solution of (2.34) with $u_1(0) = 1$ and $u_1^+(0) = 0$ and let u_2 be the solution with $u_2(0) = 0$ and $u_2^+(0) = 1$, where the index $+$ denotes the right-hand sided derivative. Consider the 2×2 matrix

$$M_0(\lambda) = \begin{pmatrix} u_1(P) & u_2(P) \\ u_1^+(P) & u_2^+(P) \end{pmatrix}, \quad (2.35)$$

which is a natural object, for if v is a solution of (2.34), then

$$\begin{pmatrix} v(P) \\ v^+(P) \end{pmatrix} = M_0(\lambda) \begin{pmatrix} v(0) \\ v^+(0) \end{pmatrix}. \quad (2.36)$$

This means that the monodromy matrix $M_0(\lambda)$ is the fundamental matrix of the system of ordinary differential equations evaluated at the period of the system.

Remark 2.7.1. *The monodromy matrices with varying evaluation points $\tilde{x} \in [0, P)$ are conjugated to each other. Thus, their eigenvalues are independent of the evaluation points and so is $\text{tr}(M_{\tilde{x}}) = \text{tr}(M)$ and $\det(M_{\tilde{x}}) = \det(M)$.*

Theorem 2.7.2 (Floquet's Theorem). *There are linearly independent solutions ψ_1, ψ_2 , such that either*

i) $\psi_1(x) = e^{m_1 x} p_1(x)$ and $\psi_2(x) = e^{m_2 x} p_2(x)$, or

ii) $\psi_1(x) = e^{m x} p_1(x)$ and $\psi_2(x) = e^{m x} (x p_1(x) + p_2(x))$,

with constants $m_1, m_2, m \in \mathbb{C}$ and P -periodic functions p_1, p_2 .

In other words, Floquet's theorem shows that the fundamental matrix $\Phi(x)$ with $\Phi(0) = I$ can be written as

$$\Phi(x) = Q(x)e^{xN},$$

with $Q(x + P) = Q(x)$ and a matrix N independent of x , which is similar to a diagonal matrix in case i) and has a Jordanblock in case ii). We want to emphasize the simple connection $M = e^{PN}$ between the monodromy matrix M defined in (2.35) and the matrix N . Therefore, we deduce

$$\mu_i = e^{m_i P},$$

where m_i are the constants of Theorem 2.7.2 and μ_i denotes the eigenvalues of the monodromy matrix. The monodromy matrix is known to have determinant 1, which implies that its eigenvalues are μ and μ^{-1} and $\text{tr}(M) = \mu + \mu^{-1}$. We can distinguish the following four cases:

- 1) $\text{tr}(M) > 2$: The eigenvalues $\mu_1 \neq \mu_2$ are positive, real numbers not equal to 1 and the linearly independent solutions are exponentially growing/decaying and of the form

$$\psi_{1,2}(x) = e^{\pm m x} p_{1,2}(x)$$

with a positive constant m .

- 2) $\text{tr}(M) < -2$: The eigenvalues $\mu_1 \neq \mu_2$ are negative, real numbers not equal to -1 and the linearly independent solutions are exponentially grow-

ing/decaying and of the form

$$\psi_{1,2}(x) = e^{(\pm m + i\pi/P)x} p_{1,2}(x)$$

with a positive constant m .

- 3) $-2 < \text{tr}(M) < 2$: The eigenvalues $\mu_1 \neq \mu_2$ lie on the complex unit circle away from $\{\pm 1\}$. The eigenfunctions are uniformly bounded and

$$\psi_{1,2}(x) = e^{\pm ilx} p_{1,2}(x)$$

with a real constant l .

- 4) $\text{tr}(M) = \pm 2$: In this case the eigenvalues are equal to $\{\pm 1\}$. The second part of Theorem 2.7.2 applies if and only if M is similar to the Jordanblock

$$\begin{pmatrix} \pm 1 & 1 \\ 0 & \pm 1 \end{pmatrix},$$

and this is the case, if and only if $\text{tr}(M)$ has a turning point at ± 2 . Otherwise, part i) applies and we have two periodic eigenfunctions in the case $\mu_1 = \mu_2 = 1$, respectively semi-periodic for $\mu_1 = \mu_2 = -1$.

To sum up, we have the following equivalences

$$\begin{aligned} |\text{tr}(M(\lambda))| \leq 2 &\Leftrightarrow \text{Floquet multipliers on the complex unit circle} \Leftrightarrow \\ &\lambda \in \sigma(-\partial_x^2|_{\Gamma}) \\ |\text{tr}(M(\lambda))| > 2 &\Leftrightarrow \text{Floquet multipliers off the complex unit circle} \Leftrightarrow \\ &\lambda \notin \sigma(-\partial_x^2|_{\Gamma}) \end{aligned}$$

2.7.2 The discrete center manifold theorem

For the reader's convenience we recall a discrete version of the center manifold theorem and refer to [Jam03]. First, we describe the general framework, in which the center manifold reduction applies. Let H be a Hilbert space and consider a closed linear operator $\Lambda : D \subset H \rightarrow H$. We equip D with the scalar product $\langle u, v \rangle_D = \langle \Lambda u, \Lambda v \rangle_H + \langle u, v \rangle_H$, which leads to the Hilbert space D continuously

embedded in H . Further, denote by $U \times V$ a neighborhood of 0 in $\mathbb{R} \times D$ and assume that the nonlinear map $N \in C^k(U \times V, H)$ for at least $k \geq 2$ satisfies

$$N(0, 0) = 0, \quad D_u N(0, 0) = 0.$$

We look for sequences $(y_n)_{n \in \mathbb{Z}}$ in V satisfying

$$y_{n+1} = \Lambda y_n + N(\varepsilon, y_n), \quad \text{in } H, \quad \forall n \in \mathbb{Z}, \quad (2.37)$$

with a constant ε independent of n .

Remark 2.7.3. *The condition $N(0, 0) = 0$ means that 0 is an equilibrium of the discrete equation, and the condition $D_u N(0, 0) = 0$ then shows that Λ is the linearization of the vector field about 0, so that N represents the nonlinear terms, which are of the order $\mathcal{O}(\|y\|_H^2)$.*

Hypothesis 2.7.4. *The operator Λ has the property of spectral separation, which means that its spectrum $\sigma(\Lambda)$ splits in the following way*

$$\sigma(\Lambda) = \sigma_s \cup \sigma_c \cup \sigma_u,$$

where $\sigma_s = \{z \in \mathbb{C} : |z| < 1\}$, $\sigma_c = \{z \in \mathbb{C} : |z| = 1\}$ and $\sigma_u = \{z \in \mathbb{C} : |z| > 1\}$. We further assume $\sup_{z \in \sigma_s} |z| < 1$ and $\inf_{z \in \sigma_u} |z| > 1$.

Hence, the hyperbolic part $\sigma_s \cup \sigma_u$ of the system has nonzero distance to the center part, i.e. there is a spectral gap around the unit circle, which allows us to define spectral projections:

$$P_c = \frac{1}{2\pi i} \int_{C(R)} (\mu - \Lambda)^{-1} d\mu - \frac{1}{2\pi i} \int_{C(r)} (\mu - \Lambda)^{-1} d\mu,$$

$$P_h = Id - \Pi_c,$$

where $C(r)$ denotes the circle with center in zero and radius r and

$$\sup_{z \in \sigma_s} |z| < r < 1 < R < \inf_{z \in \sigma_u} |z|.$$

We introduce some notation for the center space $H_c = \Pi_c H$, as well as the

hyperbolic projection $\Pi_h = I_H - \Pi_c$ and $H_h = \Pi_h H$, $D_h = \Pi_h D$. The projections provide a decomposition of H into the two invariant subspaces H_c and H_h .

Theorem 2.7.5 (Discrete center manifold theorem). *Under Hypothesis 2.7.4 there exists a neighborhood $I \times \Omega$ of 0 in $\mathbb{R} \times D$ and a map $\Phi_\varepsilon \in C_b^k(I \times H_c, D_h)$ such that for all $\varepsilon \in I$ the manifold*

$$M_\varepsilon = \{y \in D : y = x + \Phi_\varepsilon(x), x \in H_c\} \quad (2.38)$$

has the following properties

- i) M_ε is locally invariant, i.e. if $y \in M_\varepsilon \cap \Omega$, then $\Lambda y + N_\varepsilon(y) \in M_\varepsilon$.
- ii) If $(y_n)_{n \in \mathbb{Z}} \subset \Omega$ is a solution of (2.37), then $y_n \in M_\varepsilon$ for all n and the recurrence relation

$$y_{n+1}^c = f_\varepsilon(y_n^c), \quad \forall n \in \mathbb{Z}, \quad (2.39)$$

is satisfied in H_c , where the function $f \in C^k(I \times (H_c \cap \Omega), H_c)$ is defined by

$$f_\varepsilon = \Pi_c(\Lambda + N_\varepsilon) \circ (I + \Phi_\varepsilon). \quad (2.40)$$

- iii) Conversely, if $(y_n^c)_{n \in \mathbb{Z}} \subset \Omega$ is a solution of (2.39), then

$$y_n = y_n^c + \Phi_\varepsilon(y_n^c), \quad n \in \mathbb{Z}, \quad (2.41)$$

satisfies (2.37).

The manifold M is called a local center manifold and the map Φ is referred to as reduction function. This theorem allows us to reduce the local study of the discrete equation (2.37) to that of the recurrence relation (2.39) on the subspace H_c , which is particularly interesting when H_c is finite dimensional.

We finish this section with a reduction result preserving reversibility. Let (2.37) be reversible with respect to a symmetry $R \in \mathcal{L}(D)$, i.e. if u_n is a solution, then Ru_{-n} is also a solution.

Theorem 2.7.6. *Assume additionally to the assumptions in Theorem 2.7.4 that Λ admits a cut-off preserving a reversibility symmetry R , see [Jam03] Definition 2. Then, the reduced mapping is reversible and one has*

$$R \circ \Pi_c = \Pi_c \circ R, \quad R \circ \Phi_\varepsilon = \Phi_\varepsilon \circ R.$$

Chapter 3

Diffusive stability on metric necklace graphs

We consider a nonlinear diffusion equation on an infinite periodic metric graph. We prove that the terms which are irrelevant w.r.t. linear diffusion on the real line are irrelevant w.r.t. linear diffusion on the periodic metric graph, too. The proof is based on L^1 - L^∞ estimates combined with Bloch wave analysis for periodic metric graphs.

This part contains results from a collaboration with Martina Chirilus-Bruckner and Guido Schneider, see [CMS18].

3.1 Introduction

It is well known that on the real line the nonlinear terms u^p are irrelevant w.r.t. linear diffusive behavior if $p > 3$. We consider

$$\partial_t u = \partial_x^2 u + u^p, \quad u|_{t=0} = u_0, \quad (3.1)$$

with $t \geq 0$, $x \in \mathbb{R}$, $p \in \mathbb{N}$, and $u(x, t) \in \mathbb{R}$. For $p > 3$ and $C > 0$ there exists a $\delta > 0$ such that

$$\|u_0\|_{L^1} + \|u_0\|_{L^\infty} \leq \delta$$

implies

$$\|u(\cdot, t)\|_{L^1} \leq C \quad \text{and} \quad \|u(\cdot, t)\|_{L^\infty} \leq C(1+t)^{-1/2} \quad (3.2)$$

for all $t \geq 0$. The goal of this chapter is to prove that a similar result remains true, if (3.1) is posed on an infinite periodic metric graph.

A metric graph is a network of edges connected at vertices. The mathematical analysis of nonlinear PDEs on such graphs attracted recently a lot of interest, cf. [KP07, Noj14, EK15, AST16]. To avoid too many technical details, we restrict the subsequent presentation to the necklace graph shown in Figure 3.2.1 which has already been used in [GPS16] for other purposes. At the end of Section 3.2 we will discuss how to handle more general one-dimensional periodic graphs.

Stability and blow-up results for (3.1) on the real line have been developed by [Fuj66, Wei81]. The idea has been transferred to more complicated problems such as the stability of spatially periodic equilibria in the Ginzburg-Landau equation [CEE92, BK92], in pattern forming systems [Sch96, Sch98], and in pattern forming systems with a conservation law [JNRZ14]. There are various approaches to establish such results. These are the discrete and continuous renormalization approach, the use of Lyapunov functions, and L^1 - L^∞ -estimates. See [SU17, Chapter 14] for more details. Although not explicitly stated in the literature, equation (3.1) with smooth spatially periodic coefficients can be handled like these more advanced problems. Problem (3.1) posed on the necklace graph is a new challenge in the sense that we are in a very irregular situation. Restricting to solutions which are symmetric in the lower and upper semi-circle, cf Figure 5.3.1, our problem can be mapped to a problem with jump conditions at $\{n\pi : n \in \mathbb{Z}\}$.

We follow the L^1 - L^∞ -approach. In a first step the spectral picture necessary for diffusive behavior has to be computed. Since we have a spatially periodic problem the solutions of the linearized system are of Bloch wave form

$$u(x, t) = e^{\lambda_n(\ell)t} e^{i\ell x} f_n(\ell, x),$$

with $\lambda_n(\ell) \in \mathbb{R}$, $n \in \mathbb{N}$, Bloch wave number $\ell \in \mathbb{R}$, and f_n having the same periodicity w.r.t. x as the metric graph. For (3.1) posed on the necklace graph

we obtain a spectral picture as sketched in Figure 3.1.1.

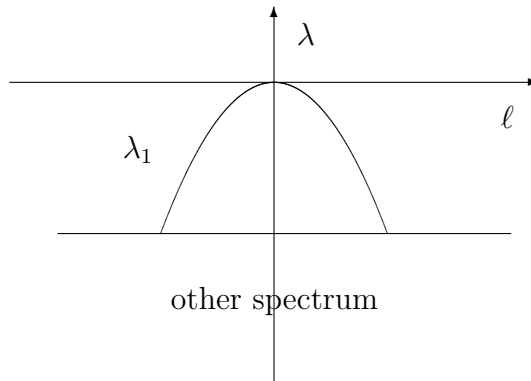


Figure 3.1.1: The eigenvalues $\lambda(\ell)$ plotted versus the Bloch wave numbers ℓ . The diffusive behavior comes from the parabola-like curve λ_1 through $(\ell, \lambda) = (0, 0)$. The rest of the spectrum leads to exponential decay. Due to the periodicity w.r.t. the Bloch wave number ℓ we can restrict ourselves to $\ell \in [-1/2, 1/2]$.

The fact that the spectrum can be estimated from above by $-C\ell^2$ near the origin is a necessary condition that a $t^{-1/2}$ decay can be established. However, the approach presented in [MSU01] and its generalization, in case of additional exponentially damped modes, presented in [SU17, Chapter 14], cannot be used directly since both do not fit together with the local existence and uniqueness theory for (3.1) posed on infinite periodic metric graphs. In Remark 3.6.7 we explain why we think that a pure L^1 - L^∞ approach will fail. As in [SU17, Chapter 14] we separate the diffusive modes from the exponentially damped modes with some projections which are defined for every fixed ℓ . However, in contrast to [SU17, Chapter 14] only the diffusive modes, corresponding to λ_1 , cf. Figure 3.1.1, are handled with L^1 and L^∞ . For the linearly exponentially damped modes we use the domain $\mathcal{H}^2 = D(\partial_x^2|_\Gamma)$, from the local existence and uniqueness theory, as suitable function space. This space is closed under point-wise multiplication. Hence the L^1 - L^∞ -estimates for the exponentially damped modes used in [SU17, Chapter 14] are replaced by L^2 -estimates for these modes. We believe that the presented approach in Section 3.6 is conceptually more transparent and simpler to apply in other situations. The detailed formulation of our stability result requires some notations and is therefore postponed to Section 3.6. Under a number of smallness assumptions on the initial conditions the

solution will satisfy $\sup_{x \in \Gamma} |u(x, t)| \leq C(1 + t)^{-1/2}$.

The present work is a first step in answering similar problems for dispersive equations, cf. [Str89], such as Klein-Gordon or NLS equations. To our knowledge, global existence results, which are based on dispersive estimates, do not exist for equations posed on non-trivial infinite periodic metric graphs so far. In [KM16] dispersive estimates for finitely many spectral bands for a problem on the real line with a periodic δ -potential has been shown.

We proceed as follows. First, we transfer (3.1) into a vector-valued problem on the real line with boundary conditions at the vertices. In order to do so we recall and use the notation from [GPS16] and explain in Section 3.2 what is meant exactly by posing (3.1) on an infinite periodic metric graph. In Section 3.3 we discuss the spectral problem associated to the linear diffusion operator ∂_x^2 defined on the metric graph Γ . In Section 3.4 we introduce the functional analytic set-up, in particular some function spaces and Bloch transform. In Section 3.5 we separate the diffusive modes from the exponentially damped modes. Then we establish linear L^1 - L^∞ estimates for the diffusive part u_c and L^2 -estimates for the exponentially damped part u_s . In Section 3.6 we prove the irrelevance of the nonlinear terms u^p w.r.t. linear diffusive behavior, i.e., we prove that the decay rates from Section 3.5 for u_c in the linear system hold in the nonlinear system, too.

Notation. Throughout this chapter, many different constants are denoted by C if they can be chosen independently of time $t \geq 0$.

3.2 The PDE on the metric graph

Considering (3.1) on the periodic metric graph Γ shown in Figure 3.2.1 means the following: For a function $u : \Gamma \rightarrow \mathbb{C}$, we denote the part on the interval $I_{n,0}$ associated to $\Gamma_{n,0}$ with $u_{n,0}$ and the parts on the intervals $I_{n,\pm}$ associated to $\Gamma_{n,\pm}$ with $u_{n,\pm}$. The scalar partial differential equation on the periodic metric graph Γ is transferred to a vector-valued partial differential equation on the real line

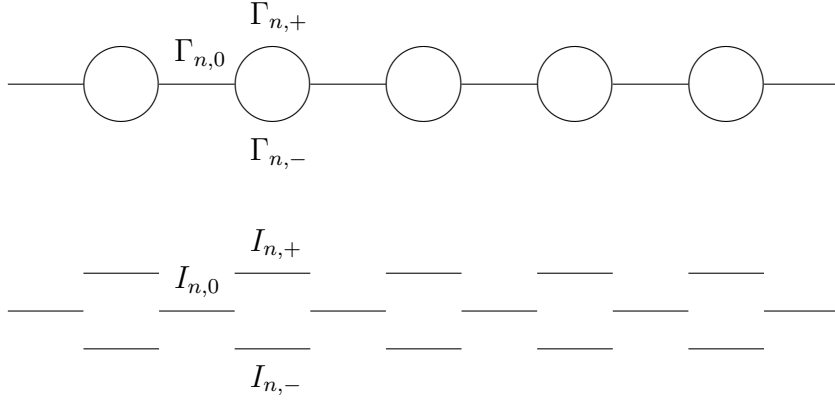


Figure 3.2.1: The periodic metric graph Γ shown in the upper panel is of the form $\Gamma = \bigoplus_{n \in \mathbb{Z}} \Gamma_n$, with $\Gamma_n = \Gamma_{n,0} \oplus \Gamma_{n,+} \oplus \Gamma_{n,-}$, where the $\Gamma_{n,0}$ are the horizontal links between the circles and the $\Gamma_{n,\pm}$ the upper and lower semicircles, all of the same length π , for $n \in \mathbb{Z}$. The part $\Gamma_{n,0}$ is identified isometrically with the interval $I_{n,0} = [2\pi n, 2\pi n + \pi]$ and the $\Gamma_{n,\pm}$ with the intervals $I_{n,\pm} = [2\pi n, 2\pi(n+1)]$. See the lower panel. For a function $u : \Gamma \rightarrow \mathbb{C}$, we denote the part on the interval $I_{n,0}$ with $u_{n,0}$ and the parts on the intervals $I_{n,\pm}$ with $u_{n,\pm}$.

by introducing

$$u_0(x) = \begin{cases} u_{n,0}(x), & x \in I_{n,0}, \\ 0, & x \in I_{n,\pm}, \end{cases} \quad (3.3)$$

and

$$u_{\pm}(x) = \begin{cases} u_{n,\pm}(x), & x \in I_{n,\pm}, \\ 0, & x \in I_{n,0}. \end{cases} \quad (3.4)$$

We collect the functions u_0 and u_{\pm} by putting them in the vector $U = (u_0, u_+, u_-)$, which rewrites the evolutionary problem (3.1) as

$$\partial_t U = \partial_x^2 U + U^p, \quad t \geq 0, \quad x \in \mathbb{R} \setminus \{k\pi : k \in \mathbb{Z}\}, \quad (3.5)$$

where we impose Kirchhoff boundary conditions at the vertex points $\{x = n\pi : n \in \mathbb{Z}\}$. The nonlinear term U^p is defined by (u_0^p, u_+^p, u_-^p) . These are given by

the continuity of the functions at the vertices

$$\begin{aligned} u_{n,0}(2\pi n + \pi, t) &= u_{n,+}(2\pi n + \pi, t) = u_{n,-}(2\pi n + \pi, t), \\ u_{n+1,0}(2\pi(n+1), t) &= u_{n,+}(2\pi(n+1), t) = u_{n,-}(2\pi(n+1), t), \end{aligned} \quad (3.6)$$

and the continuity of the fluxes at the vertices

$$\begin{aligned} \partial_x u_{n,0}(2\pi n + \pi, t) &= \partial_x u_{n,+}(2\pi n + \pi, t) + \partial_x u_{n,-}(2\pi n + \pi, t), \\ \partial_x u_{n+1,0}(2\pi(n+1), t) &= \partial_x u_{n,+}(2\pi(n+1), t) + \partial_x u_{n,-}(2\pi(n+1), t). \end{aligned} \quad (3.7)$$

Remark 3.2.1. Alternatively, the problem could be considered as a scalar problem on the real line. In order to do so we identify $\Gamma_{n,0}$ with $(3\pi n, 3\pi n + \pi)$, $\Gamma_{n,-}$ with $(3\pi n + \pi, 3\pi n + 2\pi)$ and $\Gamma_{n,+}$ with $(3\pi n + 2\pi, 3\pi(n+1))$. The transfer of the boundary conditions is straightforward, we have for instance

$$\lim_{x \rightarrow \pi, x < \pi} u(x) = \lim_{x \rightarrow \pi, x > \pi} u(x) = \lim_{x \rightarrow 2\pi, x > 2\pi} u(x).$$

The values in $x = n\pi$ with $n \in \mathbb{Z}$ are arbitrary, we can choose for instance $u(n\pi) = \lim_{x \rightarrow n\pi, x < n\pi} u(x)$. It is obvious that every reasonable periodic graph can be brought into this form. Nevertheless, we think that our approach is more natural. In [GPS16, Section 7] it is explained how to handle other one-dimensional infinite periodic metric graphs with our approach. The spectral pictures for the examples of other periodic metric graphs, presented in [GPS16, Section 7], have to be rotated by an angle of π . Moreover, the eigenvalues are real and no longer imaginary.

3.3 Spectral analysis

We start with the discussion of the linear problem

$$\partial_t U = \partial_x^2 U, \quad t \geq 0, \quad x \in \mathbb{R} \setminus \{k\pi : k \in \mathbb{Z}\}, \quad (3.8)$$

with the Kirchhoff boundary conditions (3.6) and (3.7). The ansatz $U(x, t) = W(x)e^{\lambda t}$ leads to the spectral problem

$$\partial_x^2 W = \lambda W, \quad x \in \mathbb{R} \setminus \{k\pi : k \in \mathbb{Z}\}, \quad (3.9)$$

with Kirchhoff boundary conditions at the vertices. The spectral problem has already been discussed in [GPS16]. We recall some details, which are necessary for the subsequent analysis. Since (3.9) with the Kirchhoff boundary conditions at the vertices is a periodic ordinary differential equation, there is a basis of eigenfunctions W which are given by Bloch waves

$$W(x) = e^{i\ell x} f(\ell, x), \quad \ell, x \in \mathbb{R}, \quad (3.10)$$

where $f(\ell, \cdot) = (f_0, f_+, f_-)(\ell, \cdot)$ is a 2π -periodic function for every $\ell \in \mathbb{R}$. Since these functions satisfy the continuation conditions

$$f(\ell, x) = f(\ell, x + 2\pi), \quad f(\ell, x) = f(\ell + 1, x)e^{ix}, \quad \ell, x \in \mathbb{R}, \quad (3.11)$$

we can restrict the definition of $f(\ell, x)$ to $x \in \mathbb{T}_{2\pi} = \mathbb{R}/(2\pi\mathbb{Z})$ and $\ell \in \mathbb{T}_1 = \mathbb{R}/\mathbb{Z}$. The torus $\mathbb{T}_{2\pi}$ is isometrically parameterized with $x \in [0, 2\pi]$ and the torus \mathbb{T}_1 with $\ell \in [-1/2, 1/2]$, where the endpoints of the intervals are identified to be the same. Hence, f can be found as a solution of the eigenvalue problem

$$(\partial_x + i\ell)^2 f = \lambda(\ell) f, \quad x \in \mathbb{T}_{2\pi}, \quad (3.12)$$

with associated boundary conditions

$$\begin{cases} f_0(\ell, \pi) = f_+(\ell, \pi) = f_-(\ell, \pi), \\ f_0(\ell, 0) = f_+(\ell, 2\pi) = f_-(\ell, 2\pi) \end{cases} \quad (3.13)$$

and

$$\begin{cases} (\partial_x + i\ell)f_0(\ell, \pi) = (\partial_x + i\ell)f_+(\ell, \pi) + (\partial_x + i\ell)f_-(\ell, \pi), \\ (\partial_x + i\ell)f_0(\ell, 0) = (\partial_x + i\ell)f_+(\ell, 2\pi) + (\partial_x + i\ell)f_-(\ell, 2\pi). \end{cases} \quad (3.14)$$

The supports of the functions $f_0(\ell, \cdot)$ and $f_{\pm}(\ell, \cdot)$ are contained in $I_{0,0} = [0, \pi] \subset \mathbb{T}_{2\pi}$ and $I_{0,\pm} = [\pi, 2\pi] \subset \mathbb{T}_{2\pi}$. The spectrum consists of two parts. There is a sequence of eigenvalues at $\{-m^2\}_{m \in \mathbb{N}}$ of infinite multiplicity. The associated eigenfunctions are supported compactly in each circle. Moreover, there are countably many curves of eigenvalues which correspond to the eigenvalues of the monodromy matrix M . They can be computed via roots $\rho_{1,2} = e^{2\pi i \ell}$ of $\rho^2 - \text{tr}(M)(-\lambda)\rho + 1 = 0$, where

$$\text{tr}(M)(-\lambda) = \frac{1}{4} \left[9 \cos(2\pi \sqrt{-\lambda}) - 1 \right]. \quad (3.15)$$

The spectral bands of the periodic eigenvalue problem (3.12) are shown on Figure 3.3.1.

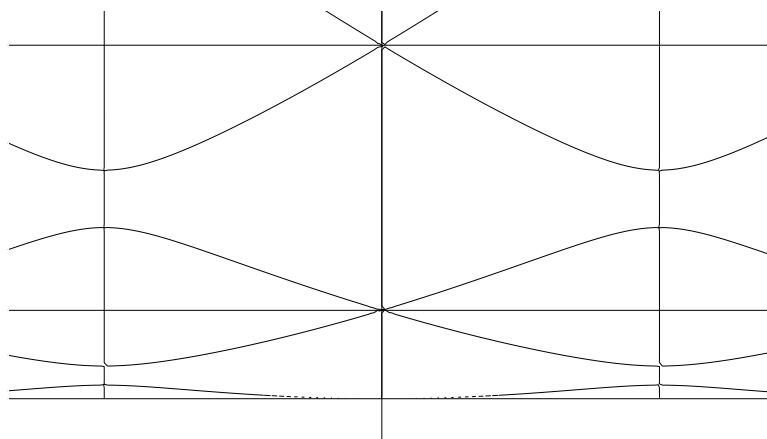


Figure 3.3.1: The eigenvalues $\lambda(\ell)$ plotted versus the Bloch wave numbers ℓ . The diffusive behavior is caused by the parabola-like curve λ_1 through $(\ell, \lambda) = (0, 0)$. All other curves lead to exponential decay.

Remark 3.3.1. At a first view it seems that the infinitely many localized eigenfunctions $\underline{W}^{m,k}$, indexed with $m \in \mathbb{N}$ and $k \in \mathbb{Z}$, with the explicit representation

$$\underline{W}_{n,0}^{m,k} = 0, \quad \underline{W}_{n,\pm}^{m,k} = \pm \delta_{n,k} \sin(mx),$$

cannot be written in Bloch form (3.10). However, the linear combination

$$w_{n,0}^m = e^{i\ell x} f_{n,0}^m(\ell, x), \quad w_{n,\pm}^m = e^{i\ell x} f_{n,\pm}^m(\ell, x),$$

with $f_{n,0}^m(\ell, x) = 0$ for $x \in [2\pi n, 2\pi n + \pi)$ and

$$f_{n,\pm}^m(\ell, x) = \pm e^{-i\ell(x-2\pi n)} \sin(mx)$$

for $x \in [2\pi n + \pi, 2\pi(n+1))$ is of the required form. It is straightforward to show that the f^m satisfy (3.11).

3.4 The functional analytic set-up

The diffusive behavior can be seen in the spectral picture plotted in Figure 3.3.1. The parabola-like curve touching $\lambda = 0$ at $\ell = 0$ leads to such diffusive behavior. Hence, a natural approach to establish the diffusive decay estimates (3.2) is an expansion of (3.5) w.r.t. the associated eigenfunctions, the Bloch modes.

3.4.1 The system in Bloch space

The concept Bloch transform \mathcal{T} generalizes Fourier transform \mathcal{F} from spatially homogeneous problems to spatially periodic problems, cf. [RS79]. It is defined by

$$\tilde{u}(\ell, x) = (\mathcal{T}u)(\ell, x) = \sum_{n \in \mathbb{Z}} u(x + 2\pi n) e^{-i\ell x - 2\pi i n \ell}. \quad (3.16)$$

The inverse of Bloch transform is given by

$$u(x) = (\mathcal{T}^{-1}\tilde{u})(x) = \int_{-1/2}^{1/2} e^{i\ell x} \tilde{u}(\ell, x) d\ell. \quad (3.17)$$

By construction, $\tilde{u}(\ell, x)$ is extended from $(\ell, x) \in \mathbb{T}_1 \times \mathbb{T}_{2\pi}$ to $(\ell, x) \in \mathbb{R} \times \mathbb{R}$ according to

$$\tilde{u}(\ell, x) = \tilde{u}(\ell, x + 2\pi) \quad \text{and} \quad \tilde{u}(\ell, x) = \tilde{u}(\ell + 1, x) e^{ix}. \quad (3.18)$$

Multiplication of two functions $u(x)$ and $v(x)$ in x -space corresponds to the convolution integral in Bloch space:

$$(\tilde{u} * \tilde{v})(\ell, x) = \int_{-1/2}^{1/2} \tilde{u}(\ell - m, x) \tilde{v}(m, x) dm, \quad (3.19)$$

where (3.18) has to be used for $|\ell - m| > 1/2$.

We apply the Bloch transform \mathcal{T} to all components of $U = (u_0, u_+, u_-)$ and obtain

$$\partial_t \tilde{U}(t, \ell, x) = \tilde{L}(\ell) \tilde{U}(t, \ell, x) + \tilde{N}(\tilde{U})(t, \ell, x), \quad (3.20)$$

where $\tilde{U} = \mathcal{T}U$, $\tilde{L} = \mathcal{T}L\mathcal{T}^{-1}$, with L the linear operator defined on the right-hand side of (3.8), and $\tilde{N}(\tilde{U}) = \mathcal{T}N(\mathcal{T}^{-1}\tilde{U})$ with $N(U) = U^p$. By definition $\tilde{U}(t, \ell, x) = (\tilde{u}_0, \tilde{u}_+, \tilde{u}_-)(t, \ell, x)$ satisfies

$$\tilde{U}(t, \ell, x) = \tilde{U}(t, \ell, x + 2\pi) \quad \text{and} \quad \tilde{U}(t, \ell, x) = \tilde{U}(t, \ell + 1, x) e^{ix}. \quad (3.21)$$

3.4.2 The function spaces

In order to analyse (3.20), we define L^2 -based spaces for fixed $\ell \in \mathbb{T}_1$.

Definition 3.4.1. *Let*

$$\begin{aligned} L_{\Gamma}^2 &:= \{ \tilde{U} = (\tilde{u}_0, \tilde{u}_+, \tilde{u}_-) \in (L^2(\mathbb{T}_{2\pi}))^3 : \\ &\quad \text{supp}(\tilde{u}_j) = I_{0,j}, \quad j \in \{0, +, -\} \} \end{aligned} \quad (3.22)$$

and

$$\begin{aligned} H_{\Gamma}^2(\ell) &:= \{ \tilde{U} \in L_{\Gamma}^2 : \tilde{u}_j \in H^2(I_{0,j}), \quad j \in \{0, +, -\}, \\ &\quad (3.13) - (3.14) \text{ are satisfied} \}, \end{aligned}$$

equipped with the norm

$$\|\tilde{U}\|_{H_{\Gamma}^2(\ell)} = \left(\|\tilde{u}_0\|_{H^2(I_{0,0})}^2 + \|\tilde{u}_+\|_{H^2(I_{0,+})}^2 + \|\tilde{u}_-\|_{H^2(I_{0,-})}^2 \right)^{1/2}.$$

The parameter ℓ is defined in $H_{\Gamma}^2(\ell)$ by means of the ℓ -dependent boundary conditions (3.13)-(3.14). We recall [GPS16, Lemma 2.1].

Lemma 3.4.2. *For fixed $\ell \in \mathbb{T}_1$, the operator $-\tilde{L}(\ell) := -(\partial_x + i\ell)^2$ is a self-adjoint, positive semi-definite operator in L_{Γ}^2 .*

The domain of the operator $\tilde{L}(\ell)$ is given by

Definition 3.4.3. *Let*

$$\begin{aligned} \tilde{\mathcal{H}}^2 = \{ \tilde{U} \in L^2(\mathbb{T}_1, L_{\Gamma}^2) : \quad & \tilde{u}_j \in L^2(\mathbb{T}_1, H^2(I_{0,j})), \quad j \in \{0, +, -\}, \\ & \text{(3.13) - (3.14) are satisfied} \}, \end{aligned}$$

equipped with the norm

$$\|\tilde{U}\|_{\tilde{\mathcal{H}}^2}^2 = \int_{-1/2}^{1/2} \left(\|\tilde{u}_0(\ell, \cdot)\|_{H^2(I_{0,0})}^2 + \|\tilde{u}_+(\ell, \cdot)\|_{H^2(I_{0,+})}^2 + \|\tilde{u}_-(\ell, \cdot)\|_{H^2(I_{0,-})}^2 \right) d\ell.$$

We have the following local existence and uniqueness result

Theorem 3.4.1. *For every $\tilde{U}_0 \in \tilde{\mathcal{H}}^2$, there exists a $T_0 = T_0(\|\tilde{U}_0\|_{\tilde{\mathcal{H}}^2}) > 0$ and a unique mild solution $\tilde{U} \in C([0, T_0], \tilde{\mathcal{H}}^2)$ of (3.20) with $\tilde{U}|_{t=0} = \tilde{U}_0$.*

Proof. In Appendix 3.7.1 we prove the local existence and uniqueness of solutions in \mathcal{H}^2 , the domain of definition of the operator $L := \partial_x^2$ in physical space. For the definition of \mathcal{H}^2 see Appendix 3.7.1. Theorem 3.4.1 follows immediately from Theorem 3.7.1 since, according to [GPS16, Lemma 4.2], Bloch transform \mathcal{T} is an isomorphism between the spaces \mathcal{H}^2 and $\tilde{\mathcal{H}}^2$. \square

We close this section with the remark that the global existence in $\tilde{\mathcal{H}}^2$ of the solutions in which we are interested follows with the subsequent diffusive estimates. They can be used as a-priori estimates such that Theorem 3.4.1 can be applied again and again. Hence, it remains to establish the polynomial decay rates (3.2).

3.5 Diffusive and exponentially damped modes

As explained in the introduction we separate the diffusive modes from the exponentially damped modes.

In the following we use the abbreviation $\tilde{\varphi}_1(\ell) = f^1(\ell, \cdot)$ and the normalization $\langle \tilde{\varphi}_1(\ell), \tilde{\varphi}_1(\ell) \rangle = 1$, where $\langle u, v \rangle = \int_0^{2\pi} \overline{u(x)}v(x)dx$.

The curve of the eigenvalue $\lambda_1(\ell)$ is separated from the rest of the spectrum, cf. Figure 3.3.1. Since $\tilde{L}(\ell)$ is a self-adjoint operator for fixed ℓ , cf. Lemma 3.4.2, we define the orthogonal projection on the diffusive modes by

$$\tilde{P}_c(\ell)\tilde{U}(\ell) = \langle \tilde{\varphi}_1(\ell), \tilde{U}(\ell) \rangle \tilde{\varphi}_1(\ell).$$

Moreover, we define by $\tilde{P}_s(\ell)\tilde{U}(\ell) = (Id - \tilde{P}_c(\ell))\tilde{U}(\ell)$ be the orthogonal projection on the exponentially damped modes. We use the projections to separate (3.20) in two parts, namely

$$\partial_t \tilde{v}_c(\ell, t) = \tilde{L}_c(\ell)\tilde{v}_c(\ell, t) + \tilde{P}_c(\ell)\tilde{N}(\tilde{U})(\ell, t), \quad (3.23)$$

$$\partial_t \tilde{v}_s(\ell, x, t) = \tilde{L}_s(\ell)\tilde{v}_s(\ell, x, t) + \tilde{P}_s(\ell)\tilde{N}(\tilde{U})(\ell, x, t). \quad (3.24)$$

where $\tilde{L}_c(\ell) = \tilde{L}(\ell)\tilde{P}_c(\ell)$ and $\tilde{L}_s(\ell) = \tilde{L}(\ell)\tilde{P}_s(\ell)$. By construction the operators $\tilde{P}_s(\ell)$ and $\tilde{P}_c(\ell)$ commute with $\tilde{L}(\ell)$. The system (3.23)-(3.24) is solved with initial conditions $\tilde{v}_c|_{t=0} = \tilde{P}_c(\tilde{U}|_{t=0})$ and $\tilde{v}_s|_{t=0} = \tilde{P}_s(\tilde{U}|_{t=0})$. Then \tilde{v}_c and \tilde{v}_s are defined via the solutions of (3.23)-(3.24).

Since the sectorial operator \tilde{L}_s has spectrum in the left half plane strictly bounded away from the imaginary axis, we obviously have the following result, cf. [Hen81, Theorem 1.5.3].

Lemma 3.5.1. *For the analytic semigroup generated by \tilde{L}_s we have the estimate*

$$\|e^{t\tilde{L}_s}\|_{\tilde{\mathcal{H}}^2 \rightarrow \tilde{\mathcal{H}}^2} \leq Ce^{-\sigma_s t/2},$$

for a $\sigma_s > 0$ and all $t \geq 0$.

For the analysis of the \tilde{v}_c we introduce the following two spaces.

Definition 3.5.2. *Let*

$$\begin{aligned} \tilde{\mathcal{X}}^1 = \{ \tilde{U} \in L^1(\mathbb{T}_1, L^2_\Gamma) : \tilde{u}_j \in L^1(\mathbb{T}_1, H^2(I_{0,j})), \quad j \in \{0, +, -\}, \\ (3.13) - (3.14) \text{ are satisfied} \}, \end{aligned}$$

equipped with the norm

$$\| \tilde{U} \|_{\tilde{\mathcal{X}}^1} = \int_{-1/2}^{1/2} (\| \tilde{u}_0(\ell, \cdot) \|_{H^2(I_{0,0})} + \| \tilde{u}_+(\ell, \cdot) \|_{H^2(I_{0,+})} + \| \tilde{u}_-(\ell, \cdot) \|_{H^2(I_{0,-})}) d\ell$$

and

$$\begin{aligned} \tilde{\mathcal{X}}^\infty = \{ \tilde{U} \in L^\infty(\mathbb{T}_1, L^2_\Gamma) : \tilde{u}_j \in L^\infty(\mathbb{T}_1, H^2(I_{0,j})), \quad j \in \{0, +, -\}, \\ (3.13) - (3.14) \text{ are satisfied} \}, \end{aligned}$$

equipped with the norm

$$\| \tilde{U} \|_{\tilde{\mathcal{X}}^\infty} = \sup_{\ell \in \mathbb{T}_1} (\| \tilde{u}_0(\ell, \cdot) \|_{H^2(I_{0,0})} + \| \tilde{u}_+(\ell, \cdot) \|_{H^2(I_{0,+})} + \| \tilde{u}_-(\ell, \cdot) \|_{H^2(I_{0,-})}).$$

Moreover, we set $\tilde{\mathcal{X}}^2 = \tilde{\mathcal{H}}^2$.

We use the representation of the \tilde{v}_c -part

$$\tilde{v}_c(\ell, x) = \widehat{v}_{c,j}(\ell) \varphi_{1,j}(\ell, x), \tag{3.25}$$

with $\widehat{v}_{c,j}(\ell) \in \mathbb{C}$, $j \in \{0, +, -\}$. Since $\varphi_{1,j} \in C^\infty(\mathbb{T}_1, H^2(I_{0,j}))$ satisfies (3.18) we have

$$\| \tilde{v}_c \|_{\tilde{\mathcal{X}}^1} = \int_{-1/2}^{1/2} \left(\sum_{j \in \{0, +, -\}} \| \widehat{v}_c(\ell) \varphi_{1,j}(\ell, \cdot) \|_{H^2(I_{0,j})} \right) d\ell \leq C \| \widehat{v}_c \|_{L^1(\mathbb{T}_1)}$$

Since the norm $\| \varphi_{1,j}(\ell, \cdot) \|_{H^2(I_{0,j})}$ is not only bounded from above, but also from below we also have

$$\| \widehat{v}_c \|_{L^1(\mathbb{T}_1)} \leq C \| \tilde{v}_c \|_{\tilde{\mathcal{X}}^1}.$$

Similarly, we find

$$\|\tilde{v}_c\|_{\tilde{\mathcal{X}}^\infty} \leq C \|\widehat{v}_c\|_{L^\infty(\mathbb{T}_1)} \quad \text{and} \quad \|\widehat{v}_c\|_{L^\infty(\mathbb{T}_1)} \leq C \|\tilde{v}_c\|_{\tilde{\mathcal{X}}^\infty}.$$

Thus, we have shown

Lemma 3.5.3. *For the analytic semigroup generated by \tilde{L}_c we obtain the estimates*

$$\|e^{t\tilde{L}_c}\|_{\tilde{\mathcal{X}}^1 \rightarrow \tilde{\mathcal{X}}^1} \leq C, \quad \|e^{t\tilde{L}_c}\|_{\tilde{\mathcal{X}}^\infty \rightarrow \tilde{\mathcal{X}}^\infty} \leq C, \quad \|e^{t\tilde{L}_c}\|_{\tilde{\mathcal{X}}^\infty \rightarrow \tilde{\mathcal{X}}^1} \leq Ct^{-1/2}.$$

Proof. Since $\lambda_1(\ell) \leq -C\ell^2$ for small ℓ and $e^{t\tilde{L}_c(\ell)}\tilde{v}_c(\ell) = e^{\lambda_1(\ell)t}\tilde{v}_c(\ell)$ we obviously get

$$\begin{aligned} \|e^{t\tilde{L}_c}\tilde{v}_c\|_{\tilde{\mathcal{X}}^1} &\leq \|e^{\lambda_1(k)t}\|_{L^\infty} \|\tilde{v}_c\|_{\tilde{\mathcal{X}}^1} \leq C \|\tilde{v}_c\|_{\tilde{\mathcal{X}}^1}, \\ \|e^{t\tilde{L}_c}\tilde{v}_c\|_{\tilde{\mathcal{X}}^\infty} &\leq \|e^{\lambda_1(k)t}\|_{L^\infty} \|\tilde{v}_c\|_{\tilde{\mathcal{X}}^\infty} \leq C \|\tilde{v}_c\|_{\tilde{\mathcal{X}}^\infty}, \\ \|e^{t\tilde{L}_c}\tilde{v}_c\|_{\tilde{\mathcal{X}}^1} &\leq \|e^{\lambda_1(k)t}\|_{L^1} \|\tilde{v}_c\|_{\tilde{\mathcal{X}}^\infty} \leq Ct^{-1/2} \|\tilde{v}_c\|_{\tilde{\mathcal{X}}^\infty}. \end{aligned}$$

□

3.6 The nonlinear decay estimates

3.6.1 Preliminaries

For the proof of the diffusive decay estimates (3.2) we first show a number of inequalities. From [GPS16, Lemma 3.1 and Lemma 4.2] we know that $\tilde{\mathcal{X}}^2 = \tilde{\mathcal{H}}^2$ is closed under the convolution (3.19).

Lemma 3.6.1. *There exists a $C > 0$ such that for all $\tilde{u}, \tilde{v} \in \tilde{\mathcal{X}}^2$ we have*

$$\|\tilde{u} * \tilde{v}\|_{\tilde{\mathcal{X}}^2} \leq C \|\tilde{u}\|_{\tilde{\mathcal{X}}^2} \|\tilde{v}\|_{\tilde{\mathcal{X}}^2}. \quad (3.26)$$

Moreover, we need

Lemma 3.6.2. *There exists a $C > 0$ such that for all $\tilde{u} \in \tilde{\mathcal{X}}^1$ and $\tilde{v} \in \tilde{\mathcal{X}}^p$ with $p \in \{2, \infty\}$ we have*

$$\|\tilde{u} * \tilde{v}\|_{\tilde{\mathcal{X}}^p} \leq C \|\tilde{u}\|_{\tilde{\mathcal{X}}^1} \|\tilde{v}\|_{\tilde{\mathcal{X}}^p}. \quad (3.27)$$

Proof. Since the function spaces $H^2(I_{0,j})$ are closed under multiplication, it follows from Young's inequality that $\|\widehat{u} * \widehat{v}\|_{L^p} \leq C \|\widehat{u}\|_{L^1} \|\widehat{v}\|_{L^p}$. For convolutions we deduce

$$\begin{aligned} & \|\tilde{u} * \tilde{v}\|_{\tilde{\mathcal{X}}^p} \\ = & \left\| \sum_{j \in \{0,+, -\}} \left\| \int_{-1/2}^{1/2} \tilde{u}_j(\ell - \ell_1, x) \tilde{v}_j(\ell_1, x) d\ell_1 \right\|_{H^2(I_{0,j})(dx)} \right\|_{L^p(d\ell)} \\ \leq & C \left\| \int_{-1/2}^{1/2} \sum_{j \in \{0,+, -\}} \|\tilde{u}_j(\ell - \ell_1, x) \tilde{v}_j(\ell_1, x)\|_{H^2(I_{0,j})(dx)} d\ell_1 \right\|_{L^p(d\ell)} \\ \leq & C \sum_{j \in \{0,+, -\}} \left\| \int_{-1/2}^{1/2} \|\tilde{u}_j(\ell - \ell_1, x)\|_{H^2(I_{0,j})(dx)} \|\tilde{v}_j(\ell_1, x)\|_{H^2(I_{0,j})(dx)} d\ell_1 \right\|_{L^p(d\ell)} \\ \leq & C \sum_{j \in \{0,+, -\}} \|\tilde{u}_j\|_{\tilde{\mathcal{X}}^1} \|\tilde{v}_j\|_{\tilde{\mathcal{X}}^p} \leq C \|\tilde{u}\|_{\tilde{\mathcal{X}}^1} \|\tilde{v}\|_{\tilde{\mathcal{X}}^p}. \end{aligned}$$

□

Lemma 3.6.3. *There exists a $C > 0$ such that for all $\tilde{u}, \tilde{v} \in \tilde{\mathcal{X}}^2$ we have*

$$\|\tilde{u} * \tilde{v}\|_{\tilde{\mathcal{X}}^\infty} \leq C \|\tilde{u}\|_{\tilde{\mathcal{X}}^2} \|\tilde{v}\|_{\tilde{\mathcal{X}}^2}. \quad (3.28)$$

Proof. We proceed as above, but use $\|\widehat{u} * \widehat{v}\|_{L^\infty} \leq C\|\widehat{u}\|_{L^2}\|\widehat{v}\|_{L^2}$. We find

$$\begin{aligned}
 & \|\widetilde{u} * \widetilde{v}\|_{\widetilde{\mathcal{X}}^\infty} \\
 = & \sum_{j \in \{0,+, -\}} \left\| \int_{-1/2}^{1/2} \widetilde{u}_j(\ell - \ell_1, x) \widetilde{v}_j(\ell_1, x) d\ell_1 \right\|_{H^2(I_{0,j})(dx)} \Big\|_{L^\infty(d\ell)} \\
 \leq & C \left\| \int_{-1/2}^{1/2} \sum_{j \in \{0,+, -\}} \|\widetilde{u}_j(\ell - \ell_1, x) \widetilde{v}_j(\ell_1, x)\|_{H^2(I_{0,j})(dx)} d\ell_1 \right\|_{L^\infty(d\ell)} \\
 \leq & C \sum_{j \in \{0,+, -\}} \left\| \int_{-1/2}^{1/2} \|\widetilde{u}_j(\ell - \ell_1, x)\|_{H^2(I_{0,j})(dx)} \|\widetilde{v}_j(\ell_1, x)\|_{H^2(I_{0,j})(dx)} d\ell_1 \right\|_{L^\infty(d\ell)} \\
 \leq & C \sum_{j \in \{0,+, -\}} \|\widetilde{u}_j\|_{\widetilde{\mathcal{X}}^2} \|\widetilde{v}_j\|_{\widetilde{\mathcal{X}}^2} \leq C\|\widetilde{u}\|_{\widetilde{\mathcal{X}}^2} \|\widetilde{v}\|_{\widetilde{\mathcal{X}}^2}.
 \end{aligned}$$

□

Moreover, we need the following embedding result.

Lemma 3.6.4. *There exists a $C > 0$ such that for all $\widetilde{u} \in \widetilde{\mathcal{X}}^2$ we have the estimate*

$$\|\widetilde{u}\|_{\widetilde{\mathcal{X}}^1} \leq C\|\widetilde{u}\|_{\widetilde{\mathcal{X}}^2}. \quad (3.29)$$

Proof. Since $\ell \in \mathbb{T}^1$ we estimate

$$\begin{aligned}
 \|\widetilde{u}\|_{\widetilde{\mathcal{X}}^1} &= \left\| \sum_{j \in \{0,+, -\}} \|\widetilde{u}_j(\ell, x)\|_{H^2(I_{0,j})(dx)} \right\|_{L^1(d\ell)} \\
 &\leq C \sum_{j \in \{0,+, -\}} \left\| \|\widetilde{u}_j(\ell, x)\|_{H^2(I_{0,j})(dx)} \cdot 1 \right\|_{L^1(d\ell)} \\
 &\leq C \sum_{j \in \{0,+, -\}} \left\| \|\widetilde{u}_j(\ell, x)\|_{H^2(I_{0,j})(dx)} \right\|_{L^2(d\ell)} \|1\|_{L^2(d\ell)} \\
 &\leq C \sum_{j \in \{0,+, -\}} \left\| \|\widetilde{u}_j(\ell, x)\|_{H^2(I_{0,j})(dx)} \right\|_{L^2(d\ell)} \leq C\|\widetilde{u}\|_{\widetilde{\mathcal{X}}^2}.
 \end{aligned}$$

□

Finally, we need the following interpolation inequality.

Lemma 3.6.5. *There exists a $C > 0$ such that for all $\widetilde{u} \in \widetilde{\mathcal{X}}^1 \cap \widetilde{\mathcal{X}}^\infty$ we have*

$$\|\widetilde{u}\|_{\widetilde{\mathcal{X}}^2}^2 \leq C\|\widetilde{u}\|_{\widetilde{\mathcal{X}}^\infty} \|\widetilde{u}\|_{\widetilde{\mathcal{X}}^1} \quad (3.30)$$

Proof. A straightforward computation yields

$$\begin{aligned}
 \|\tilde{u}\|_{\tilde{\mathcal{X}}^2}^2 &= \left\| \sum_{j \in \{0,+, -\}} \|\tilde{u}_j(\ell, x)\|_{H^2(I_{0,j})(dx)} \right\|_{L^2(d\ell)}^2 \\
 &= \left\| \sum_{j \in \{0,+, -\}} \|\tilde{u}_j(\ell, x)\|_{H^2(I_{0,j})(dx)}^2 \right\|_{L^1(d\ell)} \\
 &\leq \sum_{j \in \{0,+, -\}} \left\| \|\tilde{u}_j(\ell, x)\|_{H^2(I_{0,j})(dx)} \right\|_{L^\infty(d\ell)} \|\tilde{u}_j(\ell, x)\|_{H^2(I_{0,j})(dx)} \Big\|_{L^1(d\ell)} \\
 &\leq C \|u\|_{\tilde{\mathcal{X}}^\infty} \|\tilde{u}\|_{\tilde{\mathcal{X}}^1}
 \end{aligned}$$

□

3.6.2 Irrelevance of the nonlinear terms

We proceed as in [MSU01] and consider the variation of constant formula

$$\tilde{v}_c(t) = e^{t\tilde{L}_c} \tilde{v}_c(0) + \int_0^t e^{(t-\tau)\tilde{L}_c} \tilde{P}_c \tilde{N}(\tilde{v}_c, \tilde{v}_s)(\tau) d\tau, \quad (3.31)$$

$$\tilde{v}_s(t) = e^{t\tilde{L}_s} \tilde{v}_s(0) + \int_0^t e^{(t-\tau)\tilde{L}_s} \tilde{P}_s \tilde{N}(\tilde{v}_c, \tilde{v}_s)(\tau) d\tau \quad (3.32)$$

for (3.23)-(3.24). In the following we use the abbreviations

$$\begin{aligned}
 a(t) &= \sup_{0 \leq \tau \leq t} \|\tilde{v}_c(\tau)\|_{\tilde{\mathcal{X}}^\infty}, \\
 b(t) &= \sup_{0 \leq \tau \leq t} \|(1+\tau)^{1/2} \tilde{v}_c(\tau)\|_{\tilde{\mathcal{X}}^1}, \\
 c(t) &= \sup_{0 \leq \tau \leq t} \|(1+\tau)^{3/4} \tilde{v}_s(\tau)\|_{\tilde{\mathcal{X}}^2}
 \end{aligned}$$

and

$$r(t) = a(t) + b(t) + c(t).$$

Moreover, many different constants are now denoted with the same symbol C , if they can be chosen independently of $r(t)$ and t .

a) Lemma 3.6.2 and Lemma 3.6.4 imply

$$\begin{aligned} & \|(\tilde{v}_c + \tilde{v}_s)^{*p}\|_{\tilde{\mathcal{X}}^1} \\ & \leq C\|\tilde{v}_c + \tilde{v}_s\|_{\tilde{\mathcal{X}}^1}^p \leq C(\|\tilde{v}_c\|_{\tilde{\mathcal{X}}^1} + \|\tilde{v}_s\|_{\tilde{\mathcal{X}}^1})^p \leq C(\|\tilde{v}_c\|_{\tilde{\mathcal{X}}^1} + \|\tilde{v}_s\|_{\tilde{\mathcal{H}}^2})^p \\ & \leq C((1+t)^{-1/2}b(t) + (1+t)^{-3/4}c(t))^p \leq C(1+t)^{-p/2}r(t)^p, \end{aligned}$$

where \tilde{v}^p denotes the $p - 1$ -times convolution of \tilde{v} .

b) In the same way we obtain

$$\begin{aligned} \|(\tilde{v}_c + \tilde{v}_s)^{*p}\|_{\tilde{\mathcal{X}}^2} & \leq C\|\tilde{v}_c + \tilde{v}_s\|_{\tilde{\mathcal{X}}^1}^{p-1}\|\tilde{v}_c + \tilde{v}_s\|_{\tilde{\mathcal{X}}^2} \\ & \leq C(\|\tilde{v}_c\|_{\tilde{\mathcal{X}}^1} + \|\tilde{v}_s\|_{\tilde{\mathcal{X}}^1})^{p-1}(\|\tilde{v}_c\|_{\tilde{\mathcal{X}}^2} + \|\tilde{v}_s\|_{\tilde{\mathcal{X}}^2}) \\ & \leq C(\|\tilde{v}_c\|_{\tilde{\mathcal{X}}^1} + \|\tilde{v}_s\|_{\tilde{\mathcal{X}}^1})^{p-1}(\|\tilde{v}_c\|_{\tilde{\mathcal{X}}^1}^{1/2}\|\tilde{v}_c\|_{\tilde{\mathcal{X}}^\infty}^{1/2} + \|\tilde{v}_s\|_{\tilde{\mathcal{X}}^2}) \\ & \leq C((1+t)^{-1/2}b(t) + (1+t)^{-3/4}c(t))^{p-1} \\ & \quad \times ((1+t)^{-1/4}a(t)^{1/2}b(t)^{1/2} + (1+t)^{-3/4}c(t)) \\ & \leq C(1+t)^{(1-p)/2-1/4}r(t)^p, \end{aligned}$$

where we additionally used Lemma 3.6.5.

c) The estimates for $\|(\tilde{v}_c + \tilde{v}_s)^{*p}\|_{\tilde{\mathcal{L}}^\infty}$ are more involved. We use that

$$(\tilde{v}_c + \tilde{v}_s)^{*p} = \sum_{j=0}^p \binom{p}{j} \tilde{v}_c^{*j} * \tilde{v}_s^{*(p-j)},$$

and apply the triangle inequality. Thus, it remains to estimate $\|\tilde{v}_c^{*j} * \tilde{v}_s^{*(p-j)}\|_{\tilde{\mathcal{L}}^\infty}$.

i) Using Lemma 3.6.2, Lemma 3.6.4, and Lemma 3.6.3 yields

$$\begin{aligned} \|\tilde{v}_s^{*p}\|_{\tilde{\mathcal{X}}^\infty} & \leq \|\tilde{v}_s\|_{\tilde{\mathcal{X}}^1}^{p-2}\|\tilde{v}_s^{*2}\|_{\tilde{\mathcal{X}}^\infty} \leq \|\tilde{v}_s\|_{\tilde{\mathcal{X}}^2}^{p-2}\|\tilde{v}_s\|_{\tilde{\mathcal{X}}^2}^2 \\ & \leq C(1+t)^{-3p/4}r(t)^p. \end{aligned}$$

ii) Lemma 3.6.2 and Lemma 3.6.3 imply

$$\begin{aligned} \|\tilde{v}_c^{*(p-2)} * \tilde{v}_s^{*2}\|_{\tilde{\mathcal{X}}^\infty} & \leq \|\tilde{v}_c\|_{\tilde{\mathcal{X}}^1}^{p-2}\|\tilde{v}_s^{*2}\|_{\tilde{\mathcal{X}}^\infty} \leq \|\tilde{v}_c\|_{\tilde{\mathcal{X}}^1}^{p-2}\|\tilde{v}_s\|_{\tilde{\mathcal{X}}^2}^2 \\ & \leq C(1+t)^{(2-p)/2-3/2}r(t)^p. \end{aligned}$$

iii) All terms $\tilde{v}_c^{*j} * \tilde{v}_s^{*(p-j)}$ with $j \geq 2$ can be estimated as in i) and ii). Hence two terms remain.

iv) Using Lemma 3.6.2, Lemma 3.6.3, and Lemma 3.6.5, the first of these terms is estimated by

$$\begin{aligned}
 \|\tilde{v}_c^{*(p-1)} * \tilde{v}_s\|_{\tilde{X}^\infty} &\leq C \|\tilde{v}_c\|_{\tilde{X}^1}^{p-2} \|\tilde{v}_c * \tilde{v}_s\|_{\tilde{X}^\infty} \\
 &\leq C \|\tilde{v}_c\|_{\tilde{X}^1}^{p-2} \|\tilde{v}_c\|_{\tilde{X}^2} \|\tilde{v}_s\|_{\tilde{X}^2} \\
 &\leq C \|\tilde{v}_c\|_{\tilde{X}^1}^{p-2} \|\tilde{v}_c\|_{\tilde{X}^\infty}^{1/2} \|\tilde{v}_c\|_{\tilde{X}^1}^{1/2} \|\tilde{v}_s\|_{\tilde{X}^2} \\
 &\leq C(1+t)^{(2-p)/2-1/4-3/4} r(t)^p = (1+t)^{-p/2} r(t)^p.
 \end{aligned}$$

v) Using Lemma 3.6.2 the last term is estimated by

$$\|\tilde{v}_c^{*p}\|_{\tilde{X}^\infty} \leq C \|\tilde{v}_c\|_{\tilde{X}^1}^{p-1} \|\tilde{v}_c\|_{\tilde{X}^\infty} \leq C(1+t)^{(1-p)/2} r(t)^p.$$

Summarizing all estimates i)-v) yields

$$\|(\tilde{v}_c + \tilde{v}_s)^{*p}\|_{\tilde{X}^\infty} \leq C(1+t)^{(1-p)/2} r(t)^p.$$

We have:

Aa) First, we estimate

$$\begin{aligned}
 &\left\| \int_0^t e^{(t-\tau)\tilde{L}_c} \tilde{P}_c \tilde{N}(\tilde{v}_c, \tilde{v}_s)(\tau) d\tau \right\|_{\tilde{X}^\infty} \\
 &\leq \int_0^t \|e^{(t-\tau)\tilde{L}_c}\|_{\tilde{X}^\infty \rightarrow \tilde{X}^\infty} \|\tilde{N}(\tilde{v}_c, \tilde{v}_s)(\tau)\|_{\tilde{X}^\infty} d\tau \\
 &\leq C \int_0^t (1+\tau)^{-(p-1)/2} d\tau \cdot r(t)^p \leq Cr(t)^p,
 \end{aligned}$$

where the integral is bounded w.r.t. t since $p > 3$.

Ab) Moreover, we get

$$\begin{aligned}
 & (1+t)^{1/2} \left\| \int_0^t e^{(t-\tau)\tilde{L}_c} \tilde{P}_c \tilde{N}(\tilde{v}_c, \tilde{v}_s)(\tau) d\tau \right\|_{\tilde{X}^1} \\
 \leq & (1+t)^{1/2} \int_0^t \|e^{(t-\tau)\tilde{L}_c}\|_{\tilde{X}^\infty \rightarrow \tilde{X}^1} \|\tilde{N}(\tilde{v}_c, \tilde{v}_s)(\tau)\|_{\tilde{X}^\infty} d\tau \\
 \leq & C(1+t)^{1/2} \int_0^t (t-\tau)^{-1/2} (1+\tau)^{(1-p)/2} d\tau \cdot r(t)^p \\
 \leq & C(1+t)^{1/2} \int_0^{t/2} (t/2)^{-1/2} (1+\tau)^{(1-p)/2} d\tau \cdot r(t)^p \\
 & + C(1+t)^{1/2} \int_{t/2}^t (t-\tau)^{-1/2} (1+t/2)^{(1-p)/2} d\tau \cdot r(t)^p \\
 \leq & Cr(t)^p.
 \end{aligned}$$

B) For the linearly exponentially damped part we estimate

$$\begin{aligned}
 & (1+t)^{3/4} \left\| \int_0^t e^{(t-\tau)\tilde{L}_s} \tilde{P}_s \tilde{N}(\tilde{v}_c, \tilde{v}_s)(\tau) d\tau \right\|_{\tilde{X}^2} \\
 \leq & (1+t)^{3/4} \int_0^t \|e^{(t-\tau)\tilde{L}_s}\|_{\tilde{X}^2 \rightarrow \tilde{X}^2} \|\tilde{N}(\tilde{v}_c, \tilde{v}_s)(\tau)\|_{\tilde{X}^2} d\tau \\
 \leq & C(1+t)^{3/4} \int_0^t e^{-\sigma_s(t-\tau)} (1+\tau)^{(1-p)/2-1/4} d\tau \cdot r(t)^p \\
 \leq & Cr(t)^p,
 \end{aligned}$$

due to the uniform boundedness of

$$\begin{aligned}
 & (1+t)^{3/4} \int_0^t e^{-\sigma_s(t-\tau)} (1+\tau)^{(1-p)/2-1/4} d\tau \\
 \leq & (1+t)^{3/4} \int_0^{t/2} e^{-\sigma_s t/2} (1+\tau)^{(1-p)/2-1/4} d\tau \\
 & + (1+t)^{3/4} \int_{t/2}^t e^{-\sigma_s(t-\tau)} (1+t/2)^{(1-p)/2-1/4} d\tau.
 \end{aligned}$$

Remark 3.6.6. In the last estimate the factor $(1+t)^{3/4}$ can be replaced by $(1+t)^{(p-1)/2+1/4}$ without destroying the uniform boundedness w.r.t. the time

variable t . Therefore, the decay of $\tilde{v}_s(\cdot, t)$ can be improved to

$$\|\tilde{v}_s(\cdot, t)\|_{\tilde{\mathcal{X}}^2} \leq C(1+t)^{(1-p)/2-1/4}.$$

We used the slower decay $(1+t)^{-3/4}$ to show that the result is true even if quadratic terms, i.e. $p = 2$, are present in the linearly exponentially damped part. Hence, the approach used in the proof of Theorem 3.6.1 is an alternative to the approach given in [SU17, Chapter 14] and thus allows to redo the stability proofs for spatially periodic equilibria in a number of pattern forming systems in a slightly different manner.

C) Summing up all estimates yields the inequality

$$r(t) \leq C(r(0) + r(t)^p).$$

Comparing the curves $r \mapsto r$ and $r \mapsto C\delta + Cr^p$ for $\delta > 0$ small, it is easy to see that r cannot go beyond $2C\delta$. Hence, if $r(0) < \delta$, with $\delta > 0$ sufficiently small, we have the existence of a $C > 0$ such that $R(t) \leq 2C\delta$ for all $t \geq 0$.

Therefore, we have established

Theorem 3.6.1. *Consider (3.23)-(3.24) with $p > 3$. Then for all $C > 0$ there exists a $\delta > 0$ such that*

$$\|\tilde{v}_c|_{t=0}\|_{\tilde{\mathcal{X}}^1} + \|\tilde{v}_c|_{t=0}\|_{\tilde{\mathcal{X}}^\infty} + \|\tilde{v}_s|_{t=0}\|_{\tilde{\mathcal{X}}^2} \leq \delta$$

implies

$$\|\tilde{v}_c(\cdot, t)\|_{\tilde{\mathcal{X}}^\infty} \leq C, \quad \|\tilde{v}_c(\cdot, t)\|_{\tilde{\mathcal{X}}^1} \leq C(1+t)^{-1/2} \quad \text{and} \quad \|\tilde{v}_s(\cdot, t)\|_{\tilde{\mathcal{X}}^2} \leq C(1+t)^{-3/4}$$

for all $t \geq 0$.

A direct consequence of Theorem 3.6.1 is

$$\sup_{x \in \Gamma} |u(x, t)| \leq C(1+t)^{-1/2},$$

since $\tilde{u} \in \tilde{\mathcal{X}}^1$ is mapped continuously to $u \in L^\infty(\Gamma)$, and $\tilde{u}_s \in \tilde{\mathcal{X}}^2$ implies

$u_s \in \mathcal{X}^2$, due to [GPS16, Lemma 4.2], which again is mapped continuously to $u \in L^\infty(\Gamma)$ due to Sobolev's embedding theorem.

Remark 3.6.7. As far as we can see, we cannot solely work in $\tilde{\mathcal{X}}^1$ and $\tilde{\mathcal{X}}^\infty$. The space $\tilde{\mathcal{X}}^2$ is used in Lemma 3.5.1. Establishing this lemma in $\tilde{\mathcal{X}}^1$ and $\tilde{\mathcal{X}}^\infty$ would require additional knowledge about the eigenfunctions $\varphi_k(\ell, \cdot)$.

Remark 3.6.8. We expect that for (3.1) the decay rates for $\tilde{v}_s(\cdot, t)$ can be improved further, at least by an additional factor $t^{-1/2}$ due to the fact that $\varphi_1(0, x) = 1$. Therefore, $\varphi_1(0, x)^p = 1$ and the projection on the \tilde{v}_s -part vanishes at $\ell = 0$. This vanishing corresponds to a derivative which gives a factor $t^{-1/2}$ in case of diffusive behavior, cf. [SU17, Chapter 14].

Remark 3.6.9. In the critical case $p = 3$ stability and instability depend on the sign of the nonlinearity. In the unstable case $+u^3$ we have decay on an exponentially long time scale $\mathcal{O}(e^{-1/\delta})$ with δ the size of the initial condition.

3.7 Appendix

3.7.1 Local existence and uniqueness

For completeness we show the local existence and uniqueness of solutions of (3.5). In order to do so we consider the operator $L = \partial_x^2$ on

$$\mathcal{L}^2 = \{U = (u_0, u_+, u_-) \in (L^2(\mathbb{R}))^3 : \text{supp}(u_{n,j}) = I_{n,j}, n \in \mathbb{Z}, j \in \{0, +, -\}\}$$

with domain

$$\begin{aligned} \mathcal{H}^2 := \{U \in \mathcal{L}^2 : u_{n,j} \in H^2(I_{n,j}), n \in \mathbb{Z}, j \in \{0, +, -\} \\ (3.6) - (3.7) \text{ is satisfied}\}, \end{aligned}$$

equipped with the norm

$$\|U\|_{\mathcal{H}^2} := \left(\sum_{n \in \mathbb{Z}} \|u_{n,0}\|_{H^2(I_{n,0})}^2 + \|u_{n,+}\|_{H^2(I_{n,+})}^2 + \|u_{n,-}\|_{H^2(I_{n,-})}^2 \right)^{1/2}.$$

We recall [GPS16, Lemma 3.1] and [GPS16, Lemma 3.2].

Lemma 3.7.1. *The space \mathcal{H}^2 is closed under pointwise multiplication.*

Lemma 3.7.2. *The operator $-L$ with the domain \mathcal{H}^2 is self-adjoint and positive semi-definite in \mathcal{L}^2 .*

As a direct consequence of the last lemma, abstract semigroup theory [Paz83] implies

Corollary 3.7.3. *The sectorial operator L is the generator of an analytic semigroup $(e^{-Lt})_{t \geq 0}$. In particular there exists a constant C_L such that*

$$\|e^{Lt}\|_{\mathcal{H}^2 \rightarrow \mathcal{H}^2} \leq C_L.$$

We are now ready to prove the local existence and uniqueness of solutions of the initial value problem associated with (3.5) in \mathcal{H}^2 .

Theorem 3.7.1. *For every $U_0 \in \mathcal{H}^2$, there exists a $T_0 = T_0(\|U_0\|_{\mathcal{H}^2}) > 0$ and a unique mild solution $U \in C([0, T_0], \mathcal{H}^2)$ of (3.5) with $U|_{t=0} = U_0$.*

Proof. The estimates from Lemma 3.7.1 and Corollary 3.7.3 allow us to proceed with the general theory for semilinear dynamical systems [Paz83]. We rewrite the initial value problem associated with (3.5) as the integral equation

$$U(t, \cdot) = e^{Lt}U(0, \cdot) + \int_0^t e^{L(t-\tau)}U(\tau, \cdot)^p d\tau. \quad (3.33)$$

We search for solutions in the space

$$\mathcal{M} := \{U \in C([0, T_0], \mathcal{H}^2) : \sup_{t \in [0, T_0]} \|U(t, \cdot)\|_{\mathcal{H}^2} \leq 2C_L \|U(0, \cdot)\|_{\mathcal{H}^2}\},$$

where the constant C_L is from Corollary 3.7.3. For every $U_0 \in \mathcal{H}^2$, there is a sufficiently small $T_0 = T_0(\|U_0\|_{\mathcal{H}^2}) > 0$ such that the right-hand side of (3.33) is a contraction in the space \mathcal{M} . Therefore, the existence of a unique mild solution $U \in C([0, T_0], \mathcal{H}^2)$ follows from Banach's fixed-point theorem. \square

Part II

Nonlinear phenomena on a discrete necklace graph



Chapter 4

Dispersive estimates and asymptotic stability on a discrete necklace graph

In this chapter we consider a discrete Klein-Gordon system on a discrete necklace graph. We show that localized symmetric solutions (i.e. the part of the solution which is orthogonal to the eigenfunctions of the linearized operator) decay with a rate of $(1+t)^{-1/3}$ w.r.t. the L^∞ norm. Based on this estimate, we prove asymptotic stability of the vacuum state and provide an upper bound for the temporal decay rates. In particular, small localized symmetric initial data decay exactly with the same rates as in the linear case if the nonlinearity is of degree higher than five.

4.1 Introduction

The phenomenon of dispersive stability is well-studied for a broad range of partial differential equations. Typically, the L^∞ norm decays with an algebraic rate of type $(1+t)^{-\beta}$ for some constant $\beta > 0$. This is because initially localized solutions are dispersed by different group velocities associated with different wave numbers. The same effects are expected in discrete systems. Mielke and Patz [MP10] derived dispersive stability results for oscillator chains like one-

dimensional Fermi-Pasta-Ulam or Klein-Gordon chains. Inspired by their ideas, our proof of the dispersive decay is based on a Floquet representation of the solution kernel and uses van der Corput's lemma. The proof of global existence for small localized, symmetric solutions of a nonlinear system with power nonlinearity is standard.

We consider the discrete Klein-Gordon system

$$\begin{aligned}
 \partial_t^2 u_j(t) &= f(v_j^+(t) - u_j(t)) + f(v_j^-(t) - u_j(t)) - h(u_j(t) - w_{j-1}(t)) \\
 &\quad - r_u(u_j(t)), \\
 \partial_t^2 v_j^+(t) &= g(w_j(t) - v_j^+(t)) - f(v_j^+(t) - u_j(t)) - r_v(v_j^+(t)), \\
 \partial_t^2 v_j^-(t) &= g(w_j(t) - v_j^-(t)) - f(v_j^-(t) - u_j(t)) - r_v(v_j^-(t)), \\
 \partial_t^2 w_j(t) &= h(u_{j+1}(t) - w_j(t)) - g(w_j(t) - v_j^+(t)) - g(w_j(t) - v_j^-(t)) \\
 &\quad - r_w(w_j(t)),
 \end{aligned} \tag{4.1}$$

with interaction potentials $f, g, h : \mathbb{R} \rightarrow \mathbb{R}$, local potentials $r_u, r_v, r_w : \mathbb{R} \rightarrow \mathbb{R}$ and coordinates $u_j, v_j^\pm, w_j \in \mathbb{R}$, for all $j \in \mathbb{Z}$, on the subsequent discrete graph with periodic branching.

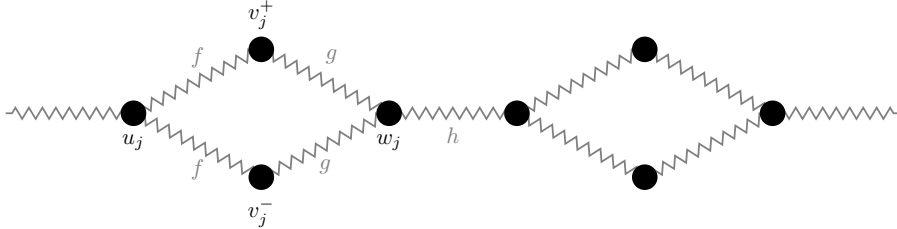


Figure 4.1.1: Discrete necklace graph with coordinates u_j, v_j^+, v_j^-, w_j and interaction forces f, g and h .

We assume that all forces vanish at the origin. Moreover, we consider Taylor expansions $f(x) = f_1 x + f_2 x^2 + \dots$ of the forces. The coordinates $(u_j, v_j^+, v_j^-, w_j)^T = X_j \in \mathbb{R}^4$ correspond to the horizontal displacement of the mass particles from its equilibrium positions. Further, we assume $f_1, g_1, h_1 > 0$ and $r_1 > 0$.

This chapter is organized as follows. In Section 4.2 we discuss the spectral situation associated to the linearization and use discrete Floquet-Bloch transform to find an explicit integral representation of the solution kernel. In Section 4.4 we prove dispersive and energy estimates. Finally, we show global existence for the nonlinear problem with sufficiently large power nonlinearity in Section 4.5.

4.2 Spectral situation and Bloch transform

In the following let $X_j = (u_j, v_j^+, v_j^-, w_j)^T$. The linear part of the Klein-Gordon system (4.1) is thus given by

$$LX_j =: MX_j + M^- X_{j-1} + M^+ X_{j+1}, \quad j \in \mathbb{Z}, \quad (4.2)$$

with matrices $M, M^-, M^+ \in \mathbb{R}^{4 \times 4}$ having constant coefficients. Note that the linear operator can be thought of as an extension of the discrete Laplacian. Our approach is based on the concept of discrete Bloch transform, which is a generalization of the concept of discrete Fourier transform. Let $X \in \ell^2(\mathbb{Z}, \mathbb{R}^4)$ and define

$$\mathcal{B}(X)(l, k) \stackrel{\text{def}}{=} \check{X}(l, k) \stackrel{\text{def}}{=} \sum_{j \in \mathbb{Z}} X_j(k) e^{-il(k+4j)}, \quad 1 \leq k \leq 4, l \in [-\pi, \pi),$$

where the index k denotes the k -th component of the four-dimensional vector X_j . The raison d'être of Bloch transform is that the linear problem transforms

into a family of diagonal multiplication operators:

$$\begin{aligned}
 (\check{L}X)(l, k) &= \sum_{j \in \mathbb{Z}} (LX)_j(k) e^{-il(k+4j)} \\
 &= \sum_{j \in \mathbb{Z}} (MX_j(k) + M^- X_{j-1}(k) + M^+ X_{j+1}(k)) e^{-il(k+4j)} \\
 &= \sum_{j \in \mathbb{Z}} ((M + M^- e^{-4il} + M^+ e^{4il}) X_j)(k) e^{-il(k+4j)} \tag{4.3} \\
 &= ((M + M^- e^{-4il} + M^+ e^{4il}) \check{X}(l))(k) \\
 &=: (M_L(l) \check{X}(l))(k).
 \end{aligned}$$

with $l \in [-\pi, \pi)$, $\check{X}(l) \in \mathbb{R}^4$ and self-adjoint 4×4 -matrices

$$M_L(l) = \begin{pmatrix} -(2f_1 + h_1 + r_{u,1}) & f_1 & f_1 & h_1 e^{-4il} \\ f_1 & -(g_1 + f_1 + (r_v)_1) & 0 & g_1 \\ f_1 & 0 & -(g_1 + f_1 + r_{v,1}) & g \\ h_1 e^{4il} & g_1 & g_1 & -(h_1 + 2g_1 + r_{w_1}) \end{pmatrix}.$$

The set of eigenvectors of $M_L(l)$ for fixed l forms an orthonormal basis of \mathbb{R}^4 . Let $\phi_n(l)$ be the eigenvector corresponding to the eigenvalue $-\omega_n(l)^2$, i.e.

$$M_L(l) \phi_n(l) = -\omega_n(l)^2 \phi_n(l), \quad 1 \leq n \leq 4. \tag{4.4}$$

The spectral curves $-\omega_n(l)^2$ can be computed explicitly as solutions of

$$\det(M_L(l) + \omega_n(l)^2) = 0.$$

The well-known Floquet-Bloch theory, cf. [RS79], implies that the spectrum has band gap structure. In particular,

$$\sigma(L) = \bigcup_{l \in [-\pi, \pi)} \sigma(M_L(l)), \tag{4.5}$$

cf. Figure 4.2.1, and $\phi_n(-l) = \overline{\phi_n(l)}$. For any l there exists an eigenvalue

$$-\omega_0^2(l) = -\omega_0^2 = -(f_1 + g_1 + (r_v)_1),$$

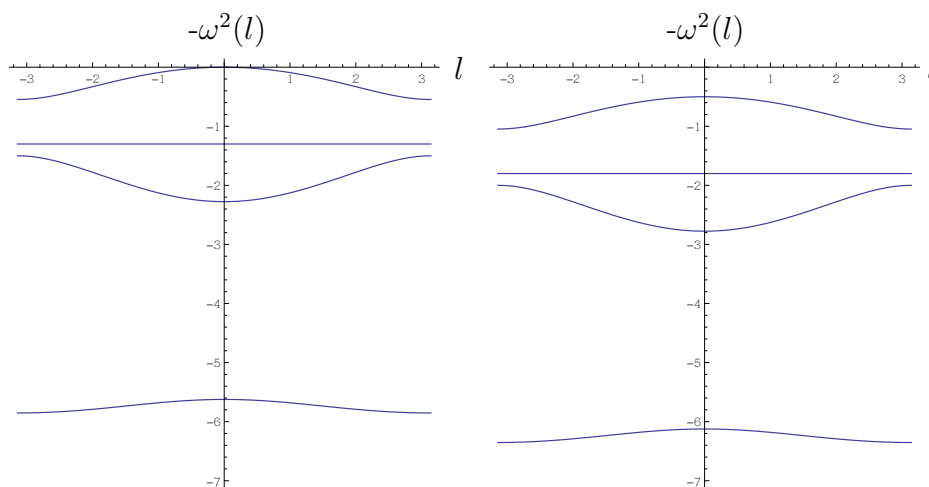


Figure 4.2.1: Floquet bands lead to the band gap structure of the spectrum.

which corresponds to a flat spectral band. The eigenstates of $-\omega_0^2$ are anti-symmetric w.r.t. the semi-circles. A basis of the eigenspace is spanned by compactly supported loop states. The second part of the spectrum is absolutely continuous and the corresponding generalized eigenfunctions are symmetric.

Remark 4.2.1. *The decomposition of the spectrum of the Laplacian on periodic, discrete graphs in an absolutely continuous part (consists of a finite number of bands) and a finite number of flat bands (eigenvalues with infinite multiplicity) is well known, cf. [KS14].*

Remark 4.2.2. *An essential feature of the model with vanishing local forces is its Galilean invariance, i.e., the transformation $(X, \dot{X}) \mapsto (X + \xi + ct, \dot{X} + c)$ is invariant for all $\xi, c \in \mathbb{R}$. In other words, we always have $0 \in \sigma(L)$ in the case of vanishing local forces. Since the Galilean invariance is broken for non-vanishing local forces, we infer $0 \notin \sigma(L)$.*

4.3 Explicit integral representation of the solution

In this section, we will calculate the integral kernel of the operator L and therefore the expression $G(L)$ for any Borel function G . Bloch transform is defined

by

$$\check{X}(l, k) = \sum_{j \in \mathbb{Z}} X_j(k) e^{-il(k+4j)} = \sum_{j \in \mathbb{Z}} x(k+4j) e^{-il(k+4j)}.$$

Here, let $x(j) \in \mathbb{R}$ count each mass particle, whereas $X_j \in \mathbb{R}^4$ counts periodicity cells, i.e., $x(m) = X_j(\tilde{m})$, with $m = 4j + \tilde{m}$, $j \in \mathbb{Z}$ and $1 \leq \tilde{m} \leq 4$ for technical reasons. We expand the vector $\check{X}(l)$ into eigenvectors $\phi_n(l)$ for any fixed value l :

$$\check{X}(l, k) = \sum_{n=1}^4 \langle \check{X}(l), \phi_n(l) \rangle_{\mathbb{R}^4} \phi_n(l, k), \quad (4.6)$$

for any component k and conclude

$$(L\check{X})(l, k) = M_L(l)\check{X}(l) = \sum_{n=1}^4 -\omega_n(l)^2 \langle \check{X}(l), \phi_n(l) \rangle \phi_n(l). \quad (4.7)$$

The eigenvectors fulfill the completeness relation,

$$\sum_{n=1}^4 \overline{\phi_n(l, k)} \phi_n(l, m) = \delta(k - m), \quad 1 \leq k, m \leq 4$$

with the Kronecker delta function δ . Extending the vectors $\phi_n(l, \cdot)$ periodically on \mathbb{Z} , leads to the relation

$$\sum_{n=1}^4 \overline{\phi_n(l, k)} \phi_n(l, m) = \sum_{j \in \mathbb{Z}} \delta(k + 4j - m), \quad k, m \in \mathbb{Z}. \quad (4.8)$$

We conclude for the k th component that

$$\begin{aligned}
 \check{X}(l, k) &= \sum_{j \in \mathbb{Z}} X_j(k) e^{-il(k+4j)} \\
 &= \sum_{j \in \mathbb{Z}} x(k+4j) e^{-il(k+4j)} \\
 &= \sum_{m \in \mathbb{Z}} x(m) e^{-ilm} \left(\sum_{j \in \mathbb{Z}} \delta(k+4j-m) \right) \\
 &= \sum_{m \in \mathbb{Z}} x(m) e^{-ilm} \left(\sum_{n=1}^4 \overline{\phi_n(l, m)} \phi_n(l, k) \right) \\
 &= \sum_{n=1}^4 \left(\sum_{m \in \mathbb{Z}} x(m) \overline{e^{ilm} \phi_n(l, m)} \right) \phi_n(l, k).
 \end{aligned}$$

This yields

$$\langle \check{X}(l), \phi_n(l) \rangle_{\mathbb{R}^4} = \sum_{m \in \mathbb{Z}} x(m) \overline{e^{ilm} \phi_n(l, m)}. \quad (4.9)$$

The inverse of Bloch transform is given by

$$x(k) = \frac{1}{2\pi} \int_{-\pi}^{\pi} \sum_{n=1}^4 \langle \check{X}(l), \phi_n(l) \rangle_{\mathbb{R}^4} e^{ilk} \phi_n(l, k) dl, \quad (4.10)$$

cf. [CBCPS12]. Inserting (4.9) in (4.10) leads to

$$\begin{aligned}
 x(k) &= \frac{1}{2\pi} \int_{-\pi}^{\pi} \sum_{n=1}^4 \sum_{m \in \mathbb{Z}} x(m) \overline{e^{ilm} \phi_n(l, m)} e^{ilk} \phi_n(l, k) dl \\
 &= \frac{1}{2\pi} \sum_{m \in \mathbb{Z}} x(m) \left(\int_{-\pi}^{\pi} \sum_{n=1}^4 \overline{e^{ilm} \phi_n(l, m)} e^{ilk} \phi_n(l, k) dl \right).
 \end{aligned} \quad (4.11)$$

We use the notation $(Lx)(k) = (LX)_j(\tilde{k})$, where $k = 4j + \tilde{k}$, with $j \in \mathbb{Z}$ and $1 \leq \tilde{k} \leq 4$. Taking into account (4.7), we proved the integral representation

$$(Lx)(k) = \frac{1}{2\pi} \sum_{m \in \mathbb{Z}} x(m) \left(\int_{-\pi}^{\pi} \sum_{n=1}^4 -\omega_n(l)^2 \overline{e^{ilm} \phi_n(l, m)} e^{ilk} \phi_n(l, k) dl \right), \quad (4.12)$$

where $-\omega_n^2(l)$ denotes the eigenvalues of the 4×4 -matrix $M_L(l)$ with corresponding eigenvectors $\phi_n(l)$.

Remark 4.3.1. *Parseval's identity shows that Bloch wave transform \mathcal{B} is continuous from ℓ^2 into L_{per}^2 , where*

$$\|\mathcal{B}u\|_{L_{per}^2}^2 = \sum_{j=1}^4 \int_{-\pi}^{\pi} |\mathcal{B}u(j, l)|^2 dl.$$

Moreover, the inverse of Bloch transform is continuous from L_{per}^2 into ℓ^2 and from L_{per}^1 into ℓ^∞ .

4.4 Dispersive decay and energy estimates

Let P_n denote the spectral projection for the self-adjoint operator L corresponding to the n th band. The spectral theorem implies

$$L = \sum_{n=1}^4 P_n L =: P_c L + P_p L,$$

where P_p denotes the projection on the eigenspace corresponding to the constant eigencurve ω_0^2 . We deduce for the projection on the absolutely continuous part of the spectrum

$$(P_c L x)(k) = \frac{1}{2\pi} \sum_{m \in \mathbb{Z}} x(m) \int_{-\pi}^{\pi} \sum_{n=1}^3 -\omega_n(l)^2 \overline{e^{ilm} \phi_n(l, m)} e^{ilk} \phi_n(l, k) dl, \quad (4.13)$$

for $k \in \mathbb{Z}$, where $\omega_n(l)^2$ and $1 \leq n \leq 3$ are the spectral curves corresponding to the absolutely continuous part.

We rewrite the Klein-Gordon system (4.1) as

$$\begin{cases} \partial_t^2 X_j(t) &= L X_j(t), \quad j \in \mathbb{Z}, t \in \mathbb{R}, \\ X(0) &= X_0, \\ \partial_t X(0) &= X_1. \end{cases} \quad (4.14)$$

By applying von Neumann's spectral theorem and the functional calculus for self-adjoint operators, the corresponding solution of (4.14) can be represented in the form

$$X_j(t) = \cos(Bt)(X_0)_j + B^{-1}\sin(Bt)(X_1)_j,$$

with $B = \sqrt{-L}$. Thanks to Euler's formula the investigation of the solution operators can be reduced to the study of their constituents

$$G_t^\beta(B) = B^{-\beta}e^{\pm iBt}, \quad \beta \in \{0, 1\}. \quad (4.15)$$

Lemma 4.4.1. *The constituents of the solution operator of (4.1) can be expressed as integral operators, which are provided by*

$$\begin{aligned} B^{-\beta}e^{\pm iBt}P_c x(j) &= \frac{1}{2\pi} \sum_{m \in \mathbb{Z}} x(m) \left(\int_{-\pi}^{\pi} \sum_{n=-3}^3 \frac{e^{\pm it\omega_n(l)}}{\omega_n(l)^\beta} \overline{e^{ilm}\phi_n(l, m)} e^{ilj}\phi_n(l, j) dl \right) \\ &= \sum_{m \in \mathbb{Z}} x(m) G_{j, m}^\beta(t) \end{aligned} \quad (4.16)$$

for $\beta \in \{0, 1\}$.

Proof. Follows directly from (4.13). □

4.4.1 Dispersive estimates

The next step is to estimate the integral expressions in Lemma 4.4.1. We prove a pointwise estimate of the constituents with decay rate $-\frac{1}{2}$, cf. Lemma 4.4.2, and a uniform estimate with decay rate $-\frac{1}{3}$, cf. Lemma 4.4.3. As a consequence, we will get dispersive estimates in weighted sequence spaces, cf. Lemma 4.4.4.

Lemma 4.4.2. *The solution kernel in Lemma 4.4.1 satisfies the estimate*

$$|G_{j, m}^\beta(t)| \lesssim (1+t)^{-1/2} |jm| \quad (4.17)$$

for any $j, m \in \mathbb{Z} \setminus \{0, \pm 1\}$ and $\beta \in \{0, 1\}$. If j or m are equal to zero or plus or minus one, we replace the product of indices on the right hand side by $\max\{|j|, |m|, 1\}$, respectively $\max\{|j| + 1, |m| + 1\}$.

Proof. At the boundary of the spectrum, the first derivative of $\omega_n(l)$ vanishes. However, we can choose the cut-off function χ , such that the second derivative does not vanish in the corresponding section and apply van der Corput's Lemma. It states that if ω is smooth and $|\omega^{(k)}(l)| \geq \lambda > 0$ for $l \in (a, b)$, where either $k \geq 2$ or $k = 1$ and ω' is monotonic, then

$$\left| \int_a^b e^{it\omega(l)} dl \right| \leq (5 \cdot 2^{k-1} - 2)(\lambda t)^{-\frac{1}{k}}.$$

Writing $F(l) = \int_a^l e^{it\omega(x)} dx$ and applying integration by parts to $\int_a^b \psi(l)F'(l)dl$, we obtain

$$\left| \int_a^b e^{it\omega(l)} \psi(l) dl \right| \leq (5 \cdot 2^{k-1} - 2)(\lambda t)^{-\frac{1}{k}} \left(|\psi(b)| + \int_a^b |\psi'(l)| dl \right). \quad (4.18)$$

Thus, integrating by parts gives

$$\begin{aligned} & \left| \int_{-\pi}^{\pi} e^{-it\omega_n(l)} \chi(l) \frac{e^{il(j-m)} \phi_n(j, -l) \phi_n(m, l)}{\omega_n(l)^\beta} dl \right| \\ & \leq \frac{1}{t^{1/2}} \left(\left| \frac{\chi(\pi) e^{i\pi(j-m)} \phi_n(j, -\pi) \phi_n(m, \pi)}{\omega_n(\pi)^\beta} \right| \right. \\ & \quad \left. + \int_{-\pi}^{\pi} \left| \partial_l \left(\chi(l) \frac{e^{il(j-m)} \phi_n(j, -l) \phi_n(m, l)}{\omega_n(l)^\beta} \right) \right| dl \right) \\ & \leq \frac{1}{t^{1/2}} |jm| \end{aligned}$$

for all n and $j, m \in \mathbb{Z} \setminus \{0\}$. The boundary terms vanish in view of the cut-off function χ . The components $\phi_n(j)$ are analytic in l and do not cause any problems. Further, ω_n is bounded away from zero for non-vanishing local forces. If the indices j or m are equal to zero or plus or minus one, we estimate the integral by $t^{-1/2} \max\{|j|, |m|, 1\}$, respectively $\max\{|j| + 1, |m| + 1\}$. Otherwise, the last integral obeys the pointwise bound $|jm|$. Using the boundedness of the integral, we obtain the required estimate for small t .

Away from the boundary of the spectrum, the first derivative does not vanish. Therefore, $1/\omega'_n(l)$ is bounded on the domain dedicated by $1 - \chi$ and integrating

by parts, we obtain

$$\begin{aligned}
 & \left| \int_{-\pi}^{\pi} e^{-it\omega_n(l)} \chi(l) \frac{e^{il(j-m)} \phi_n(j, -l) \phi_n(m, l)}{\omega_n(l)^\beta} dl \right| \\
 &= \frac{1}{t} \left| \int_{-\pi}^{\pi} \partial_l(e^{-it\omega_n(l)})(1 - \chi(l)) \frac{e^{il(j-m)} \phi_n(j, -l) \phi_n(m, l)}{\omega'_n(l)\omega_n(l)^\beta} dl \right| \\
 &= \frac{1}{t} \left| \int_{-\pi}^{\pi} e^{-it\omega_n(l)} \partial_l \left((1 - \chi(l)) \frac{e^{il(j-m)} \phi_n(j, -l) \phi_n(m, l)}{\omega'_n(l)\omega_n(l)^\beta} \right) dl \right| \\
 &\leq \frac{1}{t} |jm|,
 \end{aligned}$$

which concludes the proof. □

Lemma 4.4.3. *The solution kernel in Lemma 4.4.1 satisfies the uniform estimate*

$$|G_{j,m}^\beta(t)| \lesssim (1+t)^{-1/3}, \quad (4.19)$$

for all $j, m \in \mathbb{Z}$.

Proof. We estimate each integral in (4.16) separately for $n = 1, \dots, 3$. Explicit computations show that $\omega_n''(l_0) = 0$ only if $\omega_n'''(l_0) > 0$. Therefore, we can choose $\delta > 0$ such small that $\omega_n'''(l) \geq A > 0$ in a region U_δ around l_0 . On the other hand, we find a constant $B > 0$ with $\omega_n''(l) \geq B > 0$ for all $l \in [-\pi, \pi] \setminus U_\delta$. Applying van der Corput's lemma (4.18) gives

$$\left| \int_{-\pi}^{\pi} e^{\pm it(\omega_n(l) \mp \frac{l}{t}(m-j))} \frac{\phi_n(j, -l) \phi_n(m, l)}{\omega_n(l)^\beta} dl \right| \leq C_n (A^{-1/3} + B^{-1/2}) t^{-1/3},$$

for $t \geq 1$. Because $\partial_l^2(\omega_n(l) + \frac{l}{t}(m-j)) = \partial_l^2 \omega_n(l)$ is independent of the indices j, m , the above considerations are uniform. Using the boundedness of the integral, we obtain the estimate for small t . □

In what follows, we use discrete vector-valued function spaces defined by their norms

$$\|x\|_{\ell_s^1} := \sum_{m \in \mathbb{Z}} (1+m^2)^{\frac{s}{2}} |x_m|,$$

respectively,

$$\|x\|_{\ell^\infty} := \sup_{m \in \mathbb{Z}} (1 + m^2)^{\frac{s}{2}} |x_m|.$$

Corollary 4.4.4. *Assume that the initial data are symmetric. Then, solutions to the initial value problem obey the following decay estimates*

$$\|P_c x(t)\|_{\ell^\infty} \lesssim (1+t)^{-1/2} (\|x_0\|_{\ell^1} + \|x_1\|_{\ell^1}), \quad (4.20)$$

$$\|P_c x(t)\|_{\ell^\infty} \lesssim (1+t)^{-1/3} (\|x_0\|_{\ell^1} + \|x_1\|_{\ell^1}), \quad (4.21)$$

for all $t \in \mathbb{R}$ and initial data x_0 and x_1 .

Proof. These statements are direct consequences of Lemma 4.4.2, respectively Lemma 4.4.3. The bound is non-singular as $t \rightarrow 0$ because the discrete case enjoys an estimate $\|f\|_{\ell^\infty} \leq \|f\|_{\ell^1}$. \square

Remark 4.4.5. *For technical reasons, we identified $x(m) = X_j(\tilde{m})$, with $m = 4j + \tilde{m}$, $j \in \mathbb{Z}$ and $1 \leq \tilde{m} \leq 4$ to obtain an explicit integral representation of the solution kernel with the help of Floquet-Bloch theory. By definition $x(m)$ counts mass particles and X_j counts periodicity cells. However, the weighted norms*

$$\|x\|_{\ell^p_s} := \sum_{m \in \mathbb{Z}} (1 + m^2)^{\frac{ps}{2}} (|x_m|^p),$$

and

$$\|X\|_{\ell^p_s} := \sum_{m \in \mathbb{Z}} (1 + m^2)^{\frac{ps}{2}} (|u_m|^p + |v_m^+|^p + |v_m^-|^p + |w_m|^p),$$

are equivalent. Therefore, we can replace x by X in the formulation of Corollary 4.4.4.

4.4.2 Energy estimate

Lemma 4.4.6. *A solution of the linear Klein-Gordon system (4.1) with symmetric initial conditions obeys*

$$\|X(t)\|_{\ell^2} \lesssim \|X_0\|_{\ell^2} + C(f, g, h, r)\|X_1\|_{\ell^2}, \quad (4.22)$$

for all $t \in \mathbb{R}$ with a constant C depending on the parameters.

Proof. The linearized Klein-Gordon system is of the form

$$\partial_t^2 \check{X}(l) = (\check{L}X)(l) = (M + M^- e^{-4il} + M^+ e^{4il})\check{X}(l) =: \check{L}(l)\check{X}(l),$$

with self-adjoint, negative semi-definite matrices $\check{L}(l)$. Let $B(l) = (-\check{L}(l))^{1/2}$. Then, $e^{iB(l)t}$ defines a unitary group in \mathbb{R}^4 , such that

$$\|e^{iB(l)t}\check{Y}(l)\|_{\mathbb{R}^4} = \|\check{Y}(l)\|_{\mathbb{R}^4}, \quad \text{for all } t \in \mathbb{R},$$

for any $l \in [-\pi, \pi]$. Using continuity properties of Bloch wave transform and its inverse, see Remark 4.3.1, we estimate

$$\begin{aligned} \|X(t)\|_{\ell^2} &\lesssim \|\check{X}(t)\|_{L_{per}^2} \\ &= \|\cos(B(l)t)\check{X}_0 + B(l)^{-1}\sin(B(l)t)\check{X}_1\|_{L_{per}^2} \\ &\leq \|\cos(B(l)t)\check{X}_0\|_{L_{per}^2} + \|B(l)^{-1}\sin(B(l)t)\check{X}_1\|_{L_{per}^2} \\ &\leq \|\check{X}_0\|_{L_{per}^2} + \|\check{X}_1\|_{L_{per}^2} \\ &\lesssim \|X_0\|_{\ell^2} + C(f, g, h, r)\|X_1\|_{\ell^2}. \end{aligned}$$

The last step is valid, since the operator norm of $B(l)$ (depending on the parameters) is uniformly bounded away from zero for all $l \in [-\pi, \pi]$ in the case of non-vanishing local forces. \square

4.5 Global existence for the nonlinear problem with sufficiently large power nonlinearity

Theorem 4.5.1. *Let $p > 5$. For all constants $C > 0$ there exists a $\delta > 0$, such that solutions of (4.1) with symmetric initial conditions $\|X_0\|_{\ell^1} + \|X_1\|_{\ell^1} \leq \delta$ satisfy*

$$\|X(t)\|_{\ell^\infty} \leq \frac{C}{(1+t)^{1/3}}, \quad \|X(t)\|_{\ell^2} \leq C,$$

for all $t \in \mathbb{R}$.

This means that if the nonlinearity is of degree higher than five, small localized initial data decay exactly as in the linear case. The proof of Theorem 4.5.1 is well known.

Proof. Let $B = \sqrt{-L}$. We consider Duhamel's formula

$$X_j(t) = \cos(Bt)(X_0)_j + \int_0^t B^{-1} \sin(B(t-s))N(X)_j(s) ds.$$

From the dispersive estimate (4.21) and the energy estimate (4.22), we obtain

$$(1+t)^{1/3} \|e^{-itB} X_0\|_{\ell^\infty} \leq C_1 \begin{cases} \|X_0\|_{\ell^1}, & t \geq 1, \\ 2^{1/3} \|X_0\|_{\ell^2} & t \leq 1, \end{cases}$$

as well as,

$$\|e^{-itB} X_0\|_{\ell^2} \leq \|X_0\|_{\ell^2}, \quad t \in \mathbb{R}.$$

Using

$$(x-y)^p \leq 2^{p-1}(|x|^p + |y|^p), \quad x, y \in \mathbb{R},$$

we deduce

$$\|N(X)\|_{\ell^1} \leq C(f, g, h, r) \|X^p\|_{\ell^1} \leq C(f, g, h, r) \|X\|_{\ell^\infty}^{p-2} \|X\|_{\ell^2}^2.$$

With the abbreviations

$$\begin{aligned}\alpha(t) &= \sup_{0 \leq s \leq t} (1+s)^{1/3} \|X(s)\|_{\ell^\infty}, \\ \beta(t) &= \sup_{0 \leq s \leq t} \|X(s)\|_{\ell^2},\end{aligned}$$

it follows

$$\begin{aligned}& (1+t)^{1/3} \left\| \int_0^t \sin(B(t-s)) N(X)(s) ds \right\|_{\ell^\infty} \\ & \leq (1+t)^{1/3} \int_0^t (t-s)^{1/3} \|N(X)(s)\|_{\ell^1} ds, \\ & \leq (1+t)^{1/3} \int_0^t (t-s)^{1/3} \|X(s)\|_{\ell^\infty}^{p-2} \|X(s)\|_{\ell^2}^2 ds \\ & \leq (1+t)^{1/3} \alpha(t)^{p-2} \beta(t)^2 \int_0^t (t-s)^{-1/3} (1+s)^{-(p-2)/3} ds \\ & \leq C_2 \alpha(t)^{p-2} \beta(t)^2,\end{aligned}$$

for $p > 5$ and a constant C_2 independent of t . Moreover, we use the ℓ^2 -norm estimate for the linear part to obtain

$$\left\| \int_0^t \sin(B(t-s)) N(X)(s) ds \right\|_{\ell^2} \leq \int_0^t \|N(X)(s)\|_{\ell^2} ds \leq \int_0^t \|N(X)(s)\|_{\ell^1} ds$$

and proceed as above. Finally, we arrive at

$$\alpha(t) + \beta(t) \leq C_1 (\|X_0\|_{\ell^1} + \|X_0\|_{\ell^1}) + (C_2 + C_3) \alpha(t)^{p-2} \beta(t)^2.$$

Hence, for sufficiently small $\delta > 0$ and $\|X_0\|_{\ell^1} + \|X_0\|_{\ell^1} \leq \delta$ we proved the existence of a constant $C > 0$ such that $\alpha(t) + \beta(t) \leq C$ for all $t \geq 0$. \square

Chapter 5

Construction of breather solutions on discrete necklace graphs

We show existence of breather solutions in a nonlinear Klein-Gordon system on a discrete graph with periodic junctions. The proof is based on the Theorem of Crandall-Rabinowitz.

This part of the thesis resulted from discussions with Douglas Wright.

5.1 Introduction

We are interested in the dynamics of some nonlinear lattice differential equations on an infinite discrete graph with periodically ordered junctions. There is a competition between linear decay and the focusing effect of the nonlinearity, which allows for the existence of localized solutions. From a mathematical point of view, existence of real-valued, time-periodic and spatially localized solutions, also known as (discrete) breather solutions, is an interesting topic. Breather solutions in nonlinear PDEs are very rare. Denzler [Den93] showed that the breathers of the Sine-Gordon equation

$$\partial_t^2 u(x, t) - \partial_x^2 u(x, t) + \sin(u(x, t)) = 0, \quad x, t \in \mathbb{R},$$

disappear if the nonlinearity is perturbed. The rareness of breathers in PDEs makes it hard to believe that these non-generic, structurally unstable objects describe phenomena in nature. However, the situation is different on lattices and breather solutions come back. MacKay and Aubry [MA94] constructed breathers in Hamiltonian lattices with anharmonic on-site potentials and weak coupling. In their proof breathers are obtained by continuation from the uncoupled case in which trivial breathers exist. This means that only one oscillator is excited and the others are at rest. With the same technique, the existence of breathers was proved for diatomic Fermi-Pasta-Ulam (FPU) chains, cf. [LSM97]. Aubry et al. [AK01] have proved the existence of breathers in FPU lattices with frequencies above the phonon spectrum, when the interaction potential V is a strictly convex polynomial of degree 4. These results are obtained via a variational method.

There is an important condition for the existence of breathers, namely that the square of integer multiples of the breather frequency lie in the resolvent set of the linearized right hand side. Since the spectrum of a lattice problem is bounded, there is a good chance to find breather solutions, cf. [FW98].

Here, we consider the discrete Klein-Gordon system

$$\begin{aligned}
 \partial_t^2 u_j(t) &= f(v_j^+(t) - u_j(t)) + f(v_j^-(t) - u_j(t)) - h(u_j(t) - w_{j-1}(t)) - r_u(u_j(t)), \\
 \partial_t^2 v_j^+(t) &= g(w_j(t) - v_j^+(t)) - f(v_j^+(t) - u_j(t)) - r_v(v_j^+(t)), \\
 \partial_t^2 v_j^-(t) &= g(w_j(t) - v_j^-(t)) - f(v_j^-(t) - u_j(t)) - r_v(v_j^-(t)), \\
 \partial_t^2 w_j(t) &= h(u_{j+1}(t) - w_j(t)) - g(w_j(t) - v_j^+(t)) - g(w_j(t) - v_j^-(t)) - r_w(w_j(t)),
 \end{aligned}
 \tag{5.1}$$

with interaction potentials $f, g, h : \mathbb{R} \rightarrow \mathbb{R}$, local potentials $r_u, r_v, r_w : \mathbb{R} \rightarrow \mathbb{R}$ and coordinates $u_j, v_j^\pm, w_j \in \mathbb{R}$, for all $j \in \mathbb{Z}$ and $t \in \mathbb{R}$, on the subsequent discrete graph with periodic branching.

We assume that all forces vanish at the origin and consider Taylor expansions $f(x) = f_1 x + f_2 x^2 + \dots$ of the forces. The coordinates

$$(u_j, v_j^+, v_j^-, w_j)^T = Z_j \in \mathbb{R}^4, \tag{5.2}$$

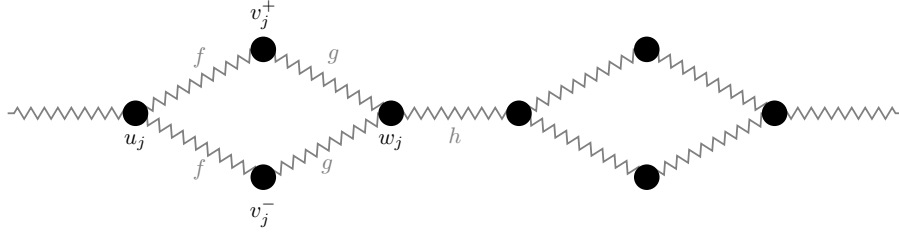


Figure 5.1.1: Topology of the discrete necklace graph

correspond to the horizontal displacement of the mass particles from its equilibrium positions. Further, we assume $f_1, g_1, h_1 > 0$ and $r_1 > 0$ and use the symbol L for the linearized operator of (5.1), respectively $N(Z)$ for the nonlinear part.

The main result, cf. Theorem 5.3.2, can be stated as follows: Let $-\omega_0^2 = -(f_1 + g_1 + (r_v)_1)$ be the eigenvalue of the linear part L in (5.1), which corresponds to the straight line in Figure 5.2.1. Suppose that the non-resonance condition $-m^2\omega_0^2 \notin \sigma_{ac}(L)$ is fulfilled for all $m \in \mathbb{N}_0$. Then, there exists a one-parameter family of real-valued solutions that are periodic in time and spatially localized. The constructed breather solutions bifurcate from eigenstates that are localized in a single ring of the periodic graph, cf. Figure 5.1.2. Hence, these non-symmetric solutions are strongly localized. To our knowledge there are no existence results for breathers on discrete graphs with periodic branching.

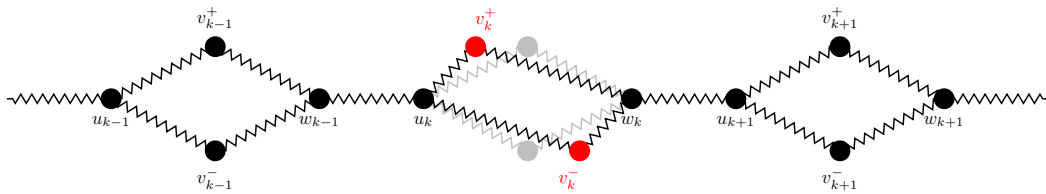


Figure 5.1.2: Antisymmetric eigenstate with support in the k th periodicity cell. Only the masses v_k^+ and v_k^- are displaced from their equilibrium positions.

This chapter is organized as follows. We compute the spectral picture for the Klein-Gordon system in Section 5.2. In Section 5.3 we apply the bifurcation theorem of Crandall-Rabinowitz in order to construct the one-parameter family

of breathers.

Notation: We equip the vector-valued sequence spaces with the norm

$$\|\{Z_j\}_{j \in \mathbb{Z}}\|_{\ell^p(\mathbb{Z}, \mathbb{R}^4)} = \left(\sum_{j \in \mathbb{Z}} |Z_j|_{\mathbb{R}^4}^p \right)^{\frac{1}{p}} < \infty$$

for $p \in [1, \infty)$.

5.2 Spectral situation

The linearized system associated to (5.1) is of the form

$$\partial_t^2 Z_j = M^0 Z_j + M^- Z_{j-1} + M^+ Z_{j+1}, \quad j \in \mathbb{Z}, \quad (5.3)$$

with $M^0, M^-, M^+ \in \mathbb{R}^{4 \times 4}$ with constant coefficients. System (5.3) is solved by Bloch waves

$$Z_j(t) = e^{i(lj - \omega t)} \check{Z}(l), \quad l, \omega \in \mathbb{R}, \quad (5.4)$$

with $\check{Z}(l) = (\check{u}(l), \check{v}^+(l), \check{v}^-(l), \check{w}(l))^T$. This leads to the spectral problem

$$M(l) \check{Z}(l) = -\omega^2(l) \check{Z}(l), \quad (5.5)$$

where

$$M(l) := M^0 + e^{-il} M^- + e^{il} M^+ = \begin{pmatrix} -(2f_1 + h_1 + (r_u)_1) & f_1 & f_1 & h_1 e^{-il} \\ f_1 & -(g_1 + f_1 + (r_v)_1) & 0 & g_1 \\ f_1 & 0 & -(g_1 + f_1 + (r_v)_1) & g_1 \\ h_1 e^{il} & g_1 & g_1 & -(h_1 + 2g_1 + (r_w)_1) \end{pmatrix}.$$

For fixed values l , we have four eigenvalues. Floquet-Bloch theory, cf. [RS79], implies that the spectrum of L has band gap structure and that

$$\sigma(L) = \bigcup_{l \in [-\pi, \pi)} \sigma(M(l)). \quad (5.6)$$

The spectrum consists of an absolutely continuous part plus an eigenvalue of infinite multiplicity, which corresponds to the flat spectral band, cf. [KS14]. The absolutely continuous part of the spectrum consists of three spectral bands.

The stiffness parameters f_1, g_1 and h_1 determine whether the eigenvalue $-\omega_0^2 = -(f_1 + g_1 + (r_v)_1)$ is isolated or located within the continuous spectrum. Typical spectral pictures are sketched in Figure 5.2.1.

Point spectrum: The eigenspace contains anti-symmetric sequences with respect to the junctions. An eigenbasis $\{E_k\}_{k \in \mathbb{Z}}$ can be chosen compactly supported in the circles. In particular, for a fixed $k \in \mathbb{Z}$, the sequence E_k is defined by

$$v_k^+(t) = \frac{1}{\sqrt{2}} = -v_k^-(t), \quad v_j^\pm = 0 \text{ for all } j \neq k, \quad u_j = w_j = 0 \text{ for all } j, \quad (5.7)$$

cf. Figure 5.1.2.

Continuous spectrum: The (generalized) eigenfunctions corresponding to the absolutely continuous spectrum are symmetric w.r.t. the semi-circles, i.e. $v_j^+ = v_j^-$ for all $j \in \mathbb{Z}$, which we refer to as \tilde{V}_{sym} .

We decompose the sequence space into its symmetric and anti-symmetric part,

$$\tilde{V}_{sym} \oplus \left(\bigoplus_{k \in \mathbb{Z}} \text{span}\{E_k\} \right).$$

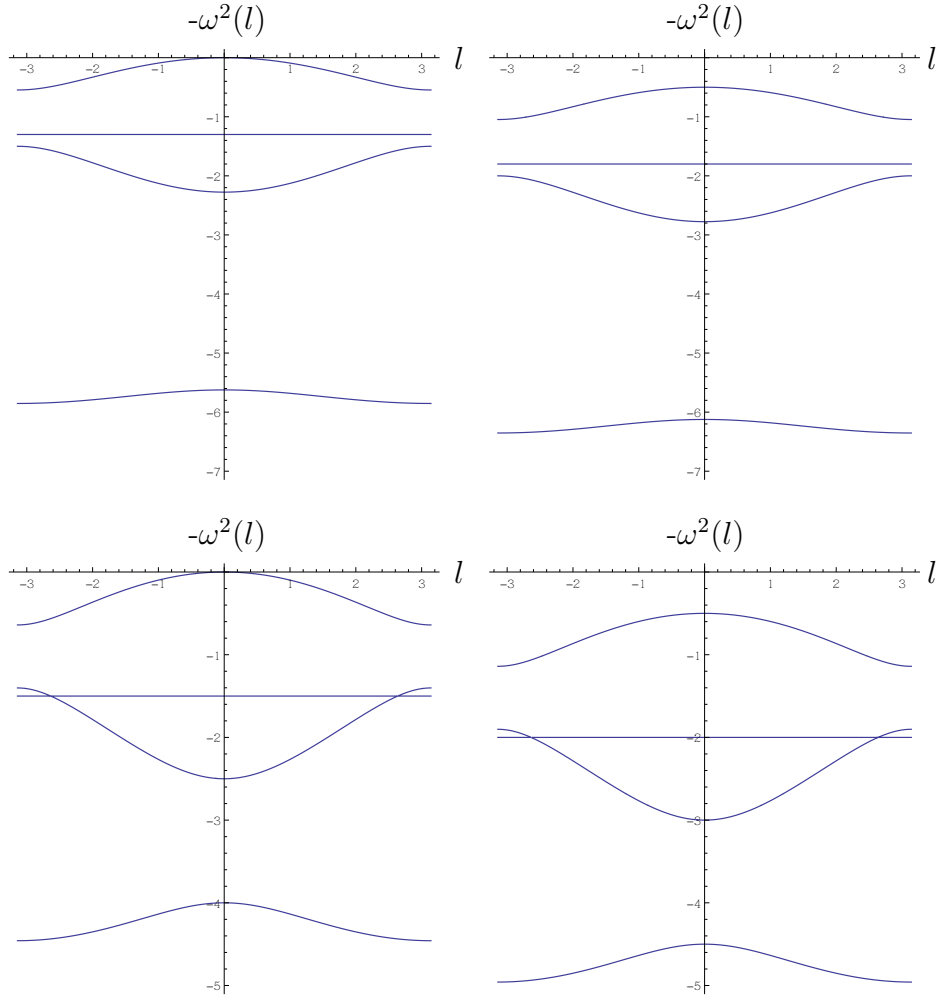


Figure 5.2.1: Spectral picture for four examples of parameter sets.
 Upper panel: isolated eigenvalue. Left: Vanishing local forces: $f_1 = 1$, $g_1 = 0.3$, $h_1 = 2$; Right: Non-vanishing local forces: $f_1 = 1$, $g_1 = 0.3$, $h_1 = 2$ and $r_1 = 0.5$
 Lower panel: embedded eigenvalue. Left: Vanishing local forces: $f_1 = 0.5$, $g_1 = 1$, $h_1 = 1$; Right: Non-vanishing local forces: $f_1 = 0.5$, $g_1 = 1$, $h_1 = 1$ and $r_1 = 0.5$

Let $p \in \mathbb{N}$ be the power of the nonlinearity

$$N^p \begin{pmatrix} u_j \\ v_j^+ \\ v_j^- \\ w_j \end{pmatrix} = \begin{pmatrix} f_p(v_j^+ - u_j)^p + f_p(v_j^- - u_j)^p - h_p(u_j - w_{j-1})^p - r_p u_j^p \\ g_p(w_j - v_j^+)^p - f_p(v_j^+ - u_j)^p - r_p (v_j^+)^p \\ g_p(w_j - v_j^-)^p - f_p(v_j^- - u_j)^p - r_p (v_j^-)^p \\ h_p(u_{j+1} - w_j)^p - g_p(w_j - v_j^+)^p - g_p(w_j - v_j^-)^p - r_p w_j^p \end{pmatrix}.$$

An explicit computation shows

$$LE_k = -\omega_0^2 E_k, \quad N(E_k) \subset \begin{cases} \text{span}\{E_k\}, & \text{for } p \text{ odd,} \\ \tilde{V}_{sym}, & \text{for } p \text{ even.} \end{cases} \quad (5.8)$$

This means that discrete eigenfunctions to other k that are not present in the initial data will not be excited at any time. Further,

$$Z \in \tilde{V}_{sym} \Rightarrow LZ, N(Z) \in \tilde{V}_{sym}, \quad (5.9)$$

i.e., the subspace \tilde{V}_{sym} is invariant under the actions of L and N for any $p \in \mathbb{N}$.

5.3 Existence of breather solutions for non-vanishing local forces

Discrete breathers arise from the combined effect of nonlinearity and discreteness. We will prove the existence of nontrivial solutions by means of bifurcation analysis. Therefore, we fix an integer $k_0 \in \mathbb{Z}$ and define the time-independent spaces

$$V_{sym} := \{ \{(u_j, v_j^+, v_j^-, w_j)^T\}_{j \in \mathbb{Z}} \in \ell^2(\mathbb{Z}, \mathbb{R}^4) \mid v_j^+ = v_j^- \text{ for all } j \in \mathbb{Z} \}, \quad (5.10)$$

$$V(k_0) := V_{sym} \oplus \text{span}\{E_{k_0}\}, \quad (5.11)$$

Let $I = \left[-\frac{\pi}{\omega_0}, \frac{\pi}{\omega_0}\right]$ with $-\omega_0^2$ the eigenvalue of L and define the time-dependent Banach spaces

$$X(k_0) := C_{per}^2(I, V(k_0)), \quad (5.12)$$

with $\|Z\|_{X(k_0)} := \max_{t \in I} \|Z(t)\|_{\ell^2} + \max_{t \in I} \|\dot{Z}(t)\|_{\ell^2} + \max_{t \in I} \|\ddot{Z}(t)\|_{\ell^2}$ and

$$Y(k_0) := C_{per}^0(I, V(k_0)), \quad (5.13)$$

with $\|Z\|_{Y(k_0)} := \max_{t \in I} \|Z(t)\|_{\ell^2}$ of periodically extendable functions with values in $V(k_0)$. Moreover, we restrict to even functions in time $X_{even}(k_0) := C_{per,even}^2(I, V(k_0))$ if the power p of the nonlinearity is even and use $X_{odd}(k_0) := C_{per,odd}^2(I, V(k_0))$ if p is odd. We suppress the indices *even* and *odd* until it becomes important. The choice of the Banach spaces is motivated by our interest in (possibly) bifurcating solutions that are real-valued, periodic in time and localized in space. We consider the mapping

$$\begin{aligned} F : X(k_0) \times \mathbb{R} &\rightarrow Y(k_0), \\ F(Z, \mu)(t) &= (1 + \mu)\ddot{Z}(t) - LZ(t) - N(Z)(t). \end{aligned} \quad (5.14)$$

The mapping F is well-defined due to observations (5.8), (5.9) and

$$\|N(Z)(t)\|_{\ell^2(\mathbb{Z}, \mathbb{R}^4)}^2 \leq C(f, g, h, r) \|Z(t)\|_{\ell^{2p}(\mathbb{Z}, \mathbb{R}^4)}^{2p} \leq C(f, g, h, r, p) \|Z(t)\|_{\ell^2(\mathbb{Z}, \mathbb{R}^4)}^{2p},$$

with parameter-depending constants C , where we made use of the embedding $\ell^2 \subset \ell^{2p}$. In particular, we will apply the Theorem of Crandall-Rabinowitz (see [Kie12, Theorem I.5.1.]):

Theorem 5.3.1. *We consider a mapping $F : U \times V \rightarrow Y$, where $U \times V \subset X \times \mathbb{R}$ is an open neighborhood of $(0, 0)$ and X and Y are Banach spaces. Suppose that*

(H0) $F(0, \mu) = 0$ for all $\mu \in \mathbb{R}$,

(H1) $F \in C^2(U \times V, Y)$,

(H2) $F(\cdot, 0)$ is a Fredholm operator of index zero with

$$\dim(\text{Ker}(D_Z F(0, 0))) = \text{codim}(\text{Ran}(D_Z F(0, 0))) = 1,$$

(H3) Let $E \in X$, $\|E\|_X = 1$ such that $\text{span}\{E\} = \text{Ker}(D_Z F(0, 0))$. Then

$$[D_{\mu Z}^2 F(0, 0)](E) \notin \text{Ran}(D_Z F(0, 0)).$$

Then there exists a nontrivial branch of solutions described by a C^1 -curve

$$\{(Z_s, \mu_s) : s \in (-s_0, s_0), (Z_0, \mu_0) = (0, 0)\},$$

which satisfies $F(Z_s, \mu_s) = 0$ locally, and all solutions in a neighborhood of $(0, 0)$ are either the trivial solution or on the nontrivial curve.

We verify the hypotheses of the previous theorem for the mapping F with Banach spaces $X(k_0)$ and $Y(k_0)$, defined in (5.14). First, we observe $F(0, \mu) = 0$ for all $\mu \in \mathbb{R}$, which means that we have a trivial solution branch, i.e. (H0) is fulfilled. Hypothesis (H1) is fulfilled due to the polynomial structure of (5.1).

We compute the required Frechet derivatives

$$[D_Z F(0, \mu)](H) = (1 + \mu)\partial_t^2 H(t) - LH(t), \quad (5.15)$$

$$[D_{\mu Z}^2 F(0, \mu)](H) = \partial_t^2 H(t), \quad (5.16)$$

for $X(k_0)$ and identify $D_{\mu Z}^2 F$ with an element of $\mathcal{L}(X(k_0), Y(k_0))$. Further, let

$$X_{\text{sym,even}} := C_{\text{per,even}}^2(I, V_{\text{sym}}), \quad X_{\text{sym,odd}} := C_{\text{per,odd}}^2(I, V_{\text{sym}}),$$

and

$$Y_{\text{sym,even}} := C_{\text{per,even}}^0(I, V_{\text{sym}}), \quad Y_{\text{sym,odd}} := C_{\text{per,odd}}^0(I, V_{\text{sym}}).$$

Again we suppress the indices *even* and *odd* until it becomes important. The

simple observation

$$D_Z F(0, 0)X_{\text{sym}} \subseteq Y_{\text{sym}}, \quad (5.17)$$

follows from (5.9). Let E_{k_0} be the normalized eigenvector of the stationary problem supported in the k_0 -th circle with eigenvalue $-\omega_0^2$. We denote the corresponding time-dependent solution of (5.1) by $E_{k_0}(t) = E_{k_0} \sin(\omega_0 t) \in X(k_0)$. Obviously, $\text{Ker}(D_Z F(0, 0)) = \text{span}\{E_{k_0}(t)\}$.

To verify (H3), we check whether it is true that

$$[D_{\mu Z}^2 F(0, 0)]E_{k_0}(t) = \partial_t^2 E_{k_0}(t) = -\omega_0^2 E_{k_0}(t) \notin \text{Ran}(D_Z F(0, 0)), \quad (5.18)$$

or equivalently, formulated as a question, does there exist an element $H \in X(k_0)$ such that

$$-\omega_0^2 E_{k_0}(t) = \partial_t^2 H(t) - LH(t).$$

By means of (5.17), we have $H(t) = \alpha E_{k_0}(t)$ with a constant $\alpha \in \mathbb{R}$. The occurring algebraic equation has no solution w.r.t α , i.e., (H3) is true.

It remains to find conditions under which $\text{codim}(\text{Ran}(D_Z F(0, 0))) = 1$. Relation (5.17) implies $\text{span}\{E_{k_0}(t)\} \not\subseteq [D_Z F(0, 0)]X_{\text{sym}}$. Hence,

$$\begin{aligned} \text{codim}(\text{Ran}(D_Z F(0, 0))) &= 1 \\ \Leftrightarrow D_Z F(0, 0) &\text{ invertible on } X_{\text{sym}} \rightarrow Y_{\text{sym}}. \end{aligned} \quad (5.19)$$

So, it remains to check under which conditions the equation

$$\xi = [D_Z F(0, 0)]\eta = (\partial_t^2 - L)\eta \quad (5.20)$$

will be invertible on the symmetric subspace. In the case of $2\pi/\omega_0$ -periodic and odd functions in time, we consider the expansion

$$\xi(t) = \sum_{m \in \mathbb{N}} \xi_m \sin(m\omega_0 t), \quad \eta(t) = \sum_{m \in \mathbb{N}} \eta_m \sin(m\omega_0 t) \quad (5.21)$$

with $\xi_m, \eta_m \in V_{\text{sym}}$ for $m \in \mathbb{N}$. This leads to the time-independent system of

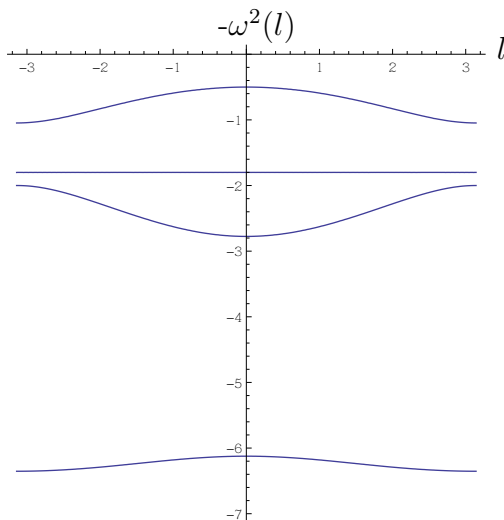


Figure 5.3.1: Spectral picture for a set of parameters satisfying the non-resonance condition ($f_1 = 0.3$, $g_1 = 1$, $h_1 = 2$ and $(r_v)_1 = 0.5$).

equations

$$\xi_m = (-m^2\omega_0^2 - L)\eta_m, \quad m \in \mathbb{N}. \quad (5.22)$$

Hence, we require that $-m^2\omega_0^2 \notin \sigma_{ac}(L)$ for all $m \in \mathbb{N}$. In particular, F is a (nonlinear) Fredholm operator of index 0. (The index does not depend on (Z, μ) , since DF depends continuously on Z and μ , cf. [Kie12, Remark I.2.2].) In the case of $2\pi/\omega_0$ -periodic and even functions in time we replace the sines in (5.21) by cosines with $m \in \mathbb{N}_0$. This leads to the requirement $-m^2\omega_0^2 \notin \sigma_{ac}(L)$ for all $m \in \mathbb{N}_0$. The spectral picture of a possible set of parameters is sketched in Figure 5.3.1.

Thus, Theorem 5.3.1 gives the existence of a non-trivial solution branch satisfying

$$(1 + \mu_s)\ddot{Z}_s(t) - LZ_s(t) - N(Z_s)(t) = 0, \quad (5.23)$$

with $Z_s \in X(k_0)$ for $s \in (-s_0, s_0)$ with $s_0 > 0$ sufficiently small. A rescaling in time leads to the following theorem.

Theorem 5.3.2. *Let $-\omega_0^2 = -(f_1 + g_1 + (r_v)_1)$ be the eigenvalue of the linear*

part in (5.1). Suppose that $-m^2\omega_0^2 \notin \sigma_{ac}(L)$ for all $m \in \mathbb{N}_0$ (non-resonance condition). Then, there exists a one-parameter family of real-valued solutions of (5.1) that are periodic in time and spatially localized.

Remark 5.3.3. To satisfy the non-resonance condition in Theorem 5.3.2, the eigenvalue $-\omega_0^2$ has to be isolated, i.e., $-\omega_0^2 \notin \sigma_{ac}(L)$. Moreover, one explicitly verifies that $-\omega_0^2 \in \sigma_{ac}(L)$ for stiffness parameters $f_1 = g_1$. Hence, a symmetry breaking is required.

Remark 5.3.4. For even powers of the nonlinearity, the non-resonance condition $-m^2\omega_0^2 \notin \sigma_{ac}(L)$, $m \in \mathbb{N}_0$, includes the requirement for $m = 0$, i.e. $0 \notin \sigma_{ac}(L)$ is required. However, Theorem 5.3.2 holds for $0 \in \sigma_{ac}(L)$ if the power of the nonlinearity is odd, i.e., in the case of vanishing local forces (FPU system).

Chapter 6

Outlook

In this chapter we shortly outline possible future research topics.

From discrete to metric graphs

The investigated Klein-Gordon systems in Sections 4 and 5 are discretized versions of Klein-Gordon equations on metric graphs. It is natural to ask, whether our proofs can be adapted to metric necklace graphs. However, the occurrence of infinitely many spectral bands leads to new challenges. The relation between discrete and continuous graphs has not been studied systematically so far.

We conjecture that our proof can be transferred to metric graphs in order to obtain a result similar to Cuccagna's for a Klein-Gordon equation with periodic potential on the real line [Cuc08]. His proof heavily relies on the fact that the periodic potential is smooth. Therefore, the operator can be considered as a perturbation of the free operator for large frequencies in this situation. This idea cannot be transferred to metric necklace graphs due to the irregularity at the vertex points and the resulting widely opened spectral gaps. To our knowledge, dispersive estimates have not been proven on non-trivial infinite periodic metric graphs so far. Kaminaga and Mine [KM16] showed dispersive estimates for only finitely many spectral bands for a periodic δ -potential on the real line, but not for the complete semigroup. It turns out that there occur additional difficulties if the spectrum consists of infinitely many bands. This is because the sum of the constants of the bandwise estimates does not converge. To overcome

this problem, a plan would be to investigate the cancellations of the oscillating integrals more carefully instead of roughly estimating them with van der Corput's lemma.

Our construction of strongly localized discrete breathers in Section 5 heavily relies on the one-dimensional invariant subspaces corresponding to the single eigenvalue, which allow us the application of the Theorem of Crandall and Rabinowitz. In the metric case the coupling of infinitely many eigenvalues and discrete modes will lead to new challenges.

Stability of breather solutions

An open question concerns asymptotic stability of the constructed localized structures, cf. [Ale18] for breathers of the Gardner equation and [CT09, KPS09] for standing waves of discrete Schrödinger equations.

In particular, it is interesting to ask whether the compactly supported breathers from Section 5 persist if a symmetric part is added to the initial data. The nonlinear coupling of infinitely many discrete modes to a continuum of dispersive modes has not been considered before in this setup. The situation of a single discrete mode was studied in [Pri15]. One scenario could be that energy of the discrete mode is transferred to the continuous modes based on some analog of Fermi's Golden Rule. The continuous modes then transport energy to infinity due to linear dispersion. One could also conjecture that the nonlinear coupling is too weak to remove all energy from the discrete modes.

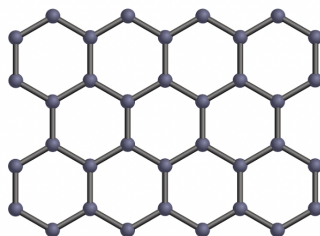


Figure 6.1: Hexagonal structure of graphene

More complex graphs

More complex and higher-dimensional graphs are an issue of further research, for instance graphs with hexagonal structure such as graphene, cf. Figure 6.1. It is desirable to characterize which dispersive equations and graphs allow us the construction of localized structures.

Bibliography

- [AK01] S. Aubry and G. Kopidakis. Aspects of discrete breathers and new directions. In *Nonlinearity and disorder: theory and applications (Tashkent, 2001)*. 2001.
- [Ale18] M. A. Alejo. Nonlinear stability of Gardner breathers. *J. Differential Equations*, 2018.
- [AST16] R. Adami, E. Serra, and P. Tilli. Threshold phenomena and existence results for NLS ground states on metric graphs. *J. Funct. Anal.*, 2016.
- [BCBLS11] C. Blank, M. Chirilus-Bruckner, V. Lescarret, and G. Schneider. Breather solutions in periodic media. *Comm. Math. Phys.*, 2011.
- [BK92] J. Bricmont and A. Kupiainen. Renormalization group and the Ginzburg-Landau equation. *Comm. Math. Phys.*, 1992.
- [BK13] G. Berkolaiko and P. Kuchment. *Introduction to quantum graphs*. Providence, RI: American Mathematical Society (AMS), 2013.
- [CBCPS12] M. Chirilus-Bruckner, C. Chong, O. Prill, and G. Schneider. Rigorous description of macroscopic wave packets in infinite periodic chains of coupled oscillators by modulation equations. *Discrete Contin. Dyn. Syst. Ser. S*, 2012.
- [CEE92] P. Collet, J.-P. Eckmann, and H. Epstein. Diffusive repair for the Ginzburg-Landau equation. *Helv Phys Acta*, 1992.

-
- [CMS18] M. Chirilus-Bruckner, D. Maier, and G. Schneider. Diffusive stability for periodic metric graphs. *Math. Nach.* 1-14, 2018.
- [CT09] S. Cuccagna and M. Tarulli. On asymptotic stability of standing waves of discrete Schrödinger equation in \mathbb{Z} . *SIAM J. Math. Anal.*, 2009.
- [Cuc08] S. Cuccagna. On dispersion for Klein Gordon equation with periodic potential in 1D. *Hokkaido Math. J.*, 2008.
- [Den93] J. Denzler. Nonpersistence of breather families for the perturbed sine Gordon equation. *Comm. Math. Phys.*, 1993.
- [Eas75] M. S. P. Eastham. *Results and problems in the spectral theory of periodic differential equations*. Springer, Berlin, 1975.
- [EK15] P. Exner and H. Kovařík. *Quantum waveguides*. Cham: Springer, 2015.
- [Fuj66] H. Fujita. On the blowing up of solutions of the Cauchy problem for $u_t = \Delta u + u^{1+\alpha}$. *J. Fac. Sci. Univ. Tokyo Sect. I*, 1966.
- [FW98] S. Flach and C. R. Willis. Discrete breathers. *Phys. Rep.*, 1998.
- [GPS16] S. Gilg, D. Pelinovsky, and G. Schneider. Validity of the NLS approximation for periodic quantum graphs. *NoDEA, Nonlinear Differ. Equ. Appl.*, 23, 2016.
- [GS01] M. D. Groves and G. Schneider. Modulating pulse solutions for a class of nonlinear wave equations. *Comm. Math. Phys.*, 2001.
- [GS05] M. D. Groves and G. Schneider. Modulating pulse solutions for quasilinear wave equations. *J. Differential Equations*, 2005.
- [GS08] M. D. Groves and G. Schneider. Modulating pulse solutions to quadratic quasilinear wave equations over exponentially long length scales. *Comm. Math. Phys.*, 2008.

-
- [Hen81] D. Henry. *Geometric theory of semilinear parabolic equations.*, volume 840 of *Lecture Notes in Mathematics*. Springer-Verlag, Berlin-New York, 1981.
- [HR17] A. Hirsch and W. Reichel. Existence of cylindrically symmetric ground states to a nonlinear curl-curl equation with non-constant coefficients. *Z. Anal. Anwend.*, 2017.
- [Jam03] G. James. Centre manifold reduction for quasilinear discrete systems. *J. Nonlinear Sci.*, 2003.
- [JNRZ14] M.A. Johnson, P. Noble, L.M. Rodrigues, and K. Zumbrun. Behavior of periodic solutions of viscous conservation laws under localized and nonlocalized perturbations. *Invent. Math.*, 2014.
- [Kie12] H. Kielhöfer. *Bifurcation theory*. Applied Mathematical Sciences. Springer, New York, 2012.
- [KL07] E. Korotyaev and I. Lobanov. Schrödinger operators on zigzag nanotubes. *Ann. Henri Poincaré*, 2007.
- [KM16] M. Kaminaga and T. Mine. Quantum diffusion in the kronig-penney model. *arxiv*, 1603.00084, 2016.
- [KP07] P. Kuchment and O. Post. On the spectra of carbon nanostructures. *Commun. Math. Phys.*, 2007.
- [KPS09] P. G. Kevrekidis, D. E. Pelinovsky, and A. Stefanov. Asymptotic stability of small bound states in the discrete nonlinear Schrödinger equation. *SIAM J. Math. Anal.*, 2009.
- [KS14] E. Korotyaev and N. Saburova. Schrödinger operators on periodic discrete graphs. *J. Math. Anal. Appl.*, 2014.
- [Kuc02] P. Kuchment. Graph models for waves in thin structures. *Waves Random Media*, 2002.
- [LSM97] R. Livi, M. Spicci, and R. S. MacKay. Breathers on a diatomic FPU chain. *Nonlinearity*, 10, 1997.

- [MA94] R. S. MacKay and S. Aubry. Proof of existence of breathers for time-reversible or hamiltonian networks of weakly coupled oscillators. *Nonlinearity*, 1994.
- [Mai18] D. Maier. Construction of breather solutions for nonlinear klein-gordon equations on periodic metric graphs. *arXiv:1812.02012 [math.AP]*, 2018.
- [MP10] A. Mielke and C. Patz. Dispersive stability of infinite-dimensional Hamiltonian systems on lattices. *Appl. Anal.*, 2010.
- [MSU01] A. Mielke, G. Schneider, and H. Uecker. Stability and diffusive dynamics on extended domains. In *Ergodic theory, analysis, and efficient simulation of dynamical systems*. Berlin: Springer, 2001.
- [MV05] S. Molchanov and B. Vainberg. Slowing down of the wave packets in quantum graphs. *Waves Random Complex Media*, 2005.
- [Noj14] D. Noja. Nonlinear Schrödinger equation on graphs: recent results and open problems. *Philos. Trans. R. Soc. Lond., Ser. A, Math. Phys. Eng. Sci.*, 2014.
- [Pan18] A. Pankov. Nonlinear Schrödinger equations on periodic metric graphs. *Discrete Contin. Dyn. Syst.*, 2018.
- [Pau36] L. Pauling. The diamagnetic anisotropy of aromatic molecules. *J. Chem. Phys*, 1936.
- [Paz83] A. Pazy. Semigroups of linear operators and applications to partial differential equations. Applied Mathematical Sciences, 44. New York etc.: Springer-Verlag. VIII., 1983.
- [Pri15] O. Prill. Asymptotic stability of the vacuum solution for one-dimensional nonlinear Klein-Gordon equations with a perturbed one-gap periodic potential with and without an eigenvalue. *ZAMM Z. Angew. Math. Mech.*, 95(8):778–821, 2015.

- [PS17] D. Pelinovsky and G. Schneider. Bifurcations of standing localized waves on periodic graphs. *Ann. Henri Poincaré*, 2017.
- [RS79] M. Reed and B. Simon. Methods of modern mathematical physics. III: Scattering theory. New York, San Francisco, London: Academic Press. XV, 1979.
- [Sch96] G. Schneider. Diffusive stability of spatial periodic solutions of the Swift-Hohenberg equation. *Comm. Math. Phys.*, 1996.
- [Sch98] G. Schneider. Nonlinear stability of Taylor-vortices in infinite cylinders. *Arch. Rat. Mech. Anal.*, 1998.
- [Str89] W. Strauss. *Nonlinear wave equations. Expository lectures from the CBMS regional conference held at George Mason University, January 16-22, 1989*. Providence, RI: American Mathematical Society, 1989.
- [SU17] G. Schneider and H. Uecker. *Nonlinear PDEs -A Dynamical Systems Approach*. Graduate Studies in Mathematics. AMS, 2017.
- [Wei81] F. Weissler. Existence and nonexistence of global solutions for a semilinear heat equation. *Israel J. Math.*, 1981.